ISSN 1023-9855

Thoracic Medicine

Volume 39 • Number 3 • September 2024

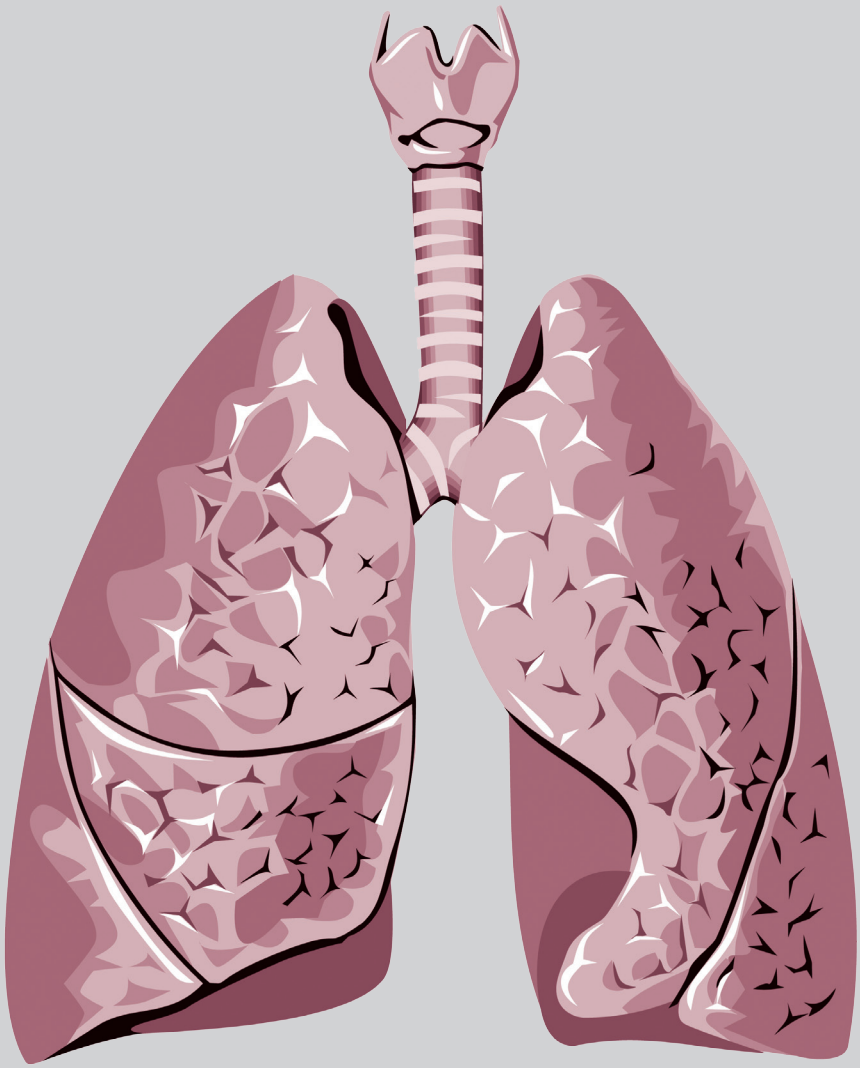

The Official Journal of

Taiwan Society of Pulmonary and Critical Care Medicine

Taiwan Society of Sleep Medicine

Taiwan Society for Respiratory Therapy

Taiwan Society of Tuberculosis and Lung Diseases

Thoracic Medicine

The Official Journal of
Taiwan Society of Pulmonary and Critical Care Medicine
Taiwan Society for Respiratory Therapy
Taiwan Society of Sleep Medicine
Taiwan Society of Tuberculosis and Lung Diseases

Thoracic Medicine

The Official Journal of
Taiwan Society of Pulmonary and Critical Care Medicine
Taiwan Society for Respiratory Therapy
Taiwan Society of Sleep Medicine
Taiwan Society of Tuberculosis and Lung Diseases

Volume 39
Number 3
September 2024

CONTENTS

Impact of DPP-4 Inhibitors on Survival of Patients with Non-Small Cell Lung Cancer – A Propensity Score-Matched Analysis

Pang-Chieh Hung[1], Kuang-Tai Kuo[1], Tung-Yu Tiong[1], Yuan-Hung Wang[2,3], *Wei-Ciao, Wu[1]

Introduction: Diabetes mellitus (DM) and cancer coexist in 8-18% of individuals with DM. Dipeptidyl peptidase-4 inhibitor (DPP4i) is one of the hypoglycemic agents (OHA) that have been found to be beneficial with various cancer patients, either in vitro or in vivo. The aim of this study was to retrospectively examine overall survival (OS) with or without the usage of DPP4i in DM patients with non-small cell lung cancer.

Methods: This single-center, propensity score-matched, retrospective comparative study using electronic medical records evaluated DM patients with non-small cell lung adenocarcinoma between January 2011 and December 2019 at Shuang Ho Hospital, Taiwan. Patients were divided into Group 1, in which DPP4i was not taken with other OHA, and Group 2, in which DPP4i was taken combined with other OHA. We compared the OS between the 2 groups and tried to find some covariate that would influence OS in DM lung cancer patients.

Results: We enrolled 193 patients (150 in the non-DDP4i group (Group 1), and 43 in the DDP4i group (Group 2)); 86 patients in Group 1 and 43 patients in Group 2 were matched using propensity scores. In the matched cohorts, patients in the non-DDP4i group had poorer OS than those in the non-DPP4i group, although without statistical significance; for 1-year, 2-year and 5-year OS, the hazard ratios were 1.37 (P = 0.304; 95% CI 0.753-2.479), 1.37 (P = 0.2; 95% CI 0.848-2.207) and 1.32 (P = 0.17; 95% CI: 0.890-1.946), respectively.

Conclusion: Dipeptidyl peptidase IV inhibitor (DPP4i) may have a benefit for OS in NSCLC patients with comorbidity of DM, although there was no significant difference due to the sample size. Among the DM lung cancer patients, female sex would be a better prognostic factor for OS. ***(Thorac Med 2024; 39: 198-207)***

Key words: DPP4i, diabetes mellitus, non-small cell lung cancer

[1]Division of Thoracic Surgery, Department of Surgery, Shuang Ho Hospital, Taipei Medical University, [2]Graduate Institute of Clinical Medicine, College of Medicine, Taipei Medical University, Taipei 11031, Taiwan. [3]Department of Medical Research, Shuang Ho Hospital, Taipei Medical University, New Taipei City 23561, Taiwan
Address reprint requests to: Dr. Wei-Ciao, Wu, No. 291, Zhongzheng Rd., Zhonghe Dist., New Taipei City

Introduction

Diabetes mellitus (DM) and cancer coexist in 8-18% of individuals. An increasing amount of evidence has revealed that DM has a positive correlation with the incidence of various cancers, including lung cancer [1-4]. Moreover, DM also plays an important role in the prognosis of cancer patients. Lung cancer patients also have many other prognostic factors that would affect overall survival (OS), such as age, pathological stage, and pathological pattern. Although the mechanisms of DM that affect cancer incidence and prognosis are not well-researched, the accepted concept is that the hyperinsulinemia, hyperglycemia, and inflammation cytokines would induce abnormalities in cancer cellular growth and division [5-7].

Oral hypoglycemic agents (OHA), including metformin, thiazolidinedione (TZD), and dipeptidyl peptidase IV inhibitor (DPP4i), have been reported to have a correlation with decreasing risk or improving OS in a dose-dependent manner among various cancer patients [5, 8]. Clinically, DPP4i has been commonly utilized mainly to control postprandial blood sugar, and is often combined with other OHA or insulin. DPP4i has the advantages of being a convenient once-daily oral regimen, having a low potential for pharmacokinetic drug-drug interactions and good efficacy and safety profiles, including cardiovascular safety, and being less harmful to renal function [9-10]. A growing body of evidence indicates that DPP4i has an interesting role in cancer biology, and could improve the clinical outcome of various cancers [11-12].

Dipeptidyl peptidase IV (DPP4), also known as cluster of differentiation 26 (CD26), is a surface T cell activation antigen expressed in many tissues, including but not limited to the kidney, gastrointestinal tract, liver and bone marrow, as well as on the surface of various cell types, such as stromal, stem, epithelial, endothelial, and immune cells, and is thought to be multifunctional and participate in different signaling pathways. DPP4i is able to modulate lymphocyte function in many aspects, especially in T cell activation and signal transduction, which would have different impacts on various autoimmune-related diseases, including cancers [13-15]. Inhibition of DPP4 expression has been reported to be a satisfactory therapeutic target in certain cancer treatments. In an in vitro study, a tumor model using a Lewis lung carcinoma and a human lung adenocarcinoma cell line was significantly suppressed when the activity of CD26/DPP4 was inhibited [16-17]. DDP4i has also been shown to improve OS in diabetes patients with chronic myeloid leukemia, colorectal cancer with lung metastasis, and prostate cancer [15, 18]. However, few studies have focused on the influence of DDP4 inhibitors on OS in diabetes patients with non-small cell lung cancer (NSCLC), or on the effective duration of DPP4i. The aim of this study was to retrospectively examine OS with or without the usage of DPP4i in DM patients with NSCLC.

Methods

Study design and patient selection

This study received ethical approval from the Institutional Review Board (IRB) of Taipei Medical University (Approval number: N202101042). We screened the electronic medical records of Shuang Ho Hospital for consecutive patients with NSCLC from January 2011 to December 2019. We found a total of 1286

NSCLC patients and screened them for DM in outpatient or hospitalization records; a total of 243 eligible patients were found. The exclusion criteria were as follows: 1) younger than 18 or older than 90 years (n=3); 2) no pathological confirmed NSCLC (n=1); 3) second or third primary lung cancer (n=38); 4) survival < 30 days (n=8). All selected patients had at least a 2-year follow-up. The patients were categorized into either the DDP4i (n = 43) or non-DPP4i (n = 150) group, based on whether DPP4i was prescribed for at least 6 months after NSCLC was diagnosed.

Clinical evaluation and outcome of the patients

Patients' DM medicine history was retrieved mainly by outpatient records. The patients in the DPP4i group were prescribed DPP4i for at least 6 months or until death after NSCLC was diagnosed. The DPP4i group patients often had combined usage with other OHA or regular insulin (RI). Commonly used DPP4i included linagliptin (Tradjenta), saxagliptin (Onglyza), vildagliptin (Galvus) and sitagliptin (Januvia).

Primary outcome focused on 1-year, 2-year and 5-year OS, which was defined as the duration between the date of first diagnosis of lung cancer and the last follow-up time or the patient's death. The last update on follow-up time was August 2022. Secondary outcome would focus on the possible risk factors for OS.

Statistical analysis and propensity score matching

Continuous variables are presented as mean ± standard deviation and categorized data are presented as n (%). Continuous patient characteristics were analyzed with the t-test for normal distribution, and categorical characteristics were analyzed with the chi-square test or Fisher's exact test. To eliminate the important covariate differences between 2 groups, we utilized propensity score matching (PSM), which used the nearest-neighbor matching algorithm with a 1:2 matching scheme for DM patients with NSCLC, whether taking DPP4i or not. The propensity score was estimated, and involved 2 variables: age and pathological stage, based on their p-value in univariate analysis and known important factors that would have an impact on OS. We matched each case so that they had a similar calculated propensity score with a caliper width of 0.2. Due to the small sample size, we could not match more covariates to make 2 groups consistent. Kaplan-Meier curves were used to obtain OS among patients, whether they used DDP4i or not, and were evaluated by log-rank test. Univariate Cox proportional-hazards models were used to estimate the significance level and hazard ratio (HR), with a 95% confidence interval (CI). For all analyses, statistically significant differences were set at $P < 0.05$. Statistical analysis was mainly performed using SPSS version 25, and Kaplan-Meier curves were drawn by the R version 4.3.1 software program (R Foundation for Statistical Computing, Vienna, Austria).

Results

Between 1 January 2011 and 31 December 2019, 1286 patients from a single institution (Shuang Ho Hospital) who were diagnosed with NSCLC were enrolled; the patient selection flowchart is presented in Figure 1. The baseline characteristics of the unmatched and matched patients are listed in each group (Table 1). The median age of both groups was 69 years, with an interquartile range (IQR) of 60 to 78 years,

Table 1. Demographic Characteristics of Participants Before and After Propensity Score Matching.

	Unmatched comparison			Matched comparison		
Characteristic	**NonDPP4i (N=150)**	**DPP4i (N=43)**	***P*- value**	**NonDPP4i (N= 86)**	**DPP4i (N=43)**	***P*- value**
Age (years)			<0.05			0.775
Median	68.0±8.9	71.5±10.4		71.5±8.8	71.5±10.4	
Range	47-88	54-89		50-88	54-89	
Gender, n (%)			0.474			0.334
Male	95(63)	24(56)		57(66)	24(56)	
Female	55(37)	19(44)		29(34)	19(44)	
BMI, kg/m^2	23.4±4.7	26.4±4.6	<0.05	23.7±4.8	26.4±4.99	<0.05
Smoke = Yes, n(%)	89(59)	18(42)	0.063	51(62)	18(42)	0.092
Location of tumor, n(%)			0.07			0.09
RUL	47(31)	13(30)		21(24)	13(30)	
RML	12(8)	5(12)		7(8)	5(12)	
RLL	15(10)	10(23)		11(13)	10(23)	
LUL	45(30)	11(26)		27(31)	11(26)	
LLL	16(11)	4(9)		9(11)	4(9)	
Multiple	15(10)	0(0)		11(13)	0(0)	
Histologic diagnosis on registration, n(%)			0.907			0.663
Adenocarcinoma	101(68)	29(68)		54(63)	29(68)	
Squamous cell carcinoma	38(25)	12(28)		25(29)	12(28)	
Adenosquamous	3(2)	1(2)		1(1)	1(2)	
Other	8(5)	1(2)		6(7)	1(2)	
TNM stage, n(%)			0.349			0.711
I	26(17)	13(30)		18(21)	13(30.2)	
II	10(7)	2(5)		5(6)	2(4.7)	
III	35(23)	8(19)		19(22)	8(18.6)	
IV	79(53)	20(46)		44(51)	20(46.5)	
CT= Yes, n(%)	83(55)	19(44)	0.263	47(55)	19(44)	0.350
RT= Yes, n(%)	52(35)	12(28)	0.518	27(36)	12(28)	0.314
TT= Yes, n(%)	33(22)	7(16)	0.547	22(26)	7(16)	0.332
IT= Yes, n(%)	5(3)	2(5)	0.653	2(2)	2(5)	0.600
OT= Yes, n(%)	53(35)	22(51)	0.09	30(35)	22(51)	0.113
Lobar resection, n(%)	33(22)	13(30)	0.165	18(21)	13(30)	0.206
Metformin= Yes, n(%)	92(61)	23(53)	0.454	52(60)	23(53)	0.570
Hypertension, n(%)	89(59)	34(79)	<0.05	57(66)	34(79)	0.154
COPD, n(%)	16(11)	5(12)	0.788	11(12)	5(12)	1
CAD, n(%)	20	12	<0.05	11(13)	12(28)	0.061

BMI: Body mass index, RT: Radiotherapy, TT: Target therapy, IT: immune therapy, OT: operation therapy, COPD: Chronic obstructive pulmonary disease. CAD: Coronary arterial disease.

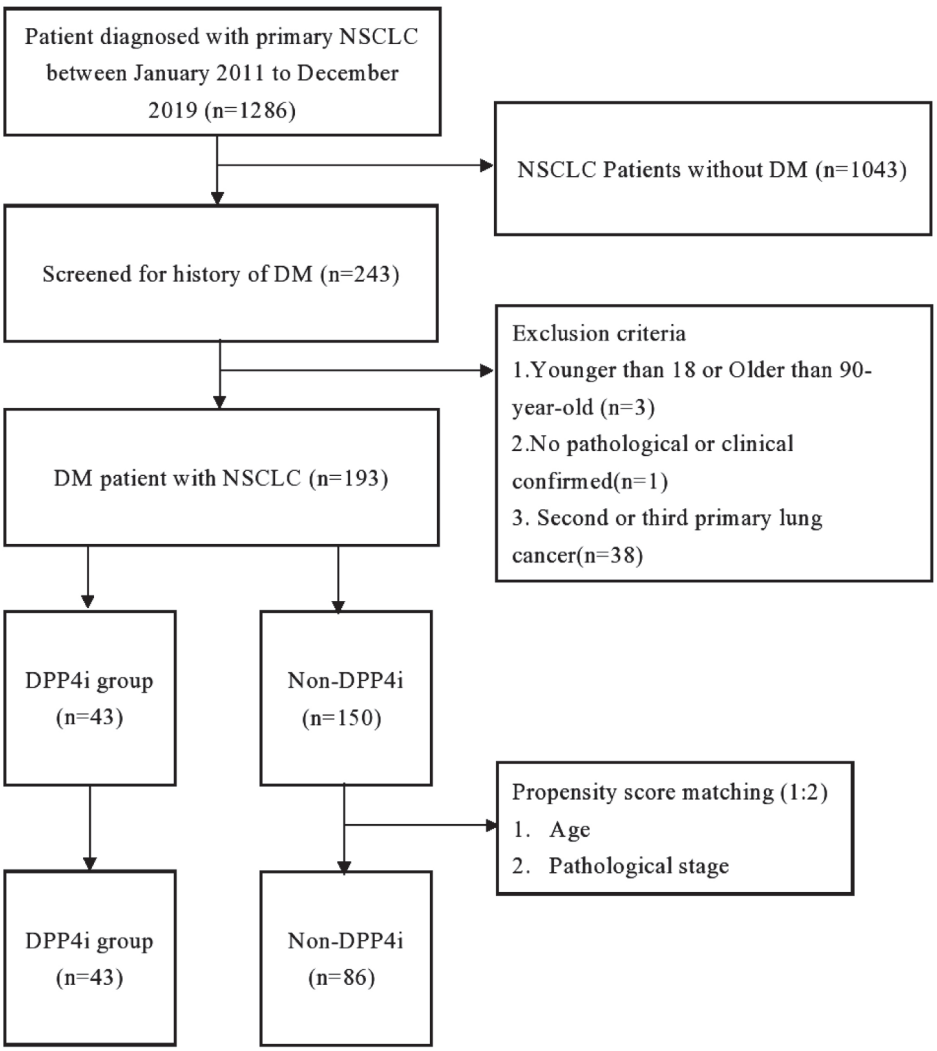

Fig. 1. Flow chart of study design and patient selection.

and there were more male than female patients in both groups.

Patients in the DPP4i group were significantly younger and more underweight than those in the non-DPP4i group. The 1:2 PSM analysis, using the abovementioned 2 variants, yielded matched pairs of 43 DM patients with lung cancer taking DPP4i and 86 DM patients with lung cancer not taking DPP4i. In the matching cohort, there was a significant difference only in BMI among inter-groups (*P*=0.003) (Table 1).

In the unmatched 5-year OS curve, the median OS was 786 days in the DPP4i group and 587 days in the non-DPP4i group. No significant difference in survival probability was observed between the 2 groups (HR = 1.25; *P* = 0.304; 95% Cl: 0.872-1.804; Figure 2).

Even after PSM, no significant difference in survival probability was observed in each group. In the matched 1-year, 2-year and 5-year OS groups, the HR of the non-DPP4i group compared with the DPP4i groups were 1.37 (*P* = 0.304; 95% CI 0.753-2.479; Figure 3A), 1.37

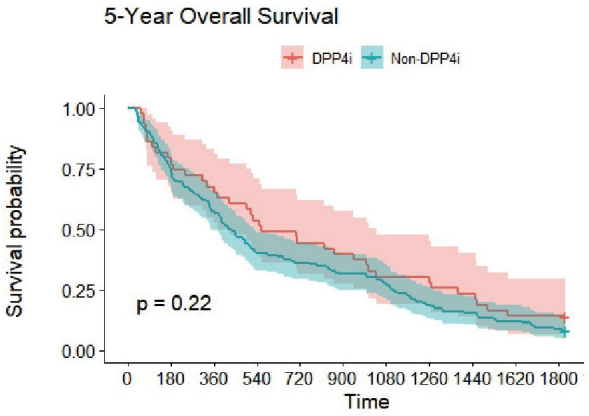

Fig. 2. 5-year Kaplan-Meier OS curve of the DPP4i (Red) and Non-DPP4i (Blue) groups before PSM.

(*P* = 0.2; 95% CI 0.848-2.207; Figure 3B) and 1.32 (*P* = 0.17; 95% Cl: 0.890-1.946; Figure 3C), respectively.

Univariate logistic regression analysis revealed the predictors of shortened OS to be smoking (odds ratio (OR),1.642; 95% CI, 1.138-2.389; *p*-value < 0.05), histological diagnosis (squamous cell carcinoma vs adenocarcinoma OR 1.654; 95% CI, 1.103-2.481; p-value < 0.05), late pathological stage (Stage III vs I OR 2.325; 95% CI, 1.321-4.092; *p*-value < 0.05;

Table 2. Prognostic Risk factors of 5 Year Overall Survival in Patients with Lung Cancer in the Matched data (n = 129).

	Univariate			Multivariable		
Varibles	**HR**	**95% CI**	***P*- value**	**HR**	**95% CI**	***P*- value**
Age (years)	1.012	0.993 -1.032	0.208			
BMI	0.968	0.927-1.011	0.142			
Gender						
Female	0.449	0.245-0.823	<0.05	0.465	0.275-0.788	<0.05
Preoperative BMI						
≥ 24(kg/m2)	0.730	0.419-1.271	0.266			
Smoke						
Yes	1.642	1.138-2.369	<0.05	1.421	0.404-1.225	0.214
Hypertension						
Yes	0.769	0.420-1.407	0.394			
SCC						
Yes	1.654	1.103-2.481	<0.05	1.742	0.404-1.225	0.06
TNM						
II	1.129	0.462-2.764	0.790	1.020	0.068-1.833	0.968
III	2.325	1.321-4.092	<0.05	1.106	0.079-0.887	0.792
IV	2.181	1.359-3.502	<0.05	1.456	0.116-1.469	0.300
Chemotherapy						
Yes	1.929	1.320-2.818	<0.05	1.589	0.981-2.572	0.06
Radiotherapy						
Yes	1.096	0.737-1.630	0.651			
Immunotherapy						
Yes	1.207	0.443-3.288	0.713			
Target therapy						
Yes	0.818	0.525-1.274	0.375			
Surgery						
Yes	0.458	0.269-0.782	<0.05	0.608	0.340-1.090	0.094
Metformin						
Yes	0.869	0.601-1.256	0.454			

* *SCC: Squamous cell carcinoma*

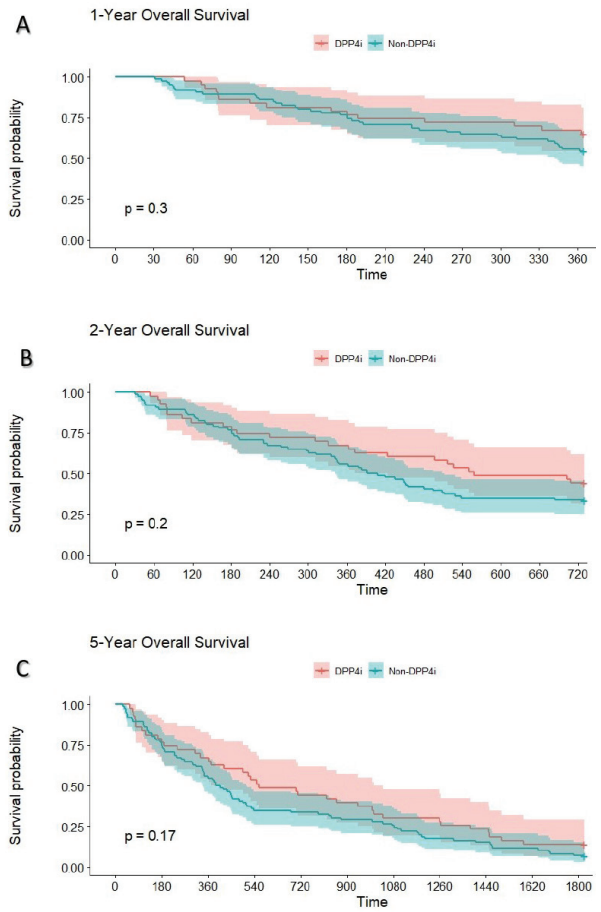

Fig. 3. (A) 1-year Kaplan-Meier OS curve of the DPP4i (Red) and Non-DPP4i (Blue) groups after PSM; (B) 2-year Kaplan-Meier OS curve of the DPP4i (Red) and Non-DPP4i (Blue) groups after PSM; (C) 5-year Kaplan-Meier OS curve of the DPP4i (Red) and Non-DPP4i (Blue) groups after PSM.

Stage IV vs I OR 2.181; 95% CI, 1.359-3.502; *p*-value < 0.05), and chemotherapy (OR,1.929; 95% CI, 1.320-2.818; *p*-value < 0.05). The predictors of better OS were sex (female vs male, OR 0.449; 95% CI, 0.245-0.823; *p*-value < 0.05) and surgery (OR 0.458; 95% CI, 0.245-0.823; *p*-value < 0.05) (Table 2). Multivariate logistic regression analysis that included all covariates revealed only that female sex yielded a longer OS. (OR 0.465; 95% CI, 0.275-0.788; *p*-value < 0.05) (Table 2).

Discussion

In our study, we compared OS between each group of DPP4i and non-DPP4i patients. No significant difference was found in OS between unmatched or PSM-matched intergroups. However, the HR of 1-year OS, 2-year OS, and 5-year OS (1.37; 1.37; 1.32, respectively) revealed a worse survival outcome in patients who did not take DPP4i. We also found that lung cancer patients that were female may have a benefit in 5-year OS. To the best of our knowledge, this is the first report on the survival benefit of DPP4i in lung cancer patients. In 2 recent studies, one of them using the Surveillance, Epidemiology, and End Results (SEER) database, usage of the DPP4 inhibitor was found to be associated with a significant improvement in OS among groups of colorectal and lung cancer patients, but there was no improvement in the group of lung cancer patients alone [18]. Another meta-analysis revealed that DPP4i seems to improve survival in prostate cancer patients, but not in breast cancer or pancreatic cancer patients [11]. Due to the complexity of chronic underlying diseases and that there are too many comorbidities, whether a combination of drugs, or the possible mechanism of DPP4i itself, would affect the OS of cancer patients, is still unclear.

For example, hypertension is another widespread chronic disease that has characteristics similar to those of DM, and it has also been demonstrated to have a positive association with the risk of several cancers, such as esophageal, liver, kidney, colorectal and breast cancer [19-20]. Antihypertensive and antihyperglycemic therapy are considered lifelong therapy, so the importance of the carcinogenic potential and the impact on cancer patient survival has

also been studied for a long time. Angiotensin I-converting enzyme inhibitors (ACEIs) and angiotensin II type-1 receptor blockers (ARBs) have been found to have benefit in progression-free survival, but there was no significant difference in OS in NSCLC patients [21]. A large propensity-matched cohort study revealed that usage of ACIEs/ARBs would improve median all-cause survival in lung cancer patients [22]. However, some studies did not find a survival benefit with ACEI/ARB use: a study conducted in Canada showed a weak association with increased deaths for breast cancer and lung cancer patients, but that calcium channel blockers (CCB) use was associated with improved survival in lung cancer patients [23].

The mechanisms of DDP4's anticancer activity have not been totally elucidated. The correlation between DDP4 and lung cancer was first described in 1993. Y. Asada, *et al*. found that CD26/DDP4 activity was positive in lung adenocarcinoma patients, rather than in squamous cell carcinoma or small cell carcinoma patients, so the expression was expected to be a biomarker to differ pathological subtypes of lung cancer [24]. Thus, there is a hypothesis that inhibition of CD26/DDP4 would suppress lung cancer growth. The inhibition of CD26/DPP4 using vildagliptin would increase the number of macrophages, NK cells and pro-inflammatory cytokine IL-12, and further, an in vivo mice study found that lung cancer growth via surfactant-activated macrophages and macrophage-mediated NK cell activity were suppressed [17, 25]. As mentioned above, DPP4 also has an important role in immune regulation. Ohnuma, *et al*. reported on the importance of DPP4 hydrolytic activity for T-cell immune reactions, which could up-regulate the co-stimulatory molecules on the antigen-presenting cells and further suppress tumor growth [26-27].

In our study, we found that OS was better in the DDP4i group, but without a significant difference. We believe that since DPP4i is designed to treat DM, not cancer, the drug dose and frequency would limit the drug's efficiency in suppressing tumor growth, especially when the cancer progresses from acquired resistance. Some in vivo studies revealed the possibility of a survival benefit when an adequate dose of DPP4i is injected [17, 25]. Having different comorbidities would also affect OS in lung cancer patients, but due to the small sample size, we could not match more subgroup covariates. Thus, above results in the study might lead to the conclusion that DPP4i did not significantly improve 5-year OS in cancer patients, including lung cancer patients, but neglect the potential survival benefit of DPP4i. In the future, further studies with a larger data base, such as Taiwan's National Health Insurance Research Database (NHIRD), should be conducted to prove the survival benefit of DPP4i in lung cancer patients.

Limitations

This study is retrospective in design, so selection bias is inevitable. Furthermore, due to the small sample size, subgroup analysis was difficult to perform, and we believe a larger sample size would help us confirm the benefit of taking DPP4i. Third, we could not trace the patient's drug compliance and change in OHA usage.

Conclusion

Dipeptidyl peptidase IV inhibitor (DPP4i) may have a benefit for OS in NSCLC patients

with the comorbidity of DM, though we did not find a significant difference due to the sample size. Among combined DM and lung cancer patients, female sex would be a better prognostic factor for OS.

Funding: self-prepared

Ethics approval and consent to participate: The study was approved by the Institutional Review Board (IRB) of the Taipei Medical University (Approval number: N202101042).

Availability of data and materials: The datasets used and analyzed in the current study are publicly accessible as indicated in the manuscript.

Conflicts of Interest: The authors declare that they have no potential financial competing interests that may in any way gain or lose financially from the publication of this manuscript at present or in the future. In addition, no non-financial competing interests were involved in the manuscript.

References

1. Larsson SC, Mantzoros CS, Wolk A. Diabetes mellitus and risk of breast cancer: a meta-analysis. Int J Cancer 2007; 121(4): 856-62.
2. Yi ZH, Luther Y, Xiong GH, *et al*. Association between diabetes mellitus and lung cancer: meta-analysis. Eur J Clin Invest 2020; 50(10): e13332.
3. Yuhara H, Steinmaus C, Cohen SE, *et al*. Is diabetes mellitus an independent risk factor for colon cancer and rectal cancer? Am J Gastroenterol 2011; 106(11): 1911.
4. Dicembrini I, Montereggi C, Nreu B, *et al*. Pancreatitis and pancreatic cancer in patientes treated with Dipeptidyl Peptidase-4 inhibitors: an extensive and updated meta-analysis of randomized controlled trials. Diabetes Res Clin Pract 2020; 159: 107981.
5. Colmers I, Bowker S, Johnson J. Thiazolidinedione use and cancer incidence in type 2 diabetes: a systematic review and meta-analysis. Diabetes Metab 2012; 38(6): 475-484.
6. Giovannucci E, Harlan DM, Archer MC, *et al*. Diabetes and cancer: a consensus report. Diabetes Care 2010; 33(7): 1674-1685.
7. Barone BB, Yeh HC, Snyder CF, *et al*. Long-term all-cause mortality in cancer patients with preexisting diabetes mellitus: a systematic review and meta-analysis. JAMA 2008; 300 (23): 2754-2764.
8. Tsai M-J, Yang C-J, Kung Y-T, *et al*. Metformin decreases lung cancer risk in diabetic patients in a dose-dependent manner. Lung Cancer 2014; 86(2):137-143.
9. Mikov M, Pavlovic N, Stanimirov B, *et al*. DPP-4 inhibitors: renoprotective potential and pharmacokinetics in type 2 diabetes mellitus patients with renal impairment. Eur J Drug Metab Pharmacokinet 2020; 45(1): 1-14.
10. Scott LJ. Sitagliptin: a review in type 2 diabetes. Drugs 2017; 77(2): 209-224.
11. Shah C, Hong YR, Bishnoi R, *et al*. Impact of DPP4 inhibitors in survival of patients with prostate, pancreas, and breast cancer. Front Oncol 2020; 10: 405.
12. Ng L, Foo DCC, Wong CKH, *et al*. Repurposing DPP-4 inhibitors for colorectal cancer: a retrospective and single center study. Cancers (Basel) 2021; 13(14): 3588.
13. Klemann C, Wagner L, Stephan M, *et al*. Cut to the chase: a review of CD26/dipeptidyl peptidase-4's (DPP4) entanglement in the immune system. Clin Exp Immunol 2016; 185(1): 1-21.
14. Shao S, Xu QQ, Yu X, *et al*. Dipeptidyl peptidase 4 inhibitors and their potential immune modulatory functions. Pharmacol Ther 2020; 209: 107503.
15. Thompson MA, Ohnuma K, Abe M, *et al*. CD26/dipeptidyl peptidase IV as a novel therapeutic target for cancer and immune disorders. Mini Rev Med Chem 2007; 7(3): 253-273.
16. Enz N, Vliegen G, De Meester I, *et al*. CD26/DPP4-a potential biomarker and target for cancer therapy. Pharmacol Ther 2019; 198: 135-159.
17. Jang JH, Janker F, Arni S, *et al*. MA04. 10 lung cancer growth is suppressed by CD26/DPP4-inhibition via enhanced NK cell and macrophage recruitment. J Thorac Oncol 2017; 12(1): S362-S363.
18. Bishnoi R, Hong YR, Shah C. *et al*. Dipeptidyl peptidase 4 inhibitors as novel agents in improving survival in

diabetic patients with colorectal cancer and lung cancer: a Surveillance Epidemiology and Endpoint Research Medicare study. Cancer Med 2019; 8(8): 3918-3927.

19. Seretis A, Cividini S, Markozannes G, *et al*. Association between blood pressure and risk of cancer development: a systematic review and meta-analysis of observational studies. Sci Rep 2019; 9(1):1-12.
20. Sanidas E, Velliou M, Papadopoulos D, *et al*. Antihypertensive drugs and risk of cancer: between scylla and charybdis. Am J Hypertens 2020; 33(12): 1049-1058.
21. Miao L, Chen W, Zhou L, *et al*. Impact of angiotensin I-converting enzyme inhibitors and angiotensin II type-1 receptor blockers on survival of patients with NSCLC. Sci Rep 2016; 6(1):1-7.
22. Mc Menamin UC, Murray LJ, Cantwell MM, *et al*. Angiotensin-converting enzyme inhibitors and angiotensin receptor blockers in cancer progression and survival: a systematic review. Cancer Causes Control 2012; 23(2): 221-230.
23. Holmes S, Grifith EJ, Musto G, *et al*. Antihypertensive medications and survival in patients with cancer: a population-based retrospective cohort study. Cancer Epidemiol 2013: 37(6): 881-885.
24. Asada Y, Aratake Y, Kotani T, *et al*. Expression of dipeptidyl aminopeptidase IV activity in human lung carcinoma. Histopathology 1993; 23(3): 265-270.
25. Jang JH, Janker F, De Meester I, *et al*. The CD26/DPP4-inhibitor vildagliptin suppresses lung cancer growth via macrophage-mediated NK cell activity. Carcinogenesis 2019: 40(2): 324-334.
26. Ohnuma K, Munakata Y, Ishii T, *et al*. Soluble CD26/dipeptidyl peptidase IV induces T cell proliferation through CD86 up-regulation on APCs. J Immunol 2001; 167(12): 6745-6755.
27. De S, Banerjee S, Ashok Kumar SK, *et al*. Critical role of dipeptidyl peptidase IV: a therapeutic target for diabetes and cancer. Mini Rev Med Chem 2019; 19(2): 88-97.

Lower Dose of First-Line Afatinib Treatment in Patients with EGFR Mutation-Positive Advanced Lung Adenocarcinoma: Real-World Data from a Tertiary Hospital in Taiwan

Wei-Cheng Hong[1], Min-Hsi Lin[1], Chiu-Fan Chen[1], Kuo-An Chu[1], Chun-Hsiang Hsu[1]

Introduction: Afatinib has favorable response rates and progression-free survival in lung cancer patients with epidermal growth factor receptor (EGFR) mutations. However, dose reduction is common due to severe side effects.

Methods: We enrolled patients with EGFR mutation-positive advanced lung adenocarcinoma from 1 January 2015 to 31 December 2019, and retrospectively analyzed the efficacy of low-dose (LD) and standard-dose (SD) afatinib treatment. Patients initially started with either 30 mg or 40 mg; those that used 40 mg daily as a final dose were included in the SD group, while those using less than 40 mg daily were in the LD group. The patients received first-line afatinib until the occurrence of disease progression, death, or intolerable adverse events. The primary outcome was time-on-treatment (ToT) and overall survival (OS).

Results: A total of 129 lung cancer patients were enrolled and received afatinib treatment. Of these, 82 (63.6%) were on LD afatinib, and 47 (36.4%) were on SD afatinib. Patients who received LD afatinib treatment tended to be older (48% vs. 28%), were more likely to be female (61% vs. 26%), and had a low BMI (26% vs. 6.4%). The median ToT was 17.9 months in the LD group and 12.7 months in the SD group (HR: 1.28; 95% confidence interval (CI): 0.86-1.91, p =0.218). Median OS was 29.5 months in the LD group and 24.6 months in the SD group (HR: 1.21; 95% CI: 0.79-1.85, p =0.372).

Conclusion: The ToT and OS of LD afatinib patients was similar to that of SD afatinib patients. ***(Thorac Med 2024; 39: 208-218)***

Key words: Lower-dose afatinib, lung adenocarcinoma, time-on-treatment, overall survival

Introduction

In treating EGFR-mutated non-small-cell lung cancer (NSCLC) patients, we observed that epidermal growth factor receptor (EGFR)-tyrosine kinase inhibitor (TKI) treatment was more beneficial than traditional chemotherapy in terms of reducing side effects and improving quality of life. However, determining its impact on overall survival (OS) is complicated, because many trials have allowed patients to switch treatments if their condition worsened.

[1]Division of Chest Medicine, Kaohsiung Veterans General Hospital, Kaohsiung, Taiwan
Address reprint requests to: Dr. Chun-Hsiang Hsu, Division of Chest Medicine, Kaohsiung Veterans General Hospital, No. 386 Dazhong First Rd., Zuoying Dist., Kaohsiung City 813414, Taiwan

For now, TKI as a stand-alone treatment is still favored as the standard of care [1]. Moreover, in a worldwide randomized phase IIb study, afatinib as a first-line treatment demonstrated a significant enhancement in progression-free survival (PFS), time until treatment failure, and overall response rate (ORR) compared to gefitinib for patients with EGFR mutation-positive NSCLC [2].

Prominent adverse drug reactions (ADRs) related to TKI treatment include diarrhea, rash/acne, stomatitis, and nail issues. Diarrhea tends to be more pronounced when afatinib is used, but these adverse events can be effectively managed through supportive care and, if necessary, dosage adjustments [3]. A meta-analysis revealed that among patients treated with first- and second-generation EGFR-TKIs, 40% encountered severe (grade 3-4) ADRs. Notably, the risk of grade 3-4 ADRs was lower with gefitinib (29.1%) than with erlotinib (54.1%) or afatinib (42.1%) [4].

The approved starting dose for afatinib is 40 mg/day. However, this dosage frequently resulted in severe ADRs, leading to dose reductions in up to 28% to 53.3% of patients in the LUX-Lung 3 and LUX-Lung 6 studies [5]. If grade ≥3 ADRs occur or specific grade 2 adverse events persist, the afatinib dose should be modified [6]. Several reports indicated that in patients with impaired kidney function (estimated glomerular filtration rate: 15-29 mL/min/1.73 m2), a lower dose of afatinib may be necessary [7-8].

This study aimed to determine if EGFR-mutated NSCLC patients who received lower final doses of afatinib experienced clinical effectiveness comparable to those receiving standard final doses.

Methods

Study population

This retrospective study used the data subset from the Cancer Registry Database provided by the Cancer Center of Kaohsiung Veterans General Hospital. The study was approved by the Institutional Review Board of Kaohsiung Veterans General Hospital (IRB number: 23-CT6-16), which waived the requirement of informed consent. All methods used in this study were performed in accordance with the directives of the Declaration of Helsinki.

We enrolled patients with EGFR mutation-positive advanced lung adenocarcinoma from 1 January 2015 to 31 December 2019, and analyzed the efficacy of first-line afatinib treatment retrospectively. We excluded patients with non-stage IV, those with non-EGFR-TKI therapy or receiving first-generation EGFR-TKI, and those with time-on-treatment (ToT) and OS less than 2 months. The patients received first-line afatinib until the occurrence of disease progression, death, or intolerable adverse events. Patients initially started with either 30 mg or 40 mg; those using 40 mg daily as a final dose were included in the SD group, and those using less than 40 mg daily were placed in the LD group. The initial dose was determined based on the preferences and experience of the physician, and then the final dose was adjusted based on the patient's tolerance.

The ToT and OS of first-line afatinib treatment were defined as the time from the start of the first treatment to the end of afatinib treatment, and the date of death, respectively.

Measurement

The primary outcome was ToT and OS. Clinical and demographic characteristics were

reviewed, including age, gender, smoking history, EGFR mutation subtype, tumor size, nodal status, BMI, Eastern Cooperative Oncology Group (ECOG) performance status, metastatic site and numbers, and comorbidities.

We also present the number of genetic tests for each group of patients and the number of patients receiving subsequent therapies, including third-generation TKIs (osimertinib or other generic medicine).

Statistical Analysis

Continuous variables with a non-normal distribution were expressed as median (range), and categorical variables were expressed as frequency (percentage [%]). The ANOVA method and Mann-Whitney test were used to compare continuous variables in different groups. The Chi-square test and Fisher's exact test were used to compare response rates in different subgroups. ToT and OS were calculated using the Kaplan-Meier method. Multivariate Cox regression analyses were applied to evaluate the effects of clinical factors on the prognosis of lung cancer patients who received TKI treatment. All statistical analyses were performed using SPSS Statistics version 28.0 software. Statistical significance was assumed at $p < 0.05$.

Results

1. Baseline characteristics of patients

A total of 129 lung cancer patients were enrolled and received afatinib treatment. Of these, 82 (63.6%) were on LD afatinib, 47 (36.4%) on SD afatinib.

The flow chart of case collection is shown in Figure 1, and clinical baseline characteristics are shown in Table 1. Only 3 patients had their dosage increased due to good tolerance; the

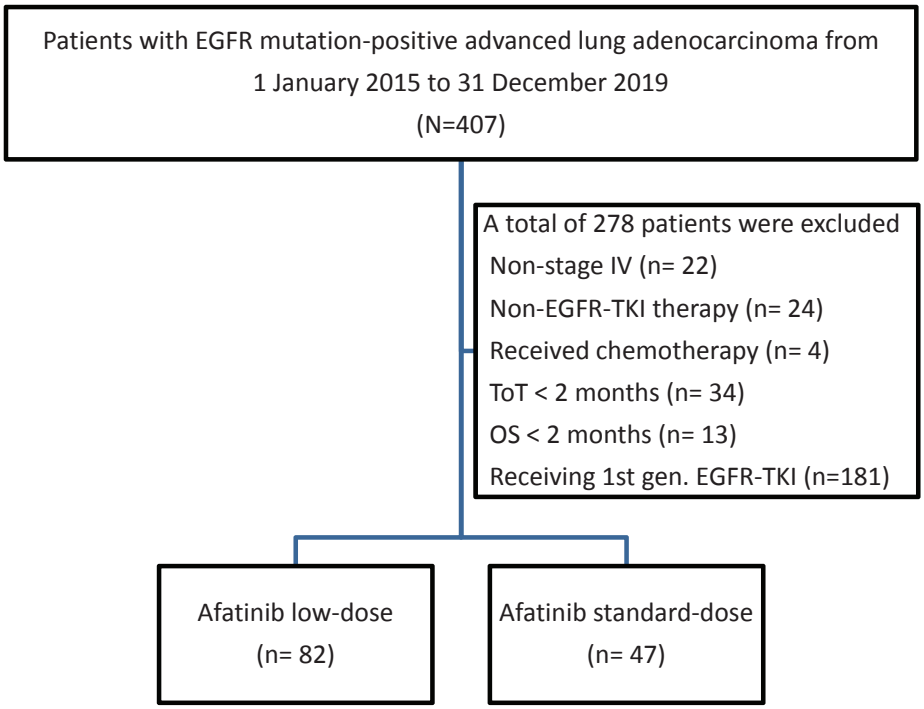

Fig. 1. Flow Chart of Case Collection.

Table 1. Comparison of Characteristics Between Patients Receiving LD Afatinib and Those Receiving SD Afatinib

Characteristic	Overall N = 129[1]	Afatinib LD N = 82[1]	Afatinib SD N = 47[1]	*p*-value[2]
Starting dose				
< 40 mg/day	54 (42%)	51 (62%)	3 (6%)	
40 mg/day	75 (58%)	31 (38%)	44 (94%)	
Gender				**<0.001**
Female	62 (48%)	50 (61%)	12 (26%)	
Male	67 (52%)	32 (39%)	35 (74%)	
Age group				**0.027**
< 65	77 (60%)	43 (52%)	34 (72%)	
≥ 65	52 (40%)	39 (48%)	13 (28%)	
Smoking status[a]				0.2
Current	9 (7.0%)	5 (6.1%)	4 (8.5%)	
Former	32 (25%)	17 (21%)	15 (32%)	
Never	88 (68%)	60 (73%)	28 (60%)	
EGFR mutation				0.8
Exon 19 deletion	61 (47%)	37 (45%)	24 (51%)	
Exon 21 L858R	58 (45%)	38 (46%)	20 (43%)	
Others	10 (7.8%)	7 (8.5%)	3 (6.4%)	
Tumor size				0.3
< 3 cm	35 (27%)	25 (30%)	10 (21%)	
≥ 3 cm	94 (73%)	57 (70%)	37 (79%)	
Nodal status				0.2
N0	21 (16%)	16 (20%)	5 (11%)	
N1/N2/N3	108 (84%)	66 (80%)	42 (89%)	
BMI group				**0.026**
< 18.5	24 (19%)	21 (26%)	3 (6.4%)	
18.5-23.9	63 (49%)	37 (45%)	26 (55%)	
≥ 24	42 (33%)	24 (29%)	18 (38%)	
ECOG group				0.7
0-1	108 (84%)	68 (83%)	40 (85%)	
2-4	21 (16%)	14 (17%)	7 (15%)	
Brain metastasis	22 (17%)	10 (12%)	12 (26%)	0.053
Bone metastasis	66 (51%)	43 (52%)	23 (49%)	0.7
Liver metastasis	17 (13%)	10 (12%)	7 (15%)	0.7
Adrenal metastasis	5 (3.9%)	3 (3.7%)	2 (4.3%)	>0.9
Lung metastasis	52 (40%)	35 (43%)	17 (36%)	0.5
Pleural metastasis	58 (45%)	42 (51%)	16 (34%)	0.059
Metastasis ≥ sites	30 (23%)	20 (24%)	10 (21%)	0.7

[1] n (%)

[2] Pearson's Chi-squared test; Fisher's exact test

[a]"Former" smokers indicates patients who had quit smoking for more than 1 year.

majority of the other patients either maintained their initial dosage or reduced it. Patients who received LD afatinib treatment tended to be older (48% vs. 28%), were more likely to be female (61% vs. 26%), and had a low BMI (26% vs. 6.4%). There were no significant differences in smoking status, EGFR gene mutation (exon 19 or 21), tumor size, nodal status, performance status, or metastatic sites or numbers, between the 2 groups.

The median ToT was 17.9 months in the LD group, and 12.7 months in the SD group (hazard ratio (HR): 1.28; 95% confidence interval (CI): 0.86-1.91, $p = 0.218$). The median OS was 29.5 months in the LD group, and 24.6 months in the SD group (HR: 1.21; 95% CI: 0.79-1.85, $p = 0.372$) (Figure 2).

(A) Time on Treatment (months) among afatinib patients according to the final dose recieved

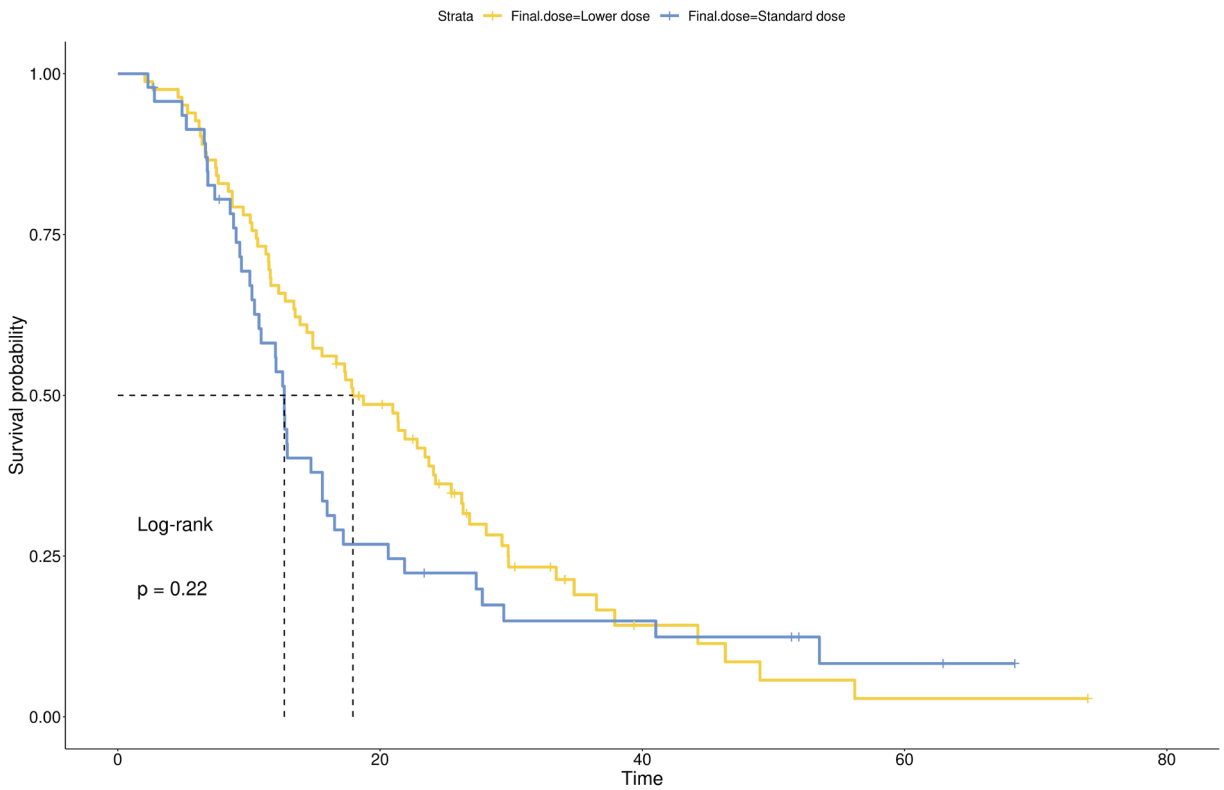

Time on Treatment (months) among afatinib patients according to the final dose recieved

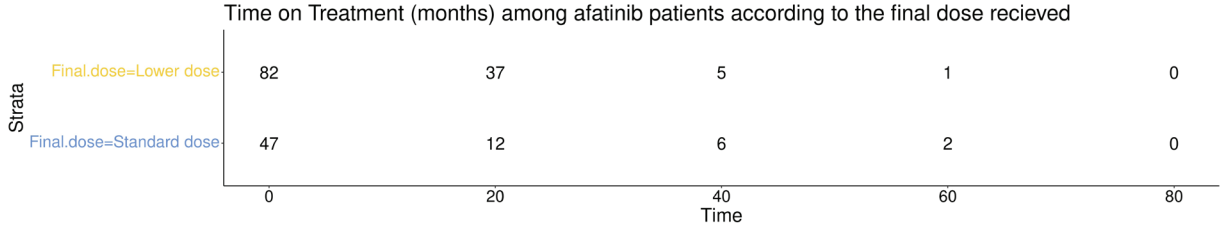

	records	events	median	Lower.CI	Upper.CI	HazardRatio	CI.95	p-value
Final.dose=Lower dose	82	67	17.9	14.9	24.2	Ref		
Final.dose=Standard dose	47	40	12.7	10.4	16.0	1.28	[0.86;1.91]	0.218

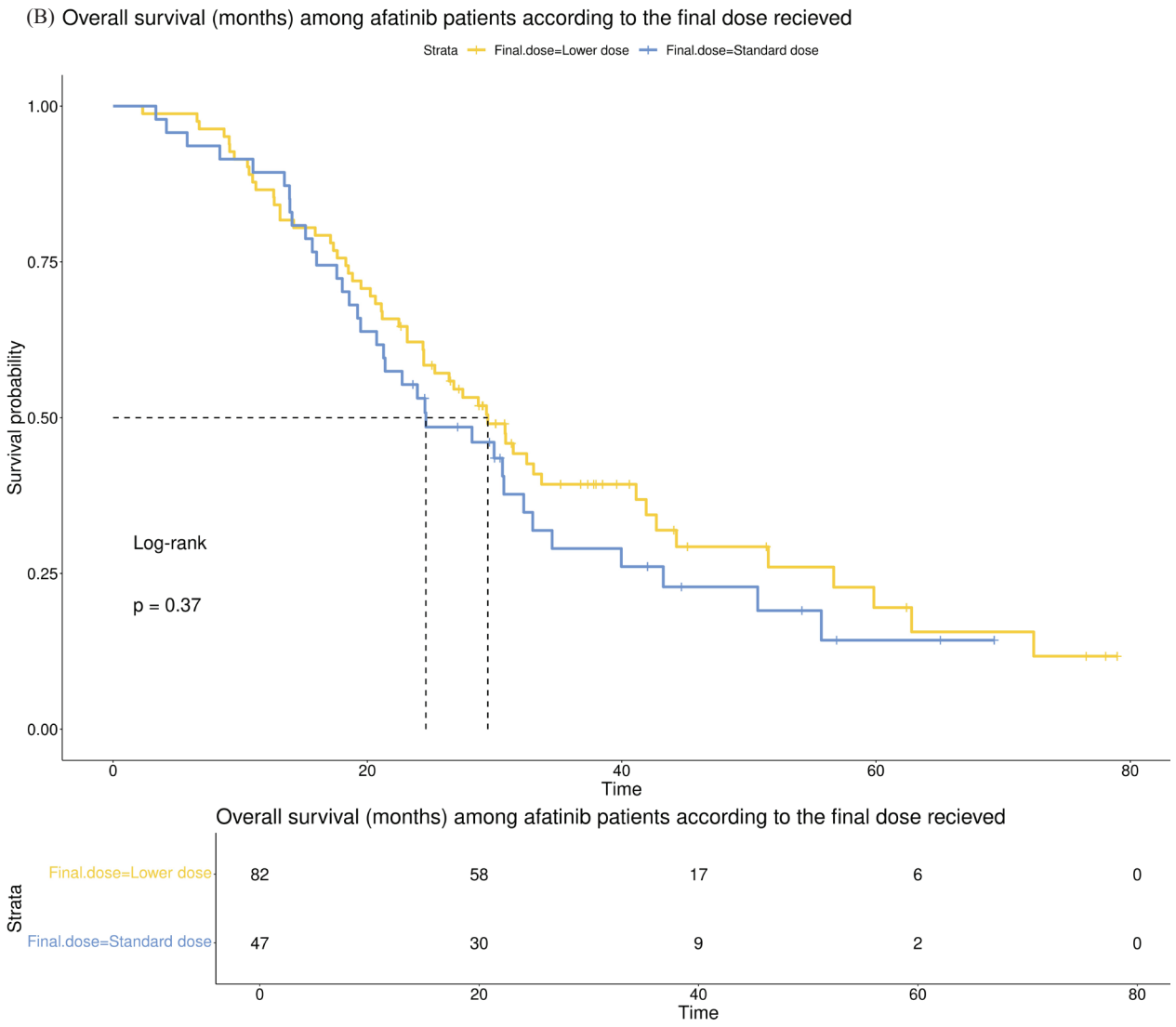

	records	events	median	Lower.CI	Upper.CI	HazardRatio	CI.95	p-value
Final.dose=Lower dose	82	56	29.5	24.4	41.9	Ref		
Final.dose=Standard dose	47	35	24.6	20.7	34.5	1.21	[0.79;1.85]	0.372

Fig. 2. ToT and OS for afatinib treatment. (A). ToT in patients receiving different final doses of afatinib. (B). OS for patients receiving different final doses of afatinib.

2. **Predictors of time-on-treatment and overall survival**

To identify factors associated with ToT and OS, we built several Cox regression models. Patients with higher BMI (BMI ≧ 24) tended to have a better ToT (HR: 0.33; 95%; CI: 0.18-0.62, p < 0.001) and OS (HR: 0.37; 95% CI: 0.19-0.70, p= 0.003), according to a Cox model adjusted for possible confounders. Patients with initial liver metastasis had a shorter ToT (HR: 2.51; 95% CI: 1.23-5.12, p=0.011), and patients with initial brain metastasis had a shorter OS (HR: 2.59; 95% CI: 1.16-5.81, p = 0.021) than those without initial brain metastasis (Table 2).

Table 2. Risk Factor Analyses of ToT and OS in Patients with Stage IV NSCLC Harboring EGFR-Activating Mutations

Factor[a]	Adjusted HR[1]	95% CI[1]	*p*-value
Multivariate analysis of ToT			
Standard afatinib dose (ref = low dose)	1.19	0.72, 1.96	0.50
Female (ref = male)	0.68	0.39, 1.19	0.18
Age ≥ 65 years (ref = < 65 years)	0.75	0.48, 1.18	0.22
BMI group			
< 18.5	—	—	
18.5-23.9	0.61	0.35, 1.08	0.090
> 24	0.33	0.18, 0.62	**<0.001**
Tumor size ≥ 3 cm (ref = < 3 cm)	1.18	0.73, 1.90	0.49
Nodal status N1/N2/N3 (ref = N0)	1.80	0.98, 3.30	0.059
EGFR mutation			
Exon 19 del	—	—	
Exon 21 L858R	1.42	0.89, 2.26	0.15
Others	1.71	0.71, 4.09	0.23
Current or ever-smoker[b] (ref = never)	1.02	0.60, 1.71	0.95
ECOG PS 2-4 (ref = 0-1)	1.42	0.77, 2.59	0.26
Brain metastasis	1.50	0.70, 3.24	0.30
Liver metastasis	2.51	1.23, 5.12	**0.011**
Bone metastasis	1.15	0.69, 1.92	0.58
Lung metastasis	0.96	0.58, 1.62	0.89
Pleural metastasis	1.57	0.90, 2.74	0.11
Metastasis ≥ 3 sites	0.96	0.46, 2.01	0.92
Multivariate analysis for OS			
Standard afatinib dose (ref = low dose)	0.96	0.55, 1.66	0.87
Female (ref = male)	0.44	0.24, 0.82	**0.010**
Age ≥ 65 years (ref = < 65 years)	0.81	0.48, 1.36	0.42
BMI group			
< 18.5	—	—	
18.5-23.9	0.53	0.29, 0.97	**0.041**
> 24	0.37	0.19, 0.70	**0.003**
Tumor size ≥ 3 cm (ref = < 3 cm)	0.87	0.52, 1.45	0.60
Nodal status N1/N2/N3 (ref = N0)	3.50	1.57, 7.80	**0.002**
EGFR mutation			
Exon 19 del	—	—	
Exon 21 L858R	1.64	0.97, 2.77	0.067
Others	2.93	1.15, 7.43	**0.024**
Current or ever-smoker[b] (ref = never)	0.81	0.46, 1.44	0.48
ECOG PS 2-4 (ref = 0-1)	1.06	0.56, 2.01	0.85
Brain metastasis	2.59	1.16, 5.81	**0.021**
Liver metastasis	2.10	0.92, 4.84	0.080
Bone metastasis	1.70	0.97, 2.97	0.062
Lung metastasis	1.09	0.62, 1.93	0.77

Pleural metastasis	1.72	0.92, 3.20	0.088
Metastasis ≥ 3 sites	0.55	0.24, 1.25	0.15

[1] HR = hazard ratio, CI = confidence interval

[a]Multivariate model adjusted for gender, age, BMI, tumor size, nodal staging, smoking status, differentiation.

[b]"Former" smokers indicates patients who had quit smoking for more than 1 year.

The number of genetic tests for each group of patients and the number of patients receiving subsequent therapies, including third-generation TKIs (osimertinib or other generic medicine) are presented in Table 3.

Table 3. Subsequent Therapies

Subsequent therapy	**Afatinib LD** N = 82	**Afatinib SD** N = 47
Re-biopsy for EGFR testing		
Liquid	12	6
Tissue	16	5
Liquid and tissue	1	1
T790M rate (T790M detected/tested)	11/30	5/12
Number of patients		
Number of regimens		
1	39	16
2	15	14
3	12	8
4	10	3
≥ 5	6	6
First subsequent therapy		
Received a first subsequent therapy	43	31
Cytotoxic chemotherapy	24	21
Osimertinib (T790M detected)	7	5
Osimertinib (T790M not detected)	3	1
Osimertinib (unknown)	9	3
Other EGFR-TKI	0	1
Immunotherapy	1	0
VEGF inhibitor	3	0
Second subsequent therapy		
Received a second subsequent therapy	28	17
Cytotoxic chemotherapy	18	11
Osimertinib (T790M detected)	1	0
Osimertinib (T790M not detected)	2	0
Osimertinib (unknown)	1	1
Other EGFR-TKI	6	5
Immunotherapy	0	1
VEGF inhibitor	0	0

Discussion

Our study showed that patients who were administered a daily dose of less than 40 mg of afatinib as their final dosing had ToT and OS outcomes that were comparable to those patients who received 40 mg daily. Also, patients treated with a daily dose of less than 40 mg of afatinib were more likely to be older, female, and have a lower BMI than those who began with 40 mg daily. These findings align with those of previous research [9, 10].

For patients with EGFR mutation-positive lung adenocarcinoma who received an initial dose of 40 mg afatinib, the median PFS was 11.1 months in the LUX-Lung 3 and 11.0 months in the LUX-Lung 6 trials [11, 12].

In a phase 2 study, 30 patients initially received afatinib at 40 mg orally daily, with dose reductions to 30 mg or 20 mg based on tolerability. The median PFS was 11.8 months and the incidence rate of grade ≥ 3 toxicities was 57%, which indicated a reduction in treatment-related adverse effects without compromising therapeutic effectiveness [13]. In another phase 2 study in which patients were initially given a lower daily dose of 20 mg afatinib, with subsequent increments of 10 mg up to a maximum of 50 mg daily, the reported PFS was 15.2 months [14].

Subgroup analyses of elderly patients in the LUX-Lung 3, LUX-Lung 6, and LUX-Lung 7 trials confirmed that afatinib is an effective and well-tolerated treatment for EGFR-mutated NSCLC patients, regardless of age [15]. One phase 2 study that included 40 elderly patients reported a shorter PFS of 12.9 months [16]. In another phase 2 study of first-line afatinib for 38 patients aged ≥ 75 years with EGFR mutation-positive advanced NSCLC, median PFS was 14.2 months (95% CI: 9.5-19.0) [17].

In a retrospective analysis involving 630 patients with metastatic EGFR-mutant NSCLC who were treated with either gefitinib or erlotinib, individuals with a higher BMI (≥ 25 kg/m^2) exhibited better PFS and OS than those with a lower BMI (< 18.5 kg/m2) [18]. For patients with advanced-stage NSCLC, regardless of their EGFR mutation status, lower BMI was associated with inferior outcomes [19-20].

The phase 3 LUX-Lung 3 and LUX-Lung 6 trials documented median OS durations of 31.4 and 33.3 months, respectively [5]. A real-world study conducted in Japan, where afatinib was used as first-line treatment, revealed a median OS of 39.5 months [21]. Another real-world study in Taiwan showed that the OS of the 30 mg and 40 mg groups, with durations of 34.0 and 25.2 months, respectively, was comparable [10].

Prior clinical trials suggested that a daily starting dose of 40 mg of afatinib was recommended for patients with EGFR mutation-positive lung cancer. Patients who had their dosage reduced to 30 mg exhibited geometric mean afatinib plasma concentrations of 23.3 ng/ml, similar to the concentrations of 22.8 ng/ml in those who continued with a 40 mg dosage [5]. One recent pharmacokinetic and pharmacogenomic analysis of LD afatinib treatment in elderly patients showed that Css (steady-state concentration) was consistent with findings from prior studies, and notably elevated in patients experiencing grade 3 adverse events [22].

There are several reasons why the clinical outcomes of SD and LD are similar. First, although the LD group had a higher proportion of elderly patients and those with a low BMI, which may lead to a poorer prognosis [23], there was also a higher proportion of females,

and female lung cancer patients typically have a better prognosis [24-25]. Second, if the dosage was adjusted due to intolerability, the serum concentration would not differ significantly [5]. Third, the side effects resulting from the reduced dosage were also fewer, which in turn reduces the likelihood of discontinuing treatment [11-12].

This study has several limitations. First, it was a single-center retrospective study, and there were significant differences in the characteristics of the 2 groups that might make the results less reliable than other standard prospective clinical trials. Second, the number of cases enrolled in the study was relatively low for a retrospective study. Third, we did not assess the renal function of the patients in this study. In elderly patients, impaired kidney function can potentially impact drug metabolism. Finally, up to 38% of patients who initially started with a 40 mg/day dosage would eventually reduce their dosage. However, only 6% of patients who initially started with a dosage lower than 40 mg/day would increase their dosage in the end. It is unclear whether the decision to not increase the dosage for the remaining 94% was due to physician choice or the patients' drug tolerance.

In conclusion, a lower dose of afatinib at a daily dose of less than 40 mg may represent an effective and well-tolerated treatment choice. A further large-scale prospective trial is urgently needed to confirm these findings.

References

1. Greenhalgh J, Boland A, Bates V, *et al*. First-line treatment of advanced epidermal growth factor receptor (EGFR) mutation positive non-squamous non-small cell lung cancer. Cochrane Database Syst Rev 2021 Mar 18; 3(3): CD010383.
2. Park K, Tan EH, O'Byrne K, *et al*. Afatinib versus gefitinib as first-line treatment of patients with EGFR mutation-positive non-small-cell lung cancer (LUX-Lung 7): a phase 2B, open-label, randomised controlled trial. Lancet Oncol 2016 May; 17(5): 577-89.
3. Califano R, Tariq N, Compton S, *et al*. Expert consensus on the management of adverse events from EGFR tyrosine kinase inhibitors in the UK. Drugs 2015 Aug; 75(12): 1335-48.
4. Ding PN, Lord SJ, Gebski V, *et al*. Risk of treatment-related toxicities from EGFR tyrosine kinase inhibitors: a meta-analysis of clinical trials of gefitinib, erlotinib, and afatinib in advanced EGFR-mutated non-small cell lung cancer. J Thorac Oncol 2017 Apr; 12(4): 633-43.
5. Yang JC, Sequist LV, Zhou C, *et al*. Effect of dose adjustment on the safety and efficacy of afatinib for EGFR mutation-positive lung adenocarcinoma: post hoc analyses of the randomized LUX-Lung 3 and 6 trials. Ann Oncol 2016 Nov; 27(11): 2103-10.
6. Boehringer Ingelheim website. Available at: https://pro.boehringer-ingelheim.com/products/giotrif/
7. US Food and Drug Administration. Label. Available from:https://www.accessdata.fda.gov/drugsatfda_docs/label/2019/201292s015lbl.pdf
8. Wiebe S, Schnell D, Külzer R, *et al*. Influence of renal impairment on the pharmacokinetics of afatinib: an open-label, single-dose study. Eur J Drug Metab Pharmacokinet 2017 Jun; 42(3): 461-69.
9. Yang CJ, Tsai MJ, Hung JY, *et al*. The clinical efficacy of afatinib 30 mg daily as starting dose may not be inferior to afatinib 40 mg daily in patients with stage IV lung adenocarcinoma harboring exon 19 or exon 21 mutations. BMC Pharmacol Toxicol 2017 Dec 13; 18(1): 82.
10. Chen YC, Tsai MJ, Lee MH, *et al*. Lower starting dose of afatinib for the treatment of metastatic lung adenocarcinoma harboring exon 21 and exon 19 mutations. BMC Cancer 2021 May 3; 21(1): 495.
11. Sequist LV, Yang JC, Yamamoto N, *et al*. Phase III study of afatinib or cisplatin plus pemetrexed in patients with metastatic lung adenocarcinoma with EGFR mutations. J Clin Oncol 2013 Sep 20; 31(27): 3327-34.
12. Wu YL, Zhou C, Hu CP, *et al*. Afatinib versus cisplatin plus gemcitabine for first-line treatment of Asian patients with advanced non-small-cell lung cancer harbouring

EGFR mutations (LUX-Lung 6): an open-label, randomised phase 3 trial. Lancet Oncol 2014 Feb; 15(2): 213-22.

13. Nakamura A, Tanaka H, Saito R, *et al*. Phase II study of low-dose afatinib maintenance treatment among patients with EGFR-mutated non-small cell lung cancer: North Japan Lung Cancer Study Group Trial 1601 (NJLCG1601). Oncologist 2020 Oct; 25(10): e1451-56.
14. Yokoyama T, Yoshioka H, Fujimoto D, *et al*; Kyoto Thoracic Oncology Research Group (KTORG). A phase II study of low starting dose of afatinib as first-line treatment in patients with EGFR mutation-positive non-small-cell lung cancer (KTORG1402). Lung Cancer 2019 Sep; 135: 175-180.
15. Wu YL, Sequist LV, Tan EH, *et al*. Afatinib as first-line treatment of older patients with EGFR mutation-positive non-small-cell lung cancer: subgroup analyses of the LUX-Lung 3, LUX-Lung 6, and LUX-Lung 7 trials. Clin Lung Cancer 2018 Jul; 19(4): e465-79.
16. Imai H, Kaira K, Suzuki K, *et al*. A phase II study of afatinib treatment for elderly patients with previously untreated advanced non-small-cell lung cancer harboring EGFR mutations. Lung Cancer 2018 Dec; 126: 41-47.
17. Minegishi Y, Yamaguchi O, Sugawara S, *et al*. A phase II study of first-line afatinib for patients aged ≥75 years with EGFR mutation-positive advanced non-small cell lung cancer: North East Japan Study Group trial NEJ027. BMC Cancer 2021 Mar 1; 21(1): 208.
18. Park S, Park S, Lee SH, *et al*. Nutritional status in the era of target therapy: poor nutrition is a prognostic factor in non-small cell lung cancer with activating epidermal growth factor receptor mutations. Korean J Intern Med 2016 Nov; 31(6): 1140-49.
19. Minami S, Ihara S, Nishimatsu K, *et al*. Low body mass index is an independent prognostic factor in patients with non-small cell lung cancer treated with epidermal growth factor receptor tyrosine kinase inhibitor. World J Oncol 2019 Dec; 10(6): 187-98.
20. Chen YM, Lai CH, Lin CY, *et al*. Body mass index, weight loss, and mortality risk in advanced-stage non-small cell lung cancer patients: a focus on EGFR mutation. Nutrients 2021 Oct 24; 13(11): 3761.
21. Tanaka H, Taima K, Itoga M, *et al*. Real-world study of afatinib in first-line or re-challenge settings for patients with EGFR mutant non-small cell lung cancer. Med Oncol 2019 May 14; 36(6): 57.
22. Mizugaki H, Oizumi S, Fujita Y, *et al*. Pharmacokinetic and pharmacogenomic analysis of low-dose afatinib treatment in elderly patients with EGFR mutation-positive non-small cell lung cancer. Eur J Cancer 2022 Jan; 160: 227-34.
23. Tas F, Ciftci R, Kilic L, *et al*. Age is a prognostic factor affecting survival in lung cancer patients. Oncol Lett 2013 Nov; 6(5): 1507-13.
24. Nakamura H, Ando K, Shinmyo T, *et al*. Female gender is an independent prognostic factor in non-small-cell lung cancer: a meta-analysis. Ann Thorac Cardiovasc Surg 2011; 17(5): 469-80.
25. Thomas L, Doyle LA, Edelman MJ. Lung cancer in women: emerging differences in epidemiology, biology, and therapy. Chest 2005 Jul; 128(1): 370-81.

Successful Treatment with Entrectinib after Crizotinib-Induced Hepatitis in a ROS1-Positive Advanced Lung Cancer Patient: A Case Report

You-Cyuan Liang[1], Shian-Chin Ko[2]

Lung cancer, a commonly occurring cancer, is responsible for the highest number of deaths in Taiwan, regardless of gender. Targeted therapy is more effective than chemotherapy in treating advanced pulmonary adenocarcinoma harboring mutant driver genes. Crizotinib is an oral small-molecule tyrosine kinase inhibitor that targets anaplastic lymphoma kinase, mesenchymal-epithelial transition factor, and c-Ros oncogene 1 receptor (ROS1) tyrosine kinase. The most common adverse effects with crizotinib use are visual disorders, gastrointestinal upset and dysgeusia. However, impaired liver function and elevated aminotransferase levels are not rare. We presented the case of a 73-year-old male who was diagnosed with ROS1-positive metastatic lung adenocarcinoma under crizotinib treatment, who suffered from poor appetite, gastric pain and fullness. Elevated serum aminotransferase and bilirubin levels were found. After excluding other causes of hepatitis, the diagnosis of crizotinib-induced liver toxicity was made. The offending drug was withdrawn and oral silymarin and intravenous glycyrrhizin were given. His liver function recovered after 6 weeks, and another targeting ROS1 drug, entrectinib, was prescribed uneventfully. Due to the potential for elevated aminotransferase levels and the development of hepatitis during crizotinib treatment, we recommend close monitoring of liver function while using crizotinib. ***(Thorac Med 2024; 39: 219-227)***

Key words: entrectinib, crizotinib, hepatitis, ROS1, lung cancer.

Introduction

Crizotinib is a tyrosine kinase inhibitor (TKI) that targets the anaplastic lymphoma kinase (ALK) fusion oncogene, ROS proto-oncogene 1 receptor tyrosine kinase (ROS1), and others. It is approved for patients with a variety of malignancies, and is mainly focused on certain ALK- or ROS1-positive cancers. At present, the Food and Drug Administration (FDA) of the United States has approved crizotinib for patients with metastatic non-small cell lung

[1]Division of Chest Medicine, Department of Internal Medicine, Chi Mei Medical Center, Tainan, Taiwan; [2]Palliative and Hospice Care Center, Chi Mei Medical Center, Tainan, Taiwan
Address reprint requests to: Dr. Shian-Chin Ko, No.901, Zhonghua Rd. Yongkang Dist., Tainan City 71004, Taiwan (R.O.C.)

cancer (NSCLC) whose tumors are ALK- or ROS1-positive, ALK-positive anaplastic large cell lymphoma or an ALK-positive inflammatory myofibroblastic tumor in pediatric patients [3]. In Taiwan, crizotinib was approved for treatment of ALK- or ROS1-positive advanced NSCLC [4].

Crizotinib has been shown to be superior to standard chemotherapy for both first-line and subsequent treatment in patients with advanced NSCLC with ALK rearrangement [5-6]. First-line crizotinib had a higher response rate and longer progression-free survival (PFS) than platinum-pemetrexed chemotherapy in patients with advanced ROS1+ NSCLC [7]. However, the use of crizotinib can be associated with side effects. Elevated serum aminotransferase is not rare with the use of crizotinib, but hepatotoxicity above grade 3 is uncommon [5].

ROS1 rearrangement is found in only 0.9-2.6% of NSCLCs, mostly in lung adenocarcinomas [8]. Since 2016, crizotinib has been the first-line reference therapy, with two-thirds of patients' tumors responding and PFS lasting about 20 months [8]. Crizotinib-induced hepatitis is rarely reported among patients with ROS1-positive lung adenocarcinoma [9]. We herein report a case of ROS1-positive metastatic lung adenocarcinoma that was treated with crizotinib. Hepatitis symptoms with elevated serum aminotransferase and bilirubin levels developed after 3 weeks of crizotinib therapy. Crizotinib-induced hepatitis was favored after excluding other etiologies, so it was discontinued immediately, and silymarin and glycyrrhizin were given. The patient's hepatitis improved after discontinuation of the offending agent for 6 weeks. Crizotinib was then replaced with entrectinib for further treatment.

Case Presentation

A 73-year-old male was incidentally found to have a right lung nodule on chest radiography during management of urinary bladder stones in February 2014. Chest computed tomography (CT) scan showed a pulmonary nodule, 3.6 cm x 2.4 cm in size, with an irregular margin and adjacent minor fissure retraction in the right middle lobe (RML) (Fig. 1A). However, CT-guided biopsy reported only chronic inflammation. Because of the chronic inflammation in the biopsy report, the patient agreed to outpatient follow-up and received antibiotic treatment. However, the lung lesions continued to grow during the outpatient follow-up process. Increased serum carcinoembryonic antigen level (6.8 ng/mL) was also found. Follow-up chest CT in July 2015 revealed a progressive RML spiculated mass, 5.1 x 4.1 cm in size (Fig. 1B). On July 27, 2015, video-assisted thoracoscopic surgery (VATS) was performed for right middle lobectomy and lymph node dissection. The pathology report revealed lung adenocarcinoma, with a tumor stage of pT2bN2M0, classified as stage IIIA according to the 7th edition of the American Joint Committee on Cancer (AJCC) staging system. Later, he was referred to the chest medicine outpatient clinic for subsequent systemic therapy, in accordance with the National Comprehensive Cancer Network (NCCN) guidelines. No mutations in the epidermal growth factor receptor (EGFR) were detected. Four cycles of adjuvant chemotherapy with vinorelbine and cisplatin were then given.

Two years later, follow-up chest CT scan in September 2017 revealed a new subsolid nodule, 6 mm in size, at the left upper lobe (LUL) of the lung (Fig. 1C). Multiple lung nodules grew slowly over 4 months (Fig. 1D). CT-

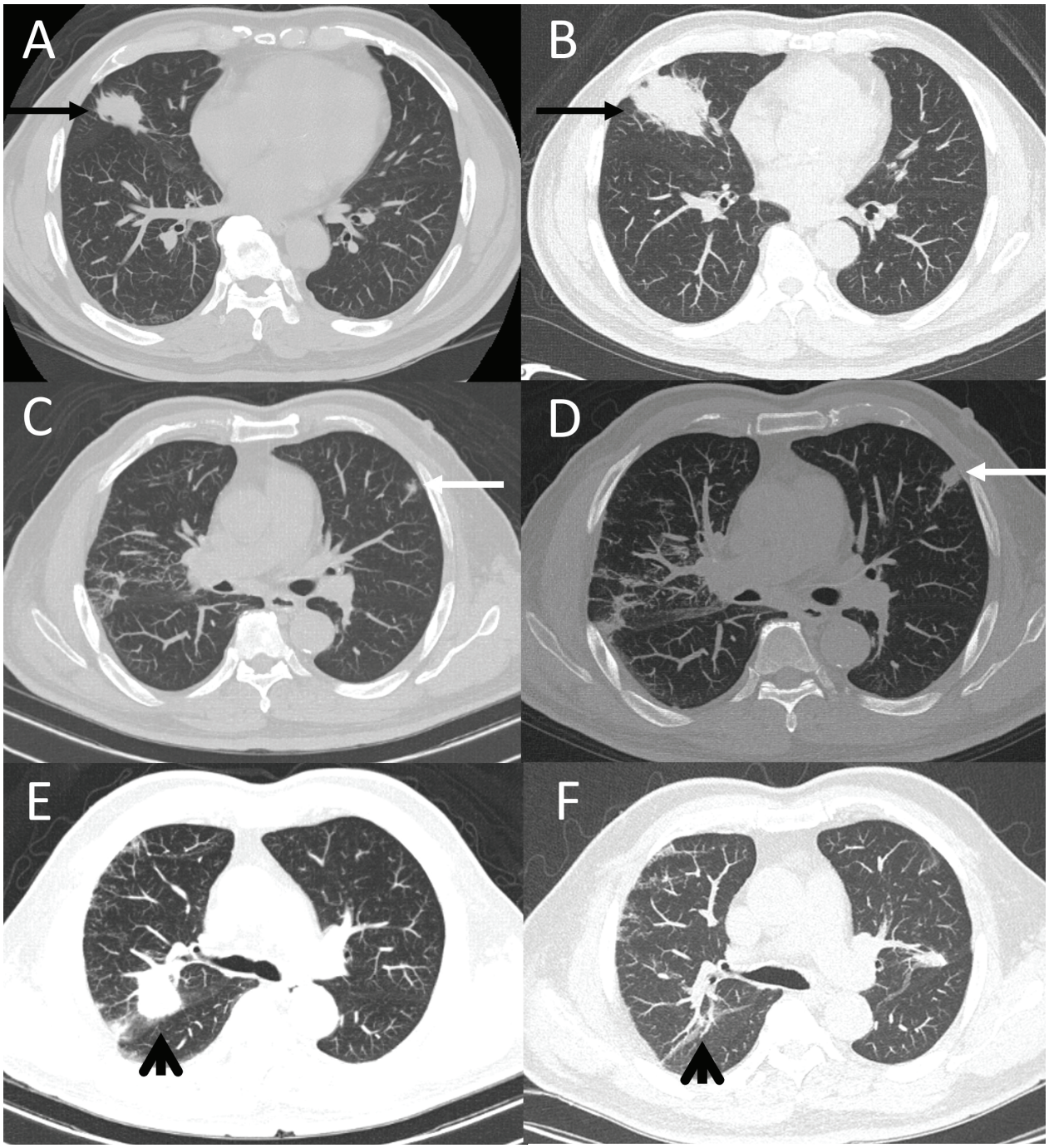

Fig. 1. Serial chest CT scan. A. Feb. 2014: right middle lobe (RML) irregular mass-like lesion of the lung with adjacent minor fissure retraction (black arrow). B, Jul. 2015: progressive RML spiculated mass. C, Sep. 2017: a new subsolid nodule over the left upper lobe (LUL) of the lung (white arrow) during follow-up. D, Jan. 2018: slow progression of the LUL subsolid nodule with suspicious subtle slow progression of the bilateral lung acinar nodules and mediastinal lymph nodes. E, Aug. 2022: progressive bilateral lung metastasis and a right upper lobe (RUL) nodule (arrowhead) before crizotinib and entrectinib treatment. F, Mar. 2023: regressive change in the RUL metastatic nodule after crizotinib (in Oct. 2022) and entrectinib (since Dec. 2022) treatment.

guided re-biopsy of the LUL nodule in March 2018 showed recurrence. Tumor re-staging was T2aN2M1a, IVA (AJCC 8th edition). Palliative chemotherapy with pemetrexed and cisplatin was given first, and then severe skin rashes with itching developed, favoring an allergic reaction to pemetrexed. Further chemotherapy with 6 cycles of gemcitabine and cisplatin was prescribed during June and November 2018, with a partial response, followed by 6 cycles of docetaxel monotherapy during October 2019 and February 2020, with stable disease, based on Response Evaluation Criteria in Solid Tumors (RECIST) 1.1 criteria [10]. Chest CT scan in July 2020 revealed progressive disease [10]. The chemotherapy regimen was changed to oral vinorelbine from July 2021 to September 2022, and limited change in bilateral lung-to-lung metastasis was noted.

Chest CT scan in August 2022 revealed progressive bilateral lung metastasis and a right upper lobe (RUL) nodule (Fig. 1E). Since the results of various chemotherapy treatments were not satisfactory, he underwent surgical re-biopsy through VATS wedge resection of the LUL in August 2022. The surgical re-biopsy specimen was sent for genetic testing using an AmoyDx Pan Lung Cancer PCR Panel, and ALK detection was performed using the immunostaining method. The genetic testing report revealed ROS1-positive adenocarcinoma. Crizotinib was prescribed in October 2022. After a 22-day regimen, the patient presented to the emergency department with the chief complaint of poor appetite, gastric pain and fullness for 3 days. Physical examination revealed slight epigastric tenderness. Laboratory examination revealed a white blood cell count of 9,900/uL, with segment neutrophils: 71.1%, lymphocytes: 14.5%, and monocytes: 7.6%. Hb was 13.2 g/dL, with aspartate aminotransferase (AST): 261 U/L, alanine aminotransferase (ALT): 436 U/L, total bilirubin: 1.46 mg/dL, direct bilirubin: 0.80 mg/dL, ammonia: 38 umol/L, alkaline phosphatase: 132 IU/L, albumin: 3.0 g/dl and lipase: 57 U/L. IgM antibodies against hepatitis A virus (anti-HAV IgM), hepatitis B surface antigen (HBsAg), IgM antibody against hepatitis B core antigen (anti-HBc IgM), and hepatitis C antibody (anti-HCV) were all negative. Antinuclear antibody (ANA) was 1:40 positive with a cytoplasmic and speckled pattern. A SARS-CoV-2 antigen rapid test was negative. Abdominal CT scan showed a periportal edema pattern, ascites, mild fatty liver, hepatic cysts in both lobes, and a stable cystic lesion in the pancreatic tail without biliary tree dilatation (Fig. 2). During hospitalization, prothrombin time was 15.3 seconds, the international normalized ratio was 1.42, and D-dimer was 3,540.9 ng/ml. IgG was 1,352 mg/dl.

A gastroenterologist was consulted, and drug-induced liver injury by crizotinib was favored as a diagnosis. Liver biopsy for definitive diagnosis was suggested, but the patient refused it. Crizotinib was discontinued immediately. Oral silymarin and intravenous glycyrrhizin were given at the patient's expense. His liver function improved gradually and serum aminotransferase and bilirubin levels returned to normal range after 6 weeks (Fig. 3).

After crizotinib withdrawal for 6 weeks, and with a recovered liver function, treatment was switched to entrectinib. The patient's liver function remained within normal range, and his condition was well controlled after changing the drug, with a partial response [10] evaluated in March 2023 (Fig. 1F). Muscle soreness and mildly elevated creatine-phospho-kinase (CPK 291 mg/dL) were found during the use of entrectinib.

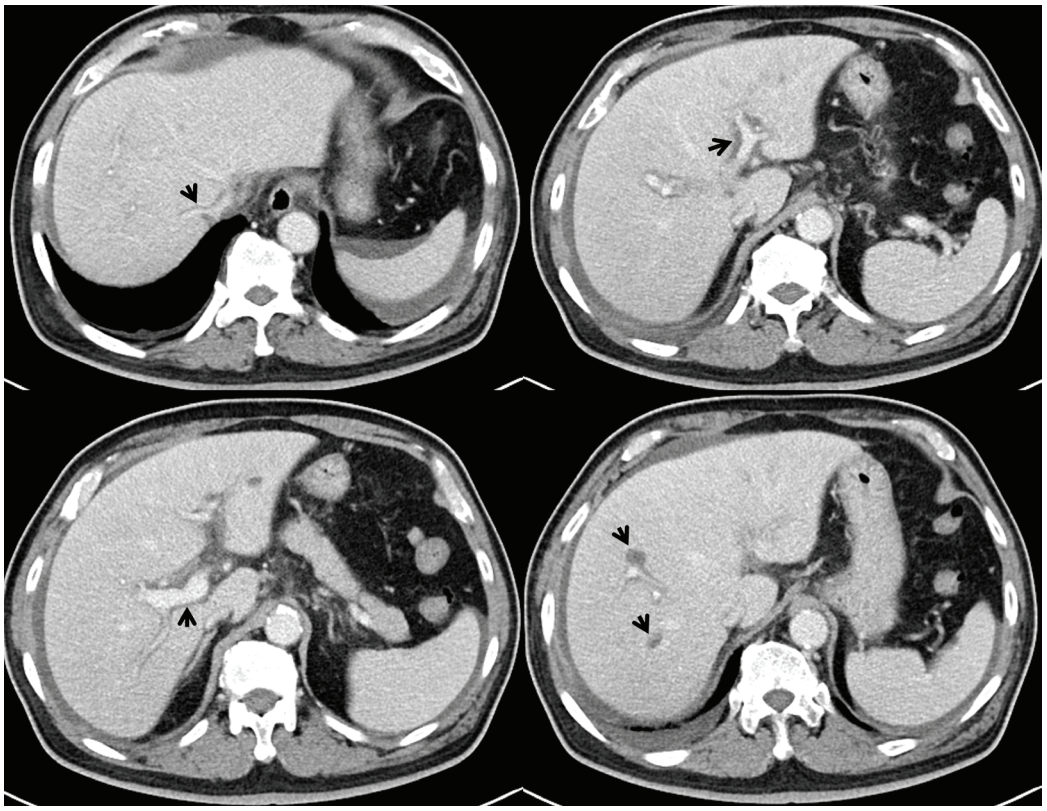

Fig. 2. Abdominal CT scan on Oct. 2022. Periportal edema (arrow head) and mild ascites were detected, which was compatible with acute hepatitis after 23 days of crizotinib treatment.

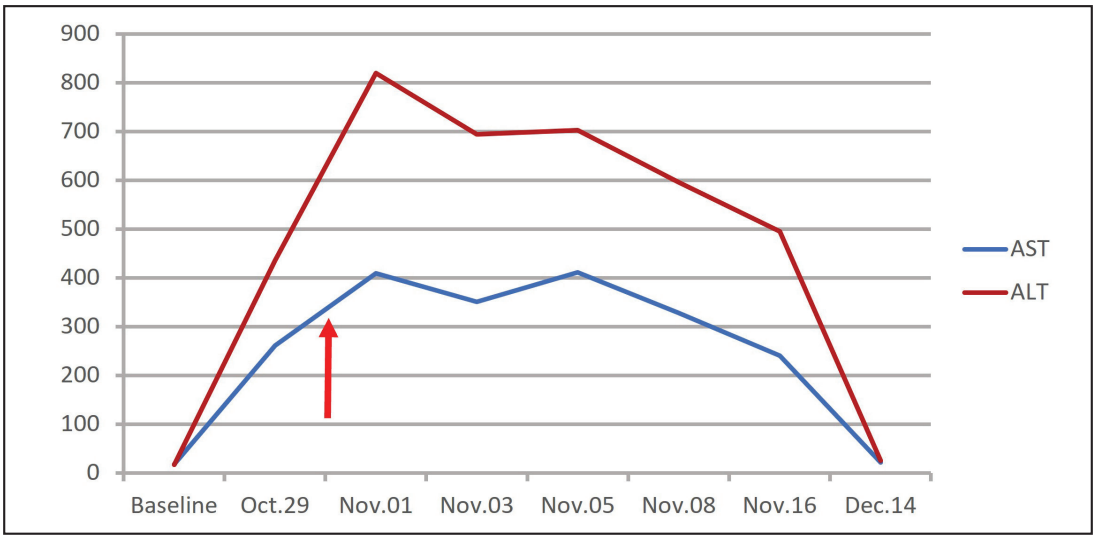

	Baseline	Oct. 29	Nov. 01	Nov. 03	Nov. 05	Nov. 08	Nov. 16	Dec. 14
AST	18	261	409	351	411	328	241	22
ALT	17	436	820	694	703	596	495	25
Bil.		1.46	2.00	1.92	1.74	1.12	0.79	0.53

Fig. 3. Clinical course of the patient treated with crizotinib. ALT, alanine aminotransferase; AST, aspartate aminotransferase; Bil., total bilirubin. Crizotinib was discontinued on Oct. 31 (red arrow).

Discussion

Elevated aminotransferase levels were seen in about 30% of patients with ALK-positive advanced NSCLC using crizotinib in phase III trials [5, 6]. Similar phenomena were also observed in patients with ROS1-positive advanced NSCLC [2]. A study published in 2021 using the FDA Adverse Event Reporting System (FAERS) database from January 2013 to December 2019 reported 6 crizotinib-induced fulminant hepatitis cases [11]. Several cases of crizotinib-induced fulminant hepatitis have also been reported [12, 13, 14]. Most cases were reported as hepatotoxicity categorized as hepatocellular injury, rather than cholestasis. However, the mechanisms behind the injuries are still not known [9]. A basic study reported using HepG2 cells in vitro and a mice model in vivo, and reported that crizotinib caused hepatotoxicity that was associated with oxidative stress, apoptosis and/or necrosis, and that crizotinib induced apoptosis via the mitochondrial pathway. Although this finding may offer a hint to help in understanding the related mechanism of liver injury, further studies are needed to understand the mechanism underlying the relationship between crizotinib-induced oxidative stress and the mitochondrial apoptotic pathway [15]. Our patient did not meet the criteria of fulminant hepatitis, but the grade 3 adverse effect of acute hepatitis was observed. A case report mentioned crizotinib-induced acute hepatitis with relapse after reintroduction with a reduced dose [16]. We chose medication replacement instead of a rechallenge of crizotinib due to the patient's worry and safety concern.

It is important to understand the risk factors for patients who are susceptible to crizotinib-induced liver injury. However, little is known about this. A retrospective, single center study published in 2018 reported that among 153 NSCLC patients treated with crizotinib from February 2012 to April 2018, those with the presence of liver disease or hepatitis B virus (HBV) and the use of H2-antagonists or proton pump inhibitors appeared to have a higher risk for hepatotoxicity [17]. Despite the study's limitation as a retrospective design and single center study, it still provides valuable data regarding those who may be candidates to undergo close monitoring of liver function. In addition, crizotinib is metabolized by CYP3A [3]. This might be another concern as to whether crizotinib has drug interactions with CYP3A4 inhibitors or inducers, and further has an impact on liver injury [18]. Our patient was not diagnosed as an HBV carrier and did not use proton pump inhibitors. He had visited an outpatient clinic where famotidine was prescribed before he presented to the emergency room that same day. Furthermore, our patient had been using the long-term CYP3A substrate amlodipine, tamsulosin, and short-term oral metoclopramide and domperidone. We considered these drugs to have a lower likelihood of causing hepatitis, which improved after crizotinib withdrawal.

In our case, oral silymarin and intravenous glycyrrhizin were prescribed for hepatitis treatment. Silymarin, extracted from milk thistle, has been used with certain hepatitis clinically. A review published in January 2024 described its therapeutic efficacy of silymarin in alcoholic liver disease, liver cirrhosis (alcoholic and non-alcoholic), liver injury (antituberculosis drug-induced), non-alcoholic fatty liver disease and nonalcoholic steatohepatitis [19]. Its therapeutic effectiveness may originate from a variety of mechanisms, such as anti-inflammatory and anti-oxidant actions [20]. Glycyrrhizin, a com-

pound from licorice root, is another drug and was developed for hepatoprotective management in China and Japan [21]. In China, magnesium isoglycyrrhizinate has been approved for the treatment of acute drug-induced liver injury, including hepatocellular and mixed liver injury [22]. However, no literature was found regarding the effect of silymarin or glycyrrhizin treatment on crizotinib-induced hepatitis. Oral desensitization may be helpful for crizotinib-induced hepatitis [18, 23]. We did not perform oral desensitization in our patient, for only case reports on its effectiveness were found [18, 23].

In cases of ROS1-positive NSCLC, in which crizotinib is not feasible for targeted therapy, the alternative is entrectinib, as in our case, because Taiwan's National Healthcare Insurance covers both crizotinib and entrectinib for ROS1-positive advanced NSCLC [4, 24]. Entrectinib is an oral, small molecule inhibitor that targets tropomyosin receptor kinase, ROS1, and ALK. It is used to treat locally advanced or metastatic solid tumors with neurotrophic tyrosine receptor kinase1/2/3, ROS1 and ALK gene fusion mutations [25]. A recent study evaluated the long-term efficacy and safety of entrectinib in ROS1-positive NSCLC [26]. Among 168 TKI–naïve patients, the objective response rate (ORR) was 68%. The median survival follow-up, median duration of response (DoR), median PFS and median overall survival (OS) were 29.1, 20.5, 15.7 and 47.8 months, respectively. The intracranial ORR of the 25 patients with measurable baseline central nervous system (CNS) metastases was 80%. The median intracranial DoR and PFS were 12.9 and 8.8 months, respectively. Among 18 patients with CNS-only progression on previous crizotinib treatment, 2 achieved a partial response (11%), and 4 had stable disease (22%). The intracranial ORR of 7 patients with measurable CNS disease in this cohort was 14% (1 partial response). Among 224 patients, 211 (94%) experienced at least 1 treatment-related adverse event (TRAE). The most frequent grade 1 to 2 TRAEs were dysgeusia in 90 patients (40%), dizziness in 82 (37%) and constipation in 71 (32%). The most frequent grade 3 TRAE was increased weight in 25 patients (11%). Grade 4 TRAEs were rare, and there were no TRAE-related deaths. Serious TRAEs occurred in 33 patients (15%), and the most frequent was pyrexia in 4 patients (2%) [26]. There is no current literature regarding fourth- or fifth-line entrectinib use in such patients. Our patient received entrectinib treatment with a partial response, as presented in Fig. 1E and Fig. 1F.

ANA could be detected in connective tissue diseases, for example, systemic lupus erythematosus [27], but healthy people and those with some non-rheumatic diseases [28], as well as certain types of autoimmune hepatitis or other liver diseases, for instance, fatty liver disease, drug-induced liver injury disease, or viral hepatitis [29], may also present ANA. Although ANA 1:40 positive was detected in our case, a variety of differential diagnoses should be considered, as mentioned above. The ANA result itself has no diagnostic value [28]. Liver biopsy could be used in the evaluation of abnormally elevated liver enzymes, and help assess the nature and severity of different liver diseases [30]. Although we did not perform biopsy in our patient, when we discontinued crizotinib, serum aminotransferases and bilirubin levels subsequently improved, suggesting that crizotinib-induced hepatitis was more likely. In addition, COVID-19 may cause elevated aminotransferases [31]. However, the SARS-CoV-2 antigen rapid test was negative and there was no as-

sociated manifestation on chest radiography in our patient, so COVID-19-induced acute liver injury was not likely.

Conclusion

Lung cancer, a commonly occurring cancer, is responsible for the highest number of deaths in Taiwan, regardless of gender [1]. Currently, crizotinib is approved for treatment of ALK- or ROS1-positive NSCLC in Taiwan [4]. However, crizotinib-induced hepatitis is an uncommon but potentially fatal side effect. Close monitoring of liver function during crizotinib administration should be taken into account. If crizotinib-induced hepatotoxicity is suspected, a liver biopsy may be considered for histological evaluation to establish the diagnosis of drug-induced liver injury [30], provided there are no contraindications. Once crizotinib-induced hepatitis is suspected or diagnosed, discontinuation of crizotinib is the preferred treatment, based on limited evidence. Whether a doctor should choose reintroduction of crizotinib with a reduced dose, desensitization, or replacement with other medications for such patients, is still unknown. Further studies are warranted regarding the etiology, evaluation, management strategies and prognosis of crizotinib-induced hepatitis.

References

1. Health Promotion Administration, Ministry of Health and Welfare, Taiwan, Cancer Registry Annual Report, 2020, Taiwan, published December 2022.
2. Shaw AT, Ou SH, Bang YJ, *et al*. Crizotinib in ROS1-rearranged non-small-cell lung cancer. N Engl J Med 2014; 371(21): 1963-71.
3. FDA, Prescribing information for Xalkori® (crizotinib), 2022 [Internet]. [cited 2023 Apr 16]. Available from: https://www.drugs.com/pro/xalkori.html
4. Taiwan Food and Drug Administration, Drug permit license for crizotinib. [cited 2023 Jul. 8]. Available from: https://info.fda.gov.tw/mlms/H0001D.aspx?Type=Lic&LicId=02025938
5. Shaw AT, Kim DW, Nakagawa K, *et al*. Crizotinib versus chemotherapy in advanced ALK-positive lung cancer. N Engl J Med 2013; 368(25): 2385-94.
6. Solomon BJ, Mok T, Kim DW, *et al*. First-line crizotinib versus chemotherapy in ALK-positive lung cancer. N Engl J Med 2014; 371(23): 2167-77.
7. Shen L, Qiang T, Li Z, *et al*. First-line crizotinib versus platinum-pemetrexed chemotherapy in patients with advanced ROS1-rearranged non-small-cell lung cancer. Cancer Med 2020; 9(10): 3310-8.
8. Gendarme S, Bylicki O, Chouaid C, *et al*. ROS-1 fusions in non-small-cell lung cancer: evidence to date. Curr Oncol 2022; 29(2): 641-58.
9. Kreitman K, Nair SP, Kothadia JP. Successful treatment of crizotinib-induced fulminant liver failure: a case report and review of literature. Case Reports Hepatol 2020; 2020: 8427960.
10. Eisenhauer EA, Therasse P, Bogaerts J, *et al*. New response evaluation criteria in solid tumours: revised RECIST guideline (version 1.1). Eur J Cancer 2009; 45(2): 228-47.
11. Zhou Z, Wang C, Ying L, *et al*. Anaplastic lymphoma kinase tyrosine kinase inhibitor-induced hepatic failure in lung cancer patients: a study of signal mining and analysis of the FDA adverse event reporting system database. J Clin Pharm Ther 2021; 46(4): 1148-54.
12. Sato Y, Fujimoto D, Shibata Y, *et al*. Fulminant hepatitis following crizotinib administration for ALK-positive non-small-cell lung carcinoma. Jpn J Clin Oncol 2014; 44(9): 872-5.
13. Charville GW, Padda SK, Sibley RK, *et al*. Resolution of crizotinib-associated fulminant hepatitis following cessation of treatment. Case Reports Hepatol 2018; 2018: 3413592.
14. van Geel RM, Hendrikx JJ, Vahl JE, *et al*. Crizotinib-induced fatal fulminant liver failure. Lung Cancer 2016; 93: 17-19.
15. Guo L, Tang T, Fang D, *et al*. An insight on the pathways involved in crizotinib and sunitinib induced hepatotoxicity in HepG2 cells and animal model. Front

Oncol 2022; 12: 749954.
16. Ripault MP, Pinzani V, Fayolle V, *et al*. Crizotinib-induced acute hepatitis: first case with relapse after reintroduction with reduced dose. Clin Res Hepatol Gastroenterol 2013; 37(1): e21-e23.
17. Jung D, Han JM, Yee J, *et al*. Factors affecting crizotinib-induced hepatotoxicity in non-small cell lung cancer patients. Med Oncol 2018; 35(12): 154.
18. Ota T, Masuda N, Matsui K, *et al*. Successful desensitization with crizotinib after crizotinib-induced liver injury in ROS1-rearranged lung adenocarcinoma. Intern Med 2019; 58(18): 2651-2655.
19. Mancak M, Altintas D, Balaban Y, *et al*. Evidence-based herbal treatments in liver diseases. Hepatol Forum 2024; 5(1): 50-60.
20. Federico A, Dallio M, Loguercio C. Silymarin/silybin and chronic liver disease: a marriage of many years. Molecules 2017; 22(2): 191.
21. Li JY, Cao HY, Liu P, *et al*. Glycyrrhizic acid in the treatment of liver diseases: literature review. Biomed Res Int 2014; 2014: 872139.
22. Li M, Luo Q, Tao Y, *et al*. Pharmacotherapies for drug-induced liver injury: a current literature review. Front Pharmacol 2022; 12: 806249.
23. Yasuda Y, Nishikawa Y, Sakamori Y, *et al*. Successful oral desensitization with crizotinib after crizotinib-induced hepatitis in an anaplastic lymphoma kinase-rearranged non-small-cell lung cancer patient: a case report. Mol Clin Oncol 2017; 7(2): 295-7.
24. Taiwan Food and Drug Administration, Drug permit license for entrectinib. [cited 2023 Jul. 14]. Available from: https://info.fda.gov.tw/MLMS/H0001D.aspx?Type=Lic&LicId=52027864
25. Jiang Q, Li M, Li H, *et al*. Entrectinib, a new multi-target inhibitor for cancer therapy. Biomed Pharmacother 2022; 150: 112974.
26. Drilon A, Chiu CH, Fan Y, *et al*. Long-term efficacy and safety of entrectinib in ROS1 fusion-positive NSCLC. JTO Clin Res Rep 2022; 3(6): 100332.
27. Aggarwal A. Role of autoantibody testing. Best Pract Res Clin Rheumatol 2014; 28(6): 907-20.
28. Grygiel-Górniak B, Rogacka N, Puszczewicz M. Antinuclear antibodies in healthy people and non-rheumatic diseases - diagnostic and clinical implications. Reumatologia 2018; 56(4): 243-48.
29. Sebode M, Weiler-Normann C, Liwinski T, *et al*. Autoantibodies in autoimmune liver disease-clinical and diagnostic relevance. Front Immunol 2018; 9: 609.
30. Khalifa A, Rockey DC. The utility of liver biopsy in 2020. Curr Opin Gastroenterol 2020; 36(3): 184-91.
31. Dufour JF, Marjot T, Becchetti C, *et al*. COVID-19 and liver disease. Gut 2022; 71(11): 2350-62.

Tocilizumab and Systemic Steroids in Severe COVID-19 with Acute Exacerbation of Idiopathic Pulmonary Fibrosis: A Case Report and Literature Review

Chung-Wen Huang[1], Chia-Min Chen[1], Ming-Ju Tsai[1,3], Tung-Chi Yeh[1]
Wei-An Chang[1,3], Cheng-Hao Chuang[1,2], Chau-Chyun Sheu[1,3]

Tocilizumab, a potent interleukin-6 (IL-6) receptor antagonist, has demonstrated a survival benefit against severe COVID-19 in clinical trials. However, the safety and efficacy of its use in populations with multiple comorbidities are unknown. Here, we report a challenging case with acute exacerbation of idiopathic pulmonary fibrosis (AE-IPF) triggered by SARS-CoV-2 infection, which is the first ever presented. AE-IPF is commonly triggered by pulmonary infection, and results in a poor prognosis with limited treatment options. Superimposed SARS-CoV-2 infection may further complicate the management and outcome. Hesitation about the prescription of tocilizumab was resolved through comprehensive multidisciplinary discussions in our interstitial lung disease board. The rationale of tocilizumab prescription is based on flourishing data on the role of IL-6 in AE-IPF, and the potential benefit of fibroblast suppression in both in vivo and in vitro studies. Successful management with much improved oxygenation and pulmonary infiltration is documented and further supports the use of tocilizumab in such a complex situation. Since there is a scarcity of effective treatments for AE-IPF, investigations on the role of IL-6 antagonist in the management of AE-IPF are needed. ***(Thorac Med 2024; 39: 228-233)***

Key words: AE-IPF, COVID-19, tocilizumab, IL-6, case report.

Introduction

Tocilizumab is a potent recombinant humanized anti-interleukin-6 receptor monoclonal antibody with accumulating experience in treating a variety of connective-tissue diseases over the last decade [1]. During the coronavirus disease 2019 (COVID-19) pandemic, tocilizumab

[1]Division of Pulmonary and Critical Care Medicine, Department of Internal Medicine, Kaohsiung Medical University Hospital, Kaohsiung Medical University, Kaohsiung, Taiwan, [2]Graduate Institute of Medicine, College of Medicine, Kaohsiung Medical University, Kaohsiung, Taiwan, [3]Department of Internal Medicine, School of Medicine, College of Medicine, Kaohsiung Medical University, Kaohsiung, Taiwan
Address reprint requests to: Dr. Cheng-Hao Chuang, Division of Pulmonary and Critical Care Medicine Department of Internal Medicine Kaohsiung Medical University Hospital Kaohsiung Medical University No. 100, Tzyou First Road, Kaohsiung City, Taiwan

was also authorized for the treatment of severe COVID-19 based on several randomized-controlled trials [2]. However, the efficacy and safety of tocilizumab in treating patients with COVID-19 complicated with acute exacerbation of idiopathic pulmonary fibrosis (AE-IPF) have never been reported. Herein, we present the case of a patient with concurrent severe COVID-19 and AE-IPF who was successfully treated with tocilizumab.

Case Presentation

A 60-year-old man with idiopathic pulmonary fibrosis (IPF), early-stage lung cancer, diabetes mellitus, and hypertension presented to the emergency room with a 5-day history of progressive dyspnea. He had been diagnosed with COVID-19 10 days before admission via rapid antigen test and completed antiviral therapy with nirmatrelvir/ritonavir. On arrival, a low but detectable viral load was found with a cycle threshold number of 29, as determined by polymerase chain reaction. Physical examination revealed tachycardia (117 beats/min), tachypnea (28 breaths/min), and severe hypoxemia with pulse oximeter oxygen saturation (SpO_2) of 80% under ambient air. Labored breathing with accessory muscle use was observed, and was partially relieved by supplemental oxygen therapy through a non-rebreathing mask. The chest radiograph and computed tomography (CT) scans showed increased bilateral reticulation and ground-glass opacity superimposed on background fibrosis and honeycombing (Figure 1 and Figure 2). Laboratory tests found borderline leukocytosis (10110 cells/μL), mildly elevated C-reactive protein (45.34 mg/L), lactate dehydrogenase (248 IU/L), d-dimer (1.4 mg/L), ferritin (192.8 ng/mL), and normal B-type natriuretic peptide (10.4 pg/L) and troponin-I (0.0034 ng/mL).

On admission to the intensive care unit, his peripheral blood oxygen saturation/frac-

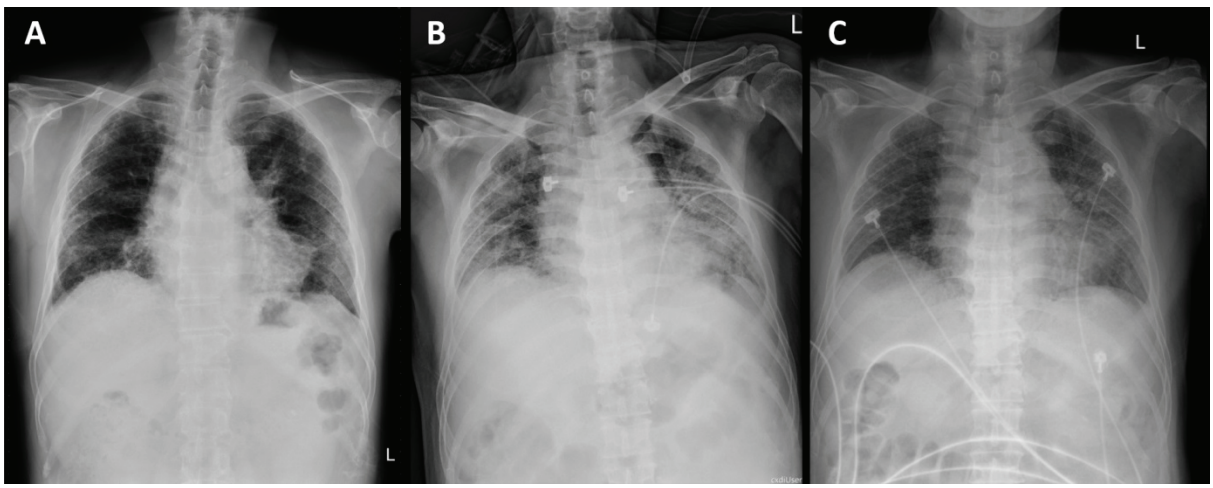

Fig. 1. Chest radiograph at (A) Four months previous, as baseline. (B) Initial presentation of acute exacerbation. (C) Three days after tocilizumab use. In a 60-year-old man, (A) Baseline peripheral reticulation and an apical-basal gradient pattern of fibrosis was seen on chest radiograph 4 months ago. Note the left upper lung tumor is not prominent on the plain film. (B) Increased bilateral interstitial infiltration and ground-glass opacity was seen on chest radiograph when he presented to the emergency room for severe COVID-19 and superimposed AE-IPF. (C) Partial resolution of bilateral ground-glass opacity was found 3 days after tocilizumab therapy.

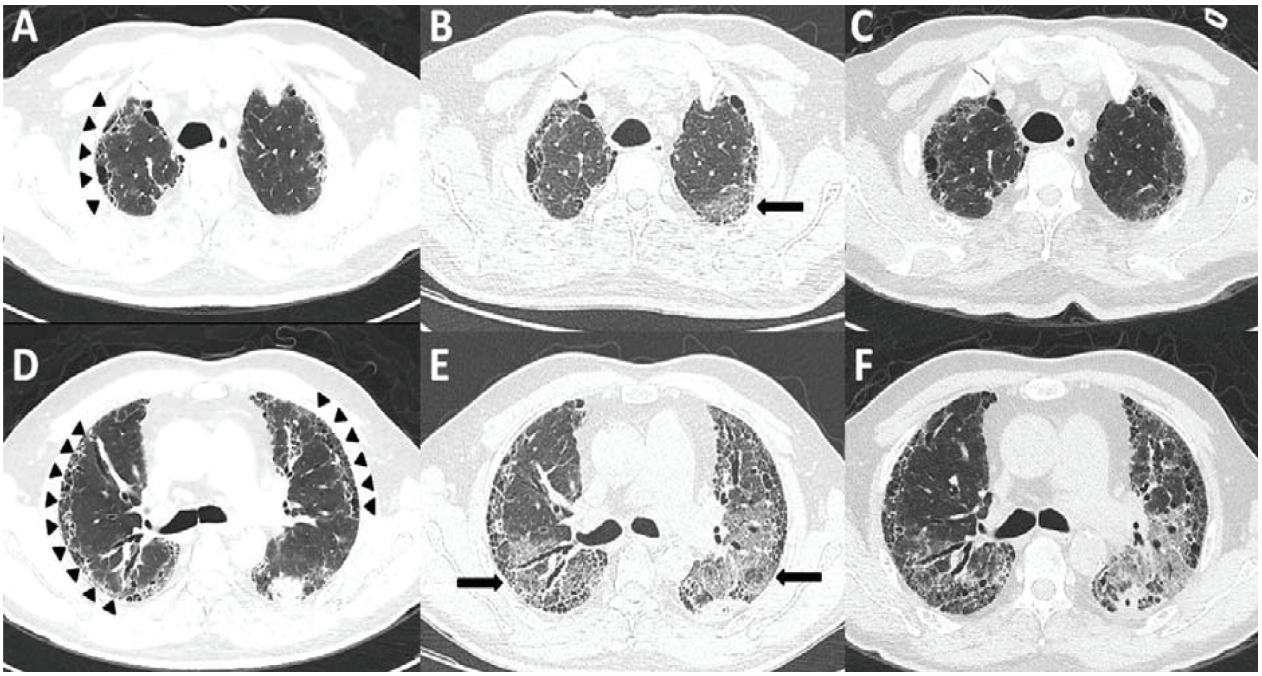

Fig. 2. Computed tomography scans: (A) and (D) Four months previous, as baseline. (B) and (E) Initial presentation of acute exacerbation. (C) and (F) Sixteen days after tocilizumab use. In a 60-year-old man, (A) and (D) A baseline usual interstitial pattern, subpleural honeycombing and traction bronchiectasis, is depicted on CT scans 4 months previous, with left upper lung tumor which received stereotactic ablative radiotherapy. (B) and (E) Significantly increased bilateral ground-glass opacity was seen when he presented to the emergency room for severe COVID-19 and superimposed AE-IPF. (C) and (F) Regression of the bilateral ground-glass opacity, especially at the right upper lung, was seen 16 days after systemic steroid and tocilizumab therapy.

tion of inspired oxygen (SpO_2/FiO_2) ratio was 138. High-flow nasal cannula with a flow rate of 45 L/min and a FiO_2 of 70% was started. In addition to maintenance of the baseline antifibrotic agent, nintedanib, a 200 mg loading dose of remdesivir on Day 1, followed by 100 mg daily for up to 4 additional days, and systemic steroid with methylprednisolone 120 mg per day were administered for AE-IPF triggered by COVID-19 infection. Broad-spectrum antibiotic therapy with cefoperazone/sulbactam was also administered to cover possible superimposed bacterial infections, although no bacteria or virus other than COVID-19 was isolated during hospitalization. Despite treatment, a persistent rapid-shallow breathing pattern and a low SpO_2/FiO_2 ratio of 158 were still noted on Day 3. Single intravenous tocilizumab (8 mg per kilogram, a total dose of 480 mg) was administered under the recommendation of the multidisciplinary team of interstitial lung disease (ILD) at our hospital, considering its effectiveness for severe COVID-19 and theoretically potential benefit for AE-IPF.

Significant regression of bilateral ground-glass opacity was observed on the follow-up chest radiograph on Day 6 (Figure 1), as well as improving SpO_2/FiO_2 ratios of 195 and 242 on Day 5 and Day 7, respectively. Mitigation of respiratory effort was also reported subjectively by the patient afterward. Methylprednisolone was tapered from 120 mg per day to 80 mg per day on Day 5, and then to 40 mg per day on Day 8, based on clinical improvement. Sys-

temic steroid was shifted to oral prednisolone of 25 mg per day on Day 11, with a 5 mg decrement every other day thereafter. The follow-up chest computed tomography (CT) scans showed partial resolution of ground-glass attenuation, especially in the right upper lobe of the lung (Figure 2). The high-flow nasal cannula was discontinued on Day 13. The patient was discharged on Day 20, with a SpO_2/FiO_2 ratio of 344 and maintenance prednisolone of 10 mg per day.

Discussion

A dysregulated immune response and an exaggerated cytokine storm are presumed causes of severe COVID-19 disease [3]. An anti-inflammation strategy is the mainstream of severe COVID-19 management, and includes systemic steroids and inhibitors targeting the specific immunomodulating pathway. Interleukin-6 (IL-6) is recognized as a major mediator of an overshooting host response, and a significantly elevated serum level of IL-6 has been observed in critical patients with COVID-19 [4]. Several randomized-controlled trials have demonstrated the treatment efficacy of tocilizumab, an IL-6 receptor antagonist, especially in reducing mortality and the need for mechanical ventilation [2]. Of note, steroids may have a role in this regard because tocilizumab tends to exhibit significant efficacy when combined with systemic steroids [5].

The exact pathophysiology of AE-IPF remains unclear. Maladaptive response to lung injury triggered by extrinsic stimuli, including viral infections, subsequent diffuse alveolar damage and activation of inflammatory cells and fibroblasts are recognized as a major paradigm of AE-IPF [6]. No strong evidence-supported treatment algorithm is available, but systemic steroid has been used widely in AE-IPF management in an attempt to interrupt flare-up inflammation [7]. In our patient, systemic steroid was administered for both COVID-19 and AE-IPF. Persistent acute hypoxemic respiratory failure, despite standard care, is the current indication for tocilizumab treatment for COVID-19 disease, but its efficacy with AE-IPF is uncertain. Diffuse bilateral ground-glass opacity and reticulation found on CT are typical but nonspecific to both COVID-19 pneumonia and AE-IPF. No characteristic clinical or laboratory presentation has been verified to evaluate the contribution of each disease in the patient.

Pulmonary embolism is another possible etiology for the acute respiratory failure in this patient, since both this malignancy and COVID-19 can lead to thrombophilia. However, the radiological presentation of significant worsening of pulmonary parenchymal reticulation and ground-glass opacities, and the absence of a typical Westermark sign or Hampton hump made pulmonary embolism less likely. In addition, a d-dimer cut-off value of 3.0 mg/L was validated in a previous multicenter retrospective cohort for the initiation of venous thromboembolism screening and anti-coagulation therapy [8], although our patient had a relatively low d-dimer level of 1.4 mg/L. Finally, successful management of acute respiratory failure without anti-coagulation therapy further supported the exclusion of pulmonary embolism.

Complex interactions between the pathophysiology of COVID-19 and AE-IPF do exist. For instance, IPF might increase host susceptibility to viral infections, including COVID-19 [9], and the acute insult triggered by COVID-19 might lead to exacerbation of IPF. Individualized therapy is needed, and measurement of the

serum IL-6 level may be helpful, but it is not available in most facilities. Besides COVID-19, enthusiasm for targeting inflammation cascades of AE-IPF is emerging. Elevated serum IL-6 levels in patients with AE-IPF was observed in a small prospective cohort, and positively correlated with mortality [10]. In vitro, increased paracrine IL-6 secretion is seen in the primary culture of fibroblasts derived from patients with IPF. Normal human pulmonary fibroblasts treated with conditioned medium of IPF pulmonary fibroblasts showed upregulation of the IL-6/STAT3/Smad3 axis, a pathway involved in pulmonary fibrosis, and the effect was inhibited by tocilizumab [11]. More studies are needed to clarify the role of IL-6 in the molecular mechanisms of AE-IPF.

However, the efficacy of tocilizumab in treating fibrosing lung diseases seems promising. Recently, a phase III randomized placebo-controlled trial (focuSSced trial) of systemic sclerosis-associated ILD (SSc-ILD) demonstrated the efficacy of tocilizumab in the preservation of lung function [12]. Based on available evidence, tocilizumab is recommended after discussion within our multidisciplinary team on ILD. The successful management experience in our case highlights the safety and potential efficacy of tocilizumab treatment in the concurrent severe COVID-19 and AE-IPF scenario. Although the clinical outcome was impressive in our patient, the optimal dose and frequency of tocilizumab treatment requires further study.

Conclusion

In conclusion, our case has provided important clinical experience regarding the safety of tocilizumab treatment combined with systemic steroids for severe COVID-19 superimposed with AE-IPF. Increasing evidence from in vitro and in vivo studies shows that IL-6 may play a critical role in the pathophysiology of both severe COVID-19 and AE-IPF. Recent clinical trials have already proved the efficacy of IL-6 inhibitor in COVID-19. More comprehensive clinical and biological investigations are needed to evaluate the potential effects of tocilizumab on AE-IPF combined with severe COVID-19.

Acknowledgments

We thank the patient and his family, who were present in the case, and the team at the Medical Intensive Care Unit and Isolation Ward of Kaohsiung Medical University Hospital.

References

1. Choy EH, De Benedetti F, Takeuchi T, *et al*. Translating IL-6 biology into effective treatments. Nat Rev Rheumatol 2020; 16(6): 335-345.
2. Shankar-Hari M, Vale CL, Godolphin PJ, *et al*. Association between administration of IL-6 antagonists and mortality among patients hospitalized for COVID-19: a meta-analysis. JAMA 2021; 326(6): 499-518.
3. Jones SA, Hunter CA. Is IL-6 a key cytokine target for therapy in COVID-19? Nat Rev Immunol 2021; 21(6): 337-339.
4. McElvaney OJ, McEvoy NL, McElvaney OF, et al. Characterization of the inflammatory response to severe COVID-19 illness. Am J Respir Crit Care Med 2020; 202(6): 812-821. doi:10.1164/rccm.202005-1583OC
5. Rubin EJ, Longo DL, Baden LR. Interleukin-6 receptor inhibition in Covid-19 - cooling the inflammatory soup. N Engl J Med 2021; 384(16): 1564-1565.
6. Collard HR, Ryerson CJ, Corte TJ, *et al*. Acute exacerbation of idiopathic pulmonary fibrosis. An international working group report. Am J Respir Crit Care Med 2016; 194(3): 265-75.
7. Kreuter M, Polke M, Walsh SLF, *et al*. Acute exacerbation of idiopathic pulmonary fibrosis: international survey

and call for harmonisation. Eur Respir J 2020; 55(4): 1901760.

8. García-Cervera C, Giner-Galvañ V, Wikman-Jorgensen P, *et al*. SEMI-COVID-19 Network. Estimation of admission D-dimer cut-off value to predict venous thrombotic events in hospitalized COVID-19 patients: analysis of the SEMI-COVID-19 Registry. J Gen Intern Med 2021; 36(11): 3478-3486.
9. Hyun L, Hayoung C, Bumhee Y, *et al*. Interstitial lung disease increases susceptibility to and severity of COVID-19. Eur Respir J 2021; 58(6): 2004125.
10. Papiris SA, Tomos IP, Karakatsani A, *et al*. High levels of IL-6 and IL-8 characterize early-on idiopathic pulmonary fibrosis acute exacerbations. Cytokine 2018; 102: 168-172.
11. Epstein Shochet G, Brook E, Bardenstein-Wald B, *et al*. TGF-beta pathway activation by idiopathic pulmonary fibrosis (IPF) fibroblast derived soluble factors is mediated by IL-6 trans-signaling. Respir Res 2020; 21(1): 56.
12. Roofeh D, Lin CJF, Goldin J, *et al*. Tocilizumab prevents progression of early systemic sclerosis-associated interstitial lung disease. Arthritis Rheumatol 2021; 73(7): 1301-1310.

Effective Management of *EGFR* L718Q Mutation Revealed by Liquid Biopsy Using 30 mg Afatinib after Osimertinib Treatment Failure

Sheng-Bin Fan[1], Chih-Jen Yang[1,2]

Developing resistance to tyrosine kinase inhibitors poses a significant challenge in treating *EGFR*-mutated non-small cell lung cancer. One known cause of resistance to osimertinib is the *EGFR* L718Q mutation, which interferes with the drug's binding efficacy and consequently leads to resistance. We reported an 81-year-old female patient who was diagnosed with adenocarcinoma in the left lower lung, exhibiting distant metastasis and an *EGFR* L858R mutation. Treatment with osimertinib led to a 25-month progression-free period before the disease progressed with an enlarged liver metastatic tumor. Although the tissue biopsy yielded inadequate samples, a liquid biopsy identified an *EGFR* L718Q mutation. This discovery led to the patient being switched to 30 mg of afatinib. Remarkable shrinkage in liver metastases was observed after 5 months of afatinib treatment, without notable adverse reactions. Presently, the patient continues to exhibit stable disease status during ongoing follow-up. ***(Thorac Med 2024; 39: 234-240)***

Key words: afatinib, osimertinib, *EGFR* L718Q mutation, non-small cell lung cancer

Background

Lung cancer is currently the leading cause of death worldwide, and has the highest mortality among all malignant tumors [1-2]. This phenomenon may be due to the fact that most lung cancers are diagnosed at an advanced stage, and choices of antineoplastic treatment have been limited. In the past, chemotherapy and radiotherapy were considered to be mainstay treatments for advanced lung cancer. Fortunately, with the evolution of molecular diagnosis, more new treatments, such as targeted therapy and immune checkpoint inhibitors, are being developed and may be considered as first-line treatment.

[1]Division of Pulmonary and Critical Care Medicine, Department of Internal Medicine, Kaohsiung Medical University Hospital, Kaohsiung Medical University, Kaohsiung, Taiwan, [2]School of Post-Baccalaureate Medicine, College of Medicine, Kaohsiung Medical University, Kaohsiung, Taiwan
Address reprint requests to: Dr. Chih-Jen Yang, Division of Pulmonary and Critical Care Medicine Department of Internal Medicine Kaohsiung Medical University Hospital Kaohsiung Medical University No. 100, Tzyou First Road, Kaohsiung City, Taiwan

Among Asian populations, the prevalence of an epidermal growth factor receptor (*EGFR*) mutation is much higher than in Caucasian patients, especially in patients with adenocarcinoma and in never-smokers [3]. Hence, *EGFR* tyrosine kinase inhibitors (TKIs) are regarded as a crucial treatment option for *EGFR*-mutated non-small cell lung cancer (NSCLC), offering improved progression-free survival (PFS) and fewer side effects than traditional cytotoxic chemotherapy [4]. Nevertheless, the emergence of acquired resistance to TKIs poses a significant challenge in treating these patients. Advancements in molecular testing continually reveal new mechanisms of resistance and mutations. Notably, the *EGFR* T790M mutation has been found to be a prevalent cause of acquired resistance following the use of first- or second-generation TKIs [5].

Osimertinib, a third-generation TKI, is established as a standard first-line therapy for NSCLC with susceptible *EGFR* mutations, and has been proven effective against acquired *EGFR* T790M-mutated NSCLC. Developing resistance to osimertinib represents a significant obstacle in the treatment of advanced lung cancer. One notable mechanism of resistance is the *EGFR* L718Q mutation. The search for effective treatments targeting this specific mutation is ongoing and remains a critical area of research [6]. In this report, we highlight a case in which a patient with an *EGFR* L718Q mutation was successfully treated with 30 mg afatinib as an effective salvage therapy after osimertinib treatment.

Case Presentation

An 81-year-old woman was referred to Kaohsiung Medical University Hospital in March 2021 due to a history of reduced appetite and unintentional weight loss. Initial diagnostic imaging revealed a bronchogenic mass in the left lower lobe of the lung, accompanied by lymphadenopathy in several regions, including the left supraclavicular area, left upper mediastinum, left hilar region, and precarinal, subcarinal, and epigastric areas. Additionally, multiple lesions were identified in the left pleura, liver, bones, and brain. Biopsies from the left lung mass and liver confirmed a diagnosis of adenocarcinoma in the left lower lobe of the lung, with extensive metastasis to non-regional lymph nodes, and the left pleura, liver, bones, and brain, thus classifying the condition as stage IVB (cT4N3M1c). The initial molecular study showed an *EGFR* L858R mutation, which was detected by cobas® *EGFR* Mutation test V2.

In April 2021, the patient opted for osimertinib treatment, starting with a daily dose of 80 mg. This decision was influenced by the patient's preference and the drug's relatively lower risk of adverse effects compared to other TKIs. Three months into the treatment, imaging studies, including computed tomography of the chest and magnetic resonance imaging of the brain, revealed positive results: there was partial reduction in the size of the lung mass, mediastinal lymph nodes, and liver mass. Notably, the brain lesion exhibited complete shrinkage. These changes indicated a partial response to the treatment (Figure 1).

However, in May 2023, the patient exhibited progressive disease characterized by a significant increase in the size of the liver metastases, indicating a PFS duration of 25 months. An attempted tissue biopsy of the hepatic metastasis did not yield sufficient tissue for genomic analysis. Subsequently, a liquid

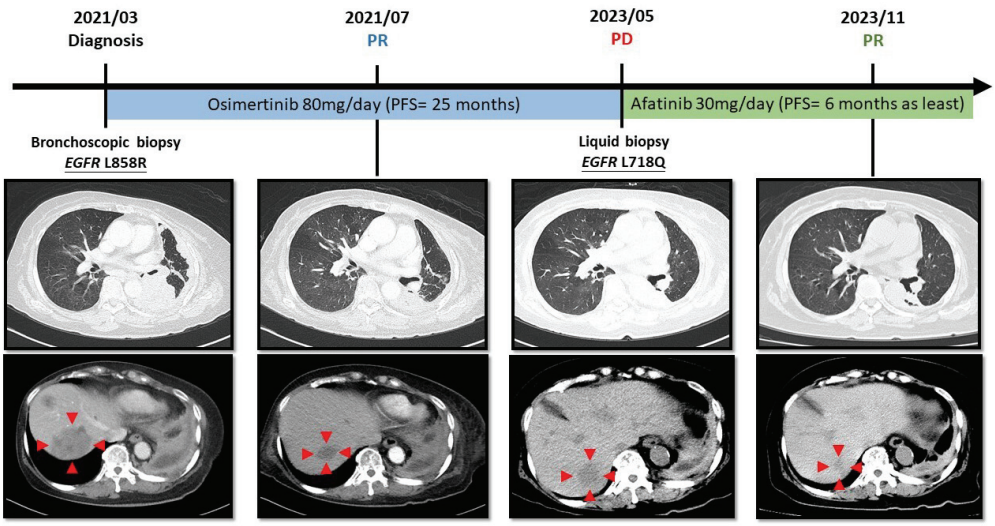

Fig. 1. Clinical course and treatment effect

Summary of Detected Somatic Alterations		
Detected Alteration(s)	Associated FDA-approved therapies	% cfDNA or Amplification
EGFR L718Q	Osimertinib is lack of response	0.04%
ATM S1923	Olparib is approved in other indication	44.0%
KRAS K117N	None	0.1%
KRAS G12S	None	0.04%

Fig. 2. Detailed results of liquid biopsy with Guardant360®

biopsy and next-generation sequencing (NGS) (Guardant360®) showed an *EGFR* L718Q/*ATM* S1923/*KRAS* K117N/ *KRAS* G12S mutation (the report is presented in Figure 2).

Following a thorough review of the literature and in-depth discussions with the patient and her family, taking into account her advanced age and potential for adverse drug reactions (ADR), a decision was made to switch from osimertinib to afatinib. Starting in June 2023, she began receiving a daily dose of 30 mg of afatinib. After 5 months of treatment, a significant reduction in liver metastases was noted, and there were no major adverse reactions. As of December 2023, the patient continued to show a stable disease status in her follow-up assessments.

Discussion

Acquired resistance to TKIs, especially resistance to osimertinib, is the main stumbling block to managing *EGFR*-mutated NSCLC in the current era. The underlying mechanisms of resistance to osimertinib are still under investigation, and are categorized as *EGFR*-dependent

(such as *EGFR* C797S, L718Q mutation, and so on) and *EGFR*-independent (such as MET, HER2, *KRAS* alterations, and so on) [6]. Identifying the optimal treatment for resistance to osimertinib is challenging, due to the scarcity of documented cases in PubMed searches and limited clinical experience among healthcare providers in managing such cases.

Among the underlying mechanisms of resistance, *EGFR* L718Q mutation is relatively rare and accounts for 7.3% to 9.7% of osimertinib resistance [7]. The L718 residue is located within the P-loop of the ATP-binding site of the *EGFR* kinase, and the L718Q mutation would interfere with binding of osimertinib by causing steric hindrance and resistance [6-9]. In a PubMed review, several case reports suggested that second-generation TKIs may be effective. This information has been summarized in Table 1: (1) Shen *et al*. used dacomitinib at a daily dose of 45 mg to treat *EGFR* L858R/L718Q-mutated NSCLC, and achieved a partial response that yielded a PFS of 5 months [9]; (2) Yang *et al*. used afatinib at a daily dose of 40 mg to treat *EGFR* L858R/L718Q-mutated NSCLC, and achieved a partial response that yielded a PFS of 4 months [10]. Despite the efficacy of second-generation TKIs, their PFS results are suboptimal. However, combined therapy with afatinib and cetuximab was observed in one study to offer a comparatively improved PFS, extending up to a minimum of 7 months [11].

In addition to second-generation TKIs, first-generation TKIs and chemotherapy have been used as treatment. Liu *et al*. and Ma *et al*. used erlotinib and icotinib for *EGFR* L858R/L718Q-mutated NSCLC, and yielded PFS of 3 months

Table 1. Literature Review of Targeted Therapy for *EGFR* L718Q-mutated NSCLC

Study	Published year	Cell type	Initial mutation	Treatment Course	Subsequent mutation	Brain Meta	Treatment	Response	PFS(month)	Mutation at PD
Liu, et al [12]	2018	Adenocarcinoma	L858R	Chemotherapy→ Gefitinib→ Osimertinib	L858R/L1718V (Lung)	-	Erlotinib 300mg/day	SD	3	L858R/C797S (Lung)
Ma, et al [13]	2018	Adenocarcinoma	L858R	Gefitinib→ Osimertinib	L858R/L718Q *TP53* R175H (Lung)	+	Icotinib	SD	1	NR
Liu, et al [24]	2019	Adenocarcinoma	L858R	Icotinib→ Osimertinib→ Chemotherapy	L858R/L1718V *BRAF* G466R (CSF)	+	Afatinib 40mg/day	ECOG Improve	4	NR
Yang, et al [10]	2020	Adenocarcinoma	L858R	Gefitinib→ Chemotherapy→ Osimertinib→	L858R/L718Q (pleural effusion)	-	Afatinib	PR	4	*KRAS* G12A
Song et al [14]	2020	adenocarcinoma	L858R	Chemotherapy→ Icotinib→ Osimertinib→	L858R/L718Q (Lung)	-	Cisplatin + Gemcitabine	PR	5	T790M
Shen, et al [9]	2021	Adenocarcinoma	L858R	Gefitinib→ Osimertinib→ Chemotherapy	L858R/L718Q (Lung)	+	Dacomitinib 45mg/day	PR	5	NR
Shen, et al [25]	2021	Adenocarcinoma	Exon 19 del	Icotinib→ Chemotherapy→ Icotinib+AntiVEGF→ Chemotherapy→ Osimertinib→ Osimertinib+erlotinib→ Crizotinib	T790M/L718Q *ALK* fusion (Blood)	-	Almonertinib 110mg/day	SD	4	NR
Zhang, et al [11]	2022	Adenocarcinoma	L858R *PIK3CA* exon 8	Almonertinib→ Chemotherapy	L858R/L718Q *TP53* (Ascites)	-	Afatinib 40mg/day + Cetuximab 250mg/m2 q2w	PR	7 at least	
Our study	**2024**	**Adenocarcinoma**	**L858R**	**Osimertinib**	**L718Q (Blood)**	**+**	**Afatinib 30mg/day**	**PR**	**6 at least**	

EGFR Epidermal growth factor receptor, NSCLC non-small cell lung cancer, PFS progression-free survical, SD stable disease, PR partial response, PD progressive disease, NR not reported, ECOG Eastern Cooperative Oncology Group

and 1 month, respectively [12-13]. Song *et al*. used chemotherapy with cisplatin and gemcitabine to treat *EGFR* L858R/L718Q-mutated NSCLC, and achieved a partial response with a PFS of 5 months [14]. Although some therapeutic strategies are available, the treatment effect is not satisfactory. Further investigation for a more precise treatment is needed.

Standard 40 mg doses of afatinib often result in severe ADRs, such as paronychia, diarrhea, and acne. Consequently, minimizing these ADRs is crucial. Our previous study revealed that a lower starting dose or reduced dosage of afatinib can markedly decrease ADR severity while still maintaining similar PFS and overall survival (OS) outcomes [15]. In this case, with concerns about the patient's age and desire to avoid ADRs, we decided to initiate 30 mg afatinib to manage *EGFR* L718Q-mutated NSCLC. PFS so far seems not inferior to that of a standard dose, compared to other studies in a literature review (Table 1), and only a grade 1 cutaneous reaction was noted.

In addition, based on our review, almost all patients with acquired *EGFR* L718Q-mutated NSCLC had an initial *EGFR* L858R mutation, and the acquired L718Q mutation always occurred after third-generation osimertinib treatment. The interrelationship of these factors might need further study.

Osimertinib resistance and a poor prognosis are often linked to *KRAS* mutations, as they activate *KRAS* as an alternative bypass mechanism, overcoming the blockage of *EGFR*-dependent survival signaling by osimertinib [6, 16]. The *KRAS* 117N mutation is rarer than *KRAS* G12S, and currently, there are no targeted therapies for either mutation. The *ATM* gene, which plays a role in cell cycle regulation and the identification and repair of DNA damage, is known for its common germline mutations. However, some studies suggest an association between *ATM* mutations and an increased risk of lung adenocarcinoma [17]. Literature discussing the link between TKI resistance and *ATM* mutations is scarce, and no targeted treatments exist for *ATM* mutations. Nevertheless, one study highlighted that co-mutations in TP53 and *ATM* showed an improved response to immune checkpoint inhibitors [18].

Utilizing tumor tissue for NGS is ideal, but challenges such as difficulty in accessing new metastatic lesions or insufficient tissue for NGS are common, and often unavoidable. One study reported that only 18% of patients with NSCLC have an adequate tumor specimen for complete tissue genotyping [19]. Moreover, progressive malignancy usually accompanies impaired physical function, so subsequent tissue proof is often inaccessible. Detecting circulating tumor DNA (ctDNA) through NGS plays a significant role in managing acquired resistance to TKIs, with liquid biopsy emerging as a promising approach. Compared to traditional biopsy, liquid biopsy has the advantage of being minimally invasive, with a better capture of tumor heterogeneity, and faster turnaround time [20]. In addition to these good points, liquid biopsy could also be used in monitoring treatment effect and prognostic evaluation [21]. Regardless of these benefits, liquid biopsy cannot replace traditional biopsy due to some disadvantages, such as the possibility of a false negative, high cost, and inability to evaluate non-DNA markers [20, 21].

In our case, a tissue biopsy of hepatic metastasis was attempted, but yielded insufficient tissue for analysis. Subsequently, a liquid biopsy revealed the *EGFR* L718Q mutation, guiding further targeted therapy. However, it is noteworthy that in another case report of *EGFR* L718Q-

mutated NSCLC, the mutation was identified only in tumor tissue genotyping, and not in liquid biopsy [12]. This discrepancy might be caused by low ctDNA shedding tumors, notably in the presence of low total body tumor burden, low extra-thoracic metastatic spread, or solitary involvement of sanctuary sites [20, 22, 23]. We consider liquid biopsy to be an invaluable diagnostic tool, yet it is important to approach negative results with careful consideration.

Conclusion

In our case, we prescribed 30 mg afatinib for *EGFR* L718Q-mutated NSCLC due to concerns about the patient's advanced age and quality of life. Obvious shrinkage of liver metastasis was then noted, yielding a PFS of at least 6 months. A review of previous studies showed that our patient was the first to receive 30 mg afatinib initially for acquired *EGFR* L718Q-mutated NSCLC, with a nearly therapeutic effect and without obvious side effects. In summary, we believe that 30 mg afatinib has sufficient therapeutic effect to treat the *EGFR* L718Q mutation. Resistance to TKI is a constant fight, so we still need more effort and more research to overcome it.

References

1. WHO. Lung cancer 2023. [cited 2023; Available from: https://www.who.int/news-room/fact-sheets/detail/lung-cancer.
2. Thandra KC, Barsouk A, Saginala K, *et al*. Epidemiology of lung cancer. Contemp Oncol (Pozn) 2021; 25(1): 45-52.
3. Zhou W, Christiani DC. East meets West: ethnic differences in epidemiology and clinical behaviors of lung cancer between East Asians and Caucasians. Chin J Cancer 2011; 30(5): 287-292.
4. Hsu WH, Yang JC, Mok TS, *et al*. Overview of current systemic management of *EGFR*-mutant NSCLC. Ann Oncol 2018; 29(suppl_1): i3-i9.
5. Westover D, Zugazagoitia J, Cho BC, *et al*. Mechanisms of acquired resistance to first- and second-generation *EGFR* tyrosine kinase inhibitors. Ann Oncol 2018; 29(suppl_1): i10-i19.
6. Zalaquett Z, Hachem MCR, Kassis Y, *et al*. Acquired resistance mechanisms to osimertinib: the constant battle. Cancer Treat Rev 2023; 116:102557.
7. Oxnard GR, Hu Y, Mileham KF, *et al*. Assessment of resistance mechanisms and clinical implications in patients with *EGFR* T790M-positive lung cancer and acquired resistance to osimertinib. JAMA Oncology 2018; 4(11): 1527-1534.
8. Callegari D, Ranaghan KE, Woods CJ, *et al*. L718Q mutant *EGFR* escapes covalent inhibition by stabilizing a non-reactive conformation of the lung cancer drug osimertinib. Chem Sci 2018 Feb 12; 9(10): 2740-2749.
9. Shen Q, Qu Z, Chen ZZ, *et al*. Case report: dacomitinib overcomes osimertinib resistance in NSCLC patient harboring L718Q mutation: a case report. Front Oncol 2021; 11: 760097.
10. Yang X, Huang C, Chen R, *et al*. Resolving resistance to osimertinib therapy with afatinib in an NSCLC patient with *EGFR* L718Q mutation. Clin Lung Cancer 2020; 21(4): e258-e260.
11. Zhang G, Yan B, Guo Y, *et al*. Case report: a patient with the rare third-generation TKI-resistant mutation *EGFR* L718Q who responded to afatinib plus cetuximab combination therapy. Front Oncol 2022; 12: 995624.
12. Liu Y, Li Y, Ou Q, *et al*. Acquired *EGFR* L718V mutation mediates resistance to osimertinib in non-small cell lung cancer but retains sensitivity to afatinib. Lung Cancer 2018; 118: 1-5.
13. Ma L, Chen R, Wang F, *et al*. *EGFR* L718Q mutation occurs without T790M mutation in a lung adenocarcinoma patient with acquired resistance to osimertinib. Ann Transl Med 2019; 7(9): 207.
14. Song Y, Jia Z, Wang Y, *et al*. Potential treatment strategy for the rare osimertinib resistant mutation *EGFR* L718Q. J Thorac Dis 2020; 12(5): 2771-2780.
15. Chen YC, Tsai MJ, Lee MH, *et al*. Lower starting dose of afatinib for the treatment of metastatic lung adenocarcinoma harboring exon 21 and exon 19

mutations. BMC Cancer 2021; 21(1): 495.
16. Cascetta P, Marinello A, Lazzari C, *et al*. *KRAS* in NSCLC: State of the art and future perspectives. Cancers (Basel) 2022; 14(21).
17. Hernandez-Martinez JM, Rosell R, Arrieta O. Somatic and germline ATM variants in non-small-cell lung cancer: therapeutic implications. Crit Rev Oncol Hematol 2023; 188: 104058.
18. Chen Y, Chen G, Li J, *et al*. Association of tumor protein p53 and ataxia-telangiectasia mutated comutation with response to immune checkpoint inhibitors and mortality in patients with non-small cell lung cancer. JAMA Netw Open 2019; 2(9): e1911895.
19. Leighl NB, Page RD, Raymond VM, *et al*. Clinical utility of comprehensive cell-free DNA analysis to identify genomic biomarkers in patients with newly diagnosed metastatic non-small cell lung Cancer. Clin Cancer Res 2019; 25(15): 4691-4700.
20. Rolfo C, Mack P, Scagliotti GV, *et al*. Liquid biopsy for advanced NSCLC: a consensus statement from the International Association for the Study of Lung Cancer. J Thorac Oncol 2021; 16(10): 1647-1662.
21. Li W, Liu JB, Hou LK, *et al*. Liquid biopsy in lung cancer: significance in diagnostics, prediction, and treatment monitoring. Mol Cancer 2022; 21(1): 25.
22. Schwartzberg LS, Horinouchi H, Chan D, *et al*. Liquid biopsy mutation panel for non-small cell lung cancer: analytical validation and clinical concordance. NPJ Precis Oncol 2020; 4: 15.
23. Müller JN, Falk M, Talwar J, *et al*. Concordance between comprehensive cancer genome profiling in plasma and tumor specimens. J Thorac Oncol 2017; 12(10): 1503-1511.
24. Liu J, Jin B, Su H, *et al*. Afatinib helped overcome subsequent resistance to osimertinib in a patient with NSCLC having leptomeningeal metastasis baring acquired *EGFR* L718Q mutation: a case report. BMC Cancer 2019; 19(1): 702.
25. Shen G, Shi L, Tian X, *et al*. Case report: response to almonertinib in a patient with metastatic NSCLC resistant to osimertinib due to acquired *EGFR* L718Q mutation. Front Pharmacol 2021; 12: 731895.

Nocardia farcinica Brain Abscess Preceded by Non-Resolving Pneumonia: A Case Report and literature Review

I-Yuan Chen[1], Chien-Wei Hsu[1,2*], Wei-Cheng Hong[1], David-Lin Lee[1,2]

Nocardia spp. are considered to be opportunistic pathogens. Pulmonary nocardiosis is the most common clinical presentation of infection, and primary infection can lead to hematogenous spread to multiple organs. The relatively slow growth on culture media and the difficulties in recognizing colony morphology result in difficulties in laboratory diagnosis, leading to delayed diagnosis. Currently, there is no universal consensus regarding the initial choice of antibiotics for nocardiosis, although trimethoprim-sulfamethoxazole remains the mainstay of a primary treatment regimen. Treatment for pulmonary nocardiosis requires at least 6 months, while central nervous system (CNS) involvement necessitates treatment for at least for 12 months. If CNS nocardiosis fails to respond to medical therapy, surgical intervention is required. Here, we report a case of brain abscess caused by *Nocardia farcinica*, which was preceded by non-resolving pneumonia for almost 5 months. Significant regression of the pneumonia patch was observed after initiating antibiotic treatment for nocardiosis. ***(Thorac Med 2024; 39: 241-248)***

Key words: *Nocardia farcinica*, nocardiosis, brain abscess

Introduction

Nocardia spp. are soil-born, Gram-positive, partially acid-fast, and filamentous bacteria, which were first described by Edmond Nocard in 1888 [1]. They are aerobic environmental bacteria and are usually considered to be opportunistic pathogens, belonging to the order Actinomycetes [2].

Inhalation is the primary route of exposure to Nocardia; therefore, pulmonary nocardiosis is the most common clinical presentation of infection. The symptoms include cough, shortness of breath, chest pain, hemoptysis, fever, night sweats, weight loss, and progressive fatigue, presenting with a subacute to acute course. Radiographic presentation can be variable, and include focal or multifocal disease, nodular or

[1]Division of Pulmonary Medicine, Kaohsiung Veterans General Hospital, [2]School of Medicine, National Yang-Ming Chiao-Tung University, Taipei, Taiwan
Address reprint requests to: Dr. Chien-Wei Hsu, Division of Pulmonary Medicine, Kaohsiung Veterans General Hospital No. 386, Dazhong 1st Rd., Zuoying Dist., Kaohsiung City 813, Taiwan (R.O.C.)

alveolar infiltrates, and cavitations [3].

Extrapulmonary nocardiosis can also occur through hematogenous dissemination or a contiguous spread of necrotizing pneumonitis into the pleura, pericardium, mediastinum, and vena cava. Abscess formation is characteristic of extrapulmonary nocardiosis. The central nervous system (CNS) is the most common extrapulmonary location for nocardiosis (up to 22.67% of all diagnosed nocardiosis in 1 series) [4].

Other frequent forms of extrapulmonary nocardiosis include involvement of bone, eyes, heart, joints, and kidneys. In addition, the skin, muscles, bones, and lymphatics are common sites of infection following traumatic inoculation [4].

Herein, we report a case of nocardiosis with CNS involvement, believed to originate from a delayed diagnosis of primary pulmonary nocardiosis.

Case Description

An 86-year-old man was admitted to the hospital in September 2021 with a complaint of worsening shortness of breath over the past 10 days. His medical history included a smoking habit of approximately 20 pack-years, hypertension, paroxysmal atrial fibrillation, and chronic obstructive pulmonary disease (COPD), group E. He had been on triple inhaled therapy (beclometasone/formoterol/glycopyrronium) for the 5 months prior to this visit. In addition, he had a diagnosis of severe thrombocytopenia with a baseline platelet count of around 20,000 per microliter, and had been treated for suspected immune thrombocytopenia purpura with prednisolone 10 mg per day for the past 8 months.

The initial chest radiograph (Fig. 1A) taken on Day 0 showed an ill-defined patchy opacity in the left upper lung field. Lab data revealed leukocytosis and prerenal azotemia. A chest computed tomography (CT) scan was performed, which showed segmental consolidation in the left upper lobe (LUL), along with a background of emphysema (Fig. 2A, Fig. 2B). The patient was then admitted with the impression of community-acquired pneumonia involving the left upper lobe and acute exacerbation of COPD.

After admission, the patient received a 1-week course of piperacillin-tazobactam and systemic corticosteroids (tapered from initial methylprednisolone 40 mg QD to prednisolone 10 mg QD). Symptoms gradually subsided and follow-up chest radiograph showed minor regression of the LUL opacity. The patient was discharged and received oral moxifloxacin in the outpatient clinic.

However, fever recurred 3 days after discharge. The patient was readmitted to receive piperacillin-tazobactam. A chest radiograph on Day 23 showed unresolved LUL opacity (Fig. 1B). A needle biopsy was performed for the LUL consolidation. The pathology report indicated organizing pneumonia, characterized by organizing fibrinous tissue in the alveolar spaces and mild chronic inflammatory cell infiltration in the alveolar septa. In addition, areas of fibrosis with fibroblasts or myofibroblast proliferation and foci of micro-abscess composed of neutrophils aggregation were observed. No microorganisms were identified from hematoxylin and eosin (H&E) stain, periodic acid–Schiff (PAS) stain, or acid-fast stain (AFS). Bacterial culture from the biopsy revealed Staphylococcus warneri, with susceptibility to oxacillin. After 2 weeks of treatment with piperacillin-tazobactam, the patient was discharged.

Fever and chills recurred on Day 56, lead-

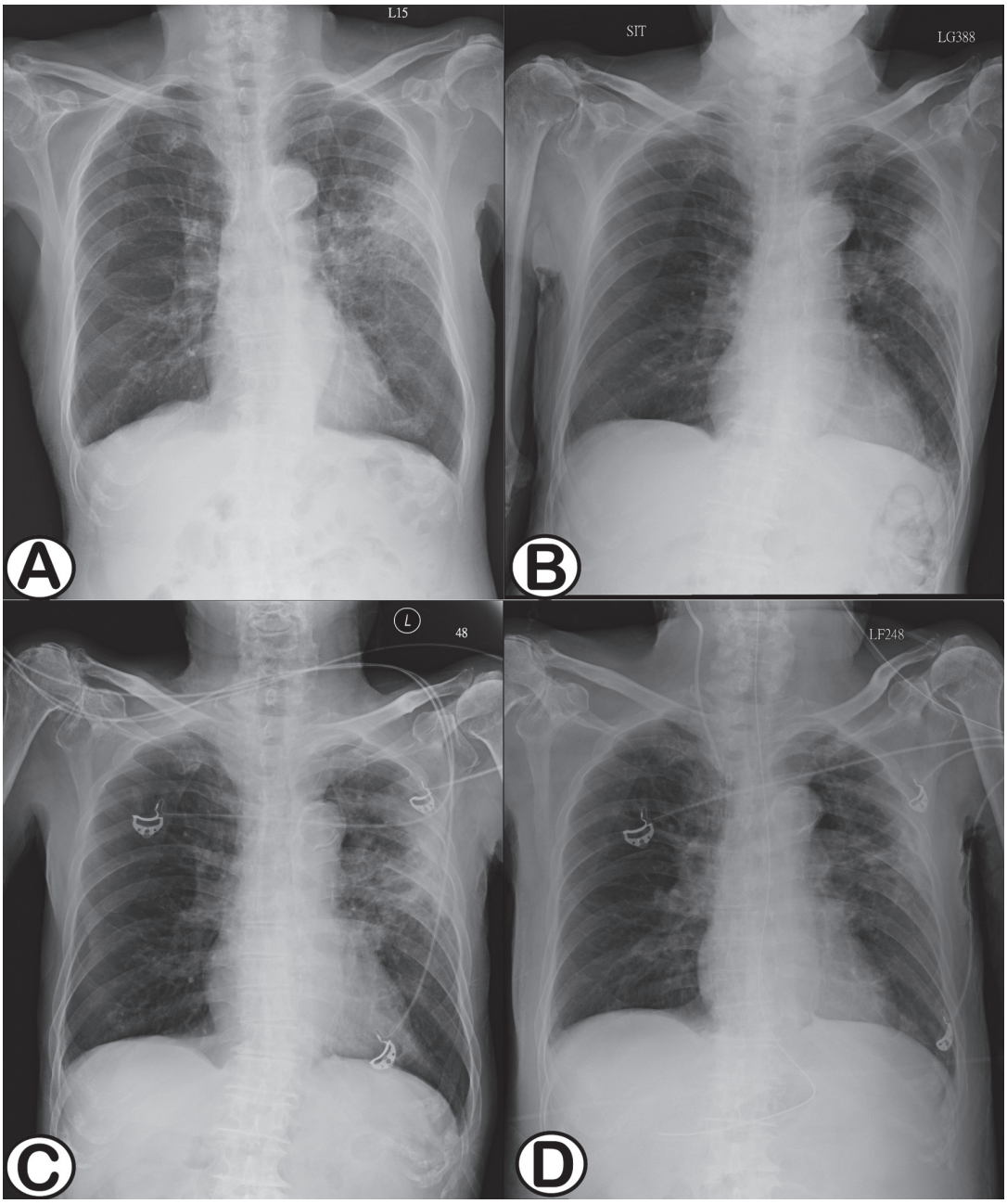

Fig. 1. Chest radiographs on (A) Day 0, first hospital visit with patchy opacity at the LUL field, (B) Day 23, delayed radiographic resolution of the patchy opacity in the LUL field, (C) Day 148, the last hospital visit due to altered mental status, showing persistence of the LUL patch, (D) Day 167, significant regression of the LUL patch after treatment with trimethoprim-sulfamethoxazole plus meropenem for 2 weeks. LUL: left upper lung.

ing to another admission for a 2-week course of broad-spectrum antibiotic treatment. Sequential chest radiographs still showed incomplete remission of the LUL patch (Fig. 1C).

On Day 148, the patient was admitted due to altered mental status and paraplegia of the left arm. The contrast-enhanced brain CT revealed a lobulated marginally-enhancing cystic

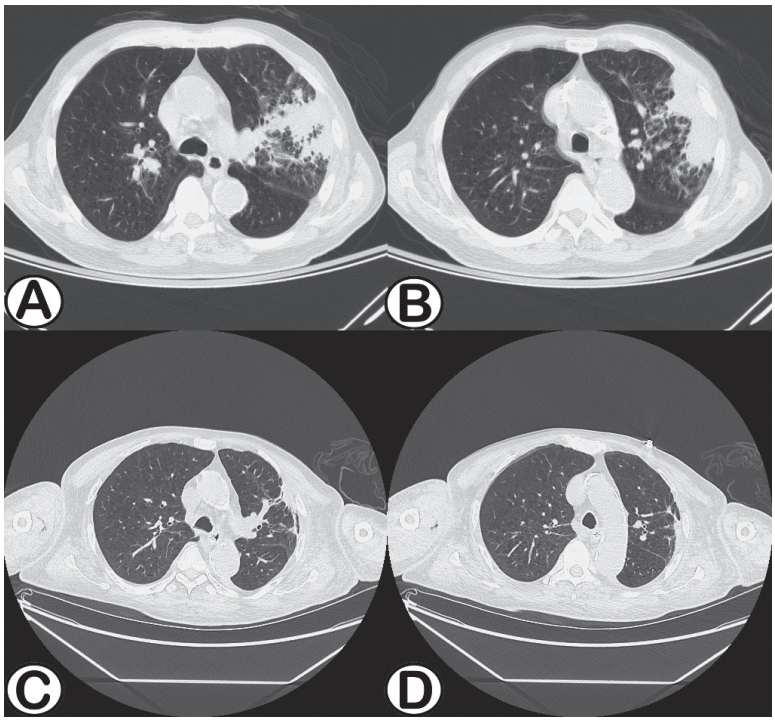

Fig. 2. (A)(B) High resolution chest computed tomography on Day 0, showing consolidation of the left upper lobe, with a background of pulmonary emphysema. (C)(D) High resolution chest computed tomography on Day 160 after 1 week of treatment with trimethoprim-sulfamethoxazole plus meropenem, revealing resolution of the consolidation in the left upper lobe.

mass lesion with perifocal edema at the right temporo-parietal lobes, leading to compression of the right lateral ventricle. Brain magnetic resonance imaging (MRI) was then performed, and showed findings consistent with a pyogenic abscess and an additional finding of abscess rupture into the right lateral ventricle (Fig. 3).

The patient received empirical ceftriaxone plus metronidazole for the brain abscess. On Day 152, surgery for external ventricular drainage was performed, and the pus obtained from the procedure revealed filamentous and branching bacilli with a positive result on AFS. Based on the suspicion of nocardiosis, the antibiotics were switched to trimethoprim-sulfamethoxazole plus meropenem, beginning on the day of surgery. Bacterial culture from the abscess yielded Nocardia farcinica 3 days after surgery. Follow-up chest radiograph demonstrated resolution of the LUL opacity (Fig. 1D). Chest CT also displayed resolution of the consolidation of the LUL (Fig. 2C, Fig. 2D). Brain CT showed resolution of the abscess (Fig. 4).

Tragically, prolonged ventilator dependence developed following surgery, and was subsequently complicated by a catheter-related bloodstream infection with candidemia, sepsis, and ultimately, mortality.

Discussion

Nocardiosis primarily affects the lungs. Various CT findings of pulmonary nocardiosis have been reported in the literature, including consolidation with or without cavitation, cavitary and non-cavitary pulmonary nodules/

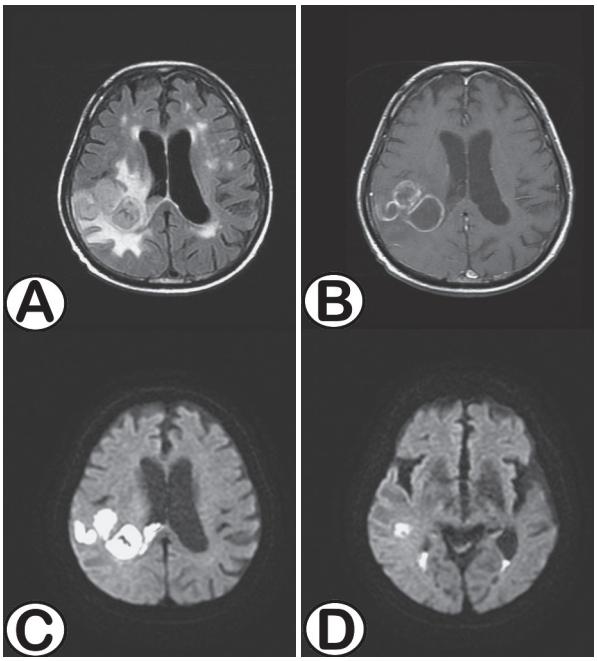

Fig. 3. Brain magnetic resonance imaging performed on Day 149, during the last admission. (A) T2-weighted-fluid-attenuated inversion recovery (T2-FLAIR), (B) T1-weighted image (T1WI) with gadolinium enhancement. (A) and (B) revealed a multi-lobulated cystic lesion with marginal enhancement, accompanied by perifocal edema and compression of the right lateral ventricle, consistent with a pyogenic abscess. In addition, the FLAIR image displayed a rupture into the right lateral ventricle, which was further confirmed by diffusion-weighted imaging. (C) DWI at the same level as (A) and (B), showing a high signal in the right lateral ventricle, indicating abscess rupture, (D) DWI at an inferior level showing high signals at the dependent portions of bilateral lateral ventricles. DWI: diffusion-weighted imaging.

masses, ground glass opacities, centrilobular nodules, interlobular septal thickening, a crazy paving pattern, pleural effusion and chest wall extension.

A recent case series summarized studies with more than 2 cases that reviewed the radiological features of pulmonary nocardiosis since 1995. The most common radiographic findings were nodules/masses with or without cavitation (121 of 148 cases). This was followed by consolidation (86 of 148 cases), cavitation (55 of 148 cases), and ground glass opacities (33 of 148 cases) [5].

Nocardiosis is often associated with an immunocompromised status; however, some of the infections occurred in immunocompetent patients [4]. There is a higher risk for nocardiosis in patients with depressed cell-mediated immunity, including lymphoma, other selected malignancies, human immunodeficiency virus (HIV) infection, solid-organ or hematopoietic stem cell transplant, and those receiving long-term treatment with steroids or other medications that suppress cell-mediated immunity [6, 7, 8]. Besides, COPD has a common association

Fig. 4. Serial brain CT of the patient. (A) Day 148, contrast-enhanced brain CT showing a lobulated marginally-enhancing cystic mass lesion with perifocal edema at the right temporo-parietal lobes, leading to compression of the right lateral ventricle, (B) Day 156, non-contrast brain CT showing placement of an external ventricular drain into the right lateral ventricle, (C) Day 162, non-contrast brain CT showing the presence of pneumocephalus after removal of the external ventricular drain and resolution of the brain abscess.

with pulmonary nocardiosis, especially in the setting of concurrent corticosteroid use [9].

In a case series of 53 patients, the majority of associated predisposing factors for Nocardia farcinica infections were immunosuppressive treatment (28%), preceding operation (26%) and hematological neoplasm (13%), followed by transplant recipient (13%), HIV infection (11%), chronic lung disease (9%), diabetes mellitus (8%) renal disease (8%), solid neoplasm (6%), alcoholism (6%), trauma (6%), and concomitant mycobacterial infection (4%). The lung and pleura were major sites of infection (43%), followed by the brain and meninges (30%), and surgical wounds (15%) [10]. In another series of 67 patients with nocardiosis caused by Nocardia farcinica, immunosuppressive treatment also accounted for the majority of risk factors. The lung (59.7%) and brain (32.8%) are the most frequently affected sites of infection [11].

When nocardiosis is clinically suspected, the lab should be informed for optimal recognition. Gram staining is the most sensitive method to visualize nocardiae in clinical samples. Using a modified Kinyoun acid-fast stain, nocardiae appear as partially acid-fast filamentous bacilli [12]. Nocardia colonies may take 2 to 14 days to appear [13]. Selective media like paraffin agar, Thayer-Martin, and charcoal-buffered yeast extract enhance Nocardia recovery and minimize contaminants [14-16]. Colonial morphology for aerial hyphae should be observed to differentiate Nocardia from related genera, including Rhodococcus, Gordonia, Tsukamurella, Corynebacterium, and Mycobacterium [17]. Chemotaxonomic and serological methods can also aid in distinguishing Nocardia from mycobacteria [18]. Due to the expertise required and discrimination limitations in the above methods, molecular identification is now the primary method for nocardiae species identification.

The Clinical & Laboratory Standards Institute (CLSI) recommends 16S rRNA, gyrB, or secA1 gene sequencing to identify Nocardia species in human clinical isolates [19]. 16S rRNA gene sequences are the gold standard, providing reliable, rapid (1-2 days), and phylogenetic information superior to phenotypic methods [18]. The gyrB gene distinguishes Nocardia from other mycolic acid-containing genera [20], and combining 16S and gyrB sequences improves identification [21]. However, the secA1 gene is preferred for its faster molecular clock and higher diversity [22].

Emerging techniques like multilocus sequence typing (MLST), whole genome analysis, and Matrix-assisted laser desorption ionization-time of flight (MALDI-TOF) proteomics are gaining popularity [23]. MLST offers superior discrimination and phylogenetic insights through multiple loci, but has interpretation challenges [23].

MALDI-TOF is reliable, rapid, and cost-effective for diverse Nocardia taxonomy, overcoming biochemical limitations [18]. Optimal results are achieved with Columbia blood agar or similar media within 48 hours of incubation [24]. Though MALDI-TOF identifies most Nocardia isolates accurately, some species may require DNA sequencing, as it remains the current gold standard for identification [25].

Sulfonamide antibiotics, most commonly trimethoprim-sulfamethoxazole, have been used to treat nocardiosis since the 1940s, and continue to be the most common antibiotics used for nocardiosis [26-27]. However, increasing resistance to sulfonamide antibiotics has been reported since the period 1995 to 2004 [28]. Alternative options include minocycline, line-

zolid, moxifloxacin, amoxicillin-clavulanate, and amikacin [29-30].

We reported a case of brain abscess caused by Nocardia farcinica. The patient had risk factors for nocardiosis, including COPD and long-term systemic corticosteroids. The existence of these risk factors and a similar presentation in patients should lead to a suspicion of nocardiosis among clinicians. In such cases, the laboratory should be informed to optimize the recognition of Nocardia. Measures such as utilizing a modified AFS, selective culture media, and adequate preparation for MALDI-TOF should be taken. These measures can potentially lead to earlier diagnosis and treatment of nocardiosis.

References

1. Nocard E. Note sur la maladie des boeufs de la Guadeloupe connue sous le nom de farcin. Ann Inst Pasteur 1888; 2: 293-302. [In France]
2. Fatahi-Bafghi M. Nocardiosis from 1888 to 2017. Microb Pathog 2018; 114: 369-84.
3. Martinez R, Reyes S, Menendez R. Pulmonary nocardiosis: risk factors, clinical features, diagnosis and prognosis. Curr Opin Pulm Med 2008; 14(3): 219-27.
4. Beaman BL, Beaman L. *Nocardia* species: host-parasite relationships. Clin Microbiol Rev 1994; 7(2): 213-64.
5. Al Umairi RS, Pandak N, Al Busaidi M, *et al*. The findings of pulmonary nocardiosis on chest high resolution computed tomography: single centre experience and review of literature. Sultan Qaboos University Med J 2022; 22(3), 357-61.
6. Wilson JW. Nocardiosis: updates and clinical overview. Mayo Clin Proc 2012; 87(4): 403-07.
7. Young LS, Rubin RH. Mycobacterial and *nocardia*l diseases in the compromised host. In: Rubin RH, Young LS, eds. A Clinical Approach to Infection in the Compromised Host. 4th ed. New York; Kluwer Academic, 2002: 257-61.
8. Long PF. A retrospective study of *Nocardia* infections associated with the acquired immune deficiency syndrome (AIDS). Infection 1994; 22(5): 362-64.
9. Martinez TR, Menendez VR, Reyes CS, *et al*. Pulmonary nocardiosis: risk factors and outcomes. Respirology 2007; 12(3): 394-400.
10. Torres OH, Domingo P, Pericas R, *et al*. Infection caused by *Nocardia farcinica*: case report and review. Eur J Clin Microbiol Infectious Dis 2000; 19: 205-12.
11. Budzik JM, Hosseini M, Mackinnon Jr. AC, *et al*. Disseminated *Nocardia farcinica*: literature review and fatal outcome in an immunocompetent patient. Surg Infect (Larchmt) 2012; 13(3): 163-70.
12. Saubolle MA, Sussland D. Nocardiosis: review of clinical and laboratory experience. J Clin Microbiol 2003; 41: 4497-501.
13. Berd D. Laboratory identification of clinically important aerobic actinomycetes. Appl Microbiol 1973; 25: 665-81.
14. Burgert SJ. Nocardiosis: a clinical review. Infect Dis Clin Pract 1999; 8: 27-32.
15. Mishra SK, Randhawa HS. Application of paraffin bait technique to the isolation of *Nocardia* asteroides from clinical specimens. Appl Microbiol 1969; 18: 686-87.
16. Murray PR, Niles AC, Heeren RL. Modified Thayer-Martin medium for recovery of *Nocardia* species from contaminated specimens. J Clin Microbiol 1988; 26: 1219-20.
17. Brown JM, McNeil MM. *Nocardia*, Rhodococcus, Gordonia, Actinomadura, Streptomyces, and other aerobic actinomycetes. In: Murray PR, *et al*. eds, Manual of Clinical Microbiology, 8th ed. Washington, D.C.; ASM Press, 2003: 370-98.
18. Brown-Elliott BA, Brown JM, Conville PS, *et al*. Clinical and laboratory features of the *Nocardia* spp. based on current molecular taxonomy. Clin Microbiol Rev 2006; 19: 259-82.
19. Susceptibility Testing of Mycobacteria, *Nocardia* spp., and Other Aerobic Actinomycetes. 3rd ed. Wayne PA; Clinical and Laboratory Standards Institute, 2018.
20. Takeda K, Kang Y, Yazawa K, *et al*. Phylogenetic studies of *Nocardia* species based on gyrB gene analyses. J Med Microbiol 2010; 59: 165-71.
21. Carrasco G, Valdezate S, Garrido N, *et al*. gyrB analysis as a tool for identifying *Nocardia* species and exploring their phylogeny. J Clin Microbiol 2015; 53: 997-1001.
22. Conville PS, Witebsky FG. Organisms designated as *Nocardia* asteroides drug pattern type VI are members of

the species *Nocardia* cyriacigeorgica. J Clin Microbiol 2007; 45: 2257-59.
23. Rita MT, Melissa EB, Brent L. Updated review on *Nocardia* species: 2006-2021. Clin Microbiol Rev 2022; 35(4): e0002721.
24. McTaggart LR, Chen Y, Poopalarajah R, *et al*. Incubation time and culture media impact success of identification of *Nocardia* spp. by MALDI-ToF mass spectrometry. Diagn Microbiol Infect Dis 2018; 92: 270-74.
25. Girard V, Mailler S, Welker M, *et al*. Identification of Mycobacterium spp. and *Nocardia* spp. from solid and liquid cultures by matrix-assisted laser desorption ionization-time of flight mass spectrometry (MALDI-TOF MS). Diagn Microbiol Infect Dis 2016; 86: 277-83.
26. Glover RP, Herrell WE, Heilman FR, *et al*. *Nocardia* asteroides infection simulating pulmonary tuberculosis. JAMA 1948; 136: 172-75.
27. Wallace, Jr. RJ, Septimus EJ, Williams Jr. TW, *et al*. Use of trimethoprim-sulfamethoxazole for treatment of infections due to *Nocardia*. Rev Infect Dis 1982; 4: 315-25.
28. Uhde KB, Pathak S, McCullum Jr. I, *et al*. Antimicrobial-resistant *Nocardia* isolates, United States, 1995-2004. Clin Infect Dis 2010; 51: 1445-48.
29. Mamelak AN, Obana WG, Flaherty JF, *et al*. *Nocardia*l brain abscess: treatment strategies and factors influencing outcome. Neurosurgery 1994; 35: 622-31.
30. Welsh O, Vera-Cabrera L, Salinas-Carmona MC. Mycetoma. Clin Dermatol 2007; 25: 195-202.

Delayed Acquired Diaphragmatic Hernia after Penetrating Trauma, A Case Report and Review of the Literature

Hung-Hsiang Chao[1], Wei-Chang Huang[2, 3, 4], Chih-Hung Lin[5], Yi-Chun Hsiao[2]

Acquired diaphragmatic hernia is a rare complication following major traumas. The insidious nature and symptoms of the disease make it difficult to diagnose. We present the case of a patient with traumatic diaphragmatic hernia that was diagnosed 16 months after a knife stabbing. The patient underwent video-assisted thoracoscopic surgery, and there was no recurrence during the follow-up period. Our case may highlight the possibility of managing a delayed diaphragmatic hernia via minimally-invasive thoracoscopic surgery in selected patients. We also reviewed recent literature on traumatic diaphragmatic hernia. ***(Thorac Med 2024; 39: 249-255)***

Key words: traumatic diaphragmatic hernia, video-assisted thoracic surgery

Introduction

Acquired diaphragmatic rupture with organ herniation represents a rare and elusive complication that can emerge after traumatic incidents. The incidence of acquired diaphragmatic hernia varied from 0.5% to 3.6% in different studies [1, 2]. Traumatic diaphragmatic hernias are traditionally classified into 3 phases and are categorized into 2 types: acute and delayed [3]. Acute traumatic diaphragmatic hernia refers to symptomatic herniation within 14 days after a traumatic event, and usually takes place within 1 day. In contrast, the delayed-type hernia could occur months or even years later. The non-specific symptoms of herniation, including dyspnea, chest pain and gastrointestinal discomfort, make it difficult for physicians to diagnose the disease in the beginning. Treatment usually involves surgical intervention with laparotomy

[1]Department of Internal Medicine, Taichung Veterans General Hospital, Taichung, Taiwan. [2]Division of Chest Medicine, Department of Internal Medicine, Taichung Veterans General Hospital, Taichung, Taiwan. [3]Department of Post-Baccalaureate Medicine, College of Medicine, National Chung Hsing University, Taichung, Taiwan. [4]School of Medicine, Chung Shan Medical University, Taichung, Taiwan. [5]Division of Thoracic Surgery, Department of Surgery, Taichung Veterans General Hospital, Taichung, Taiwan
Address reprint requests to: Dr. Yi-Chun Hsiao, Division of Chest Medicine, Department of Internal Medicine, Taichung Veterans General Hospital, No.1650, Sect. 4, Taiwan Blvd., Taichung, 407 Taiwan

or thoracotomy [4]. We present the case of a patient with a delayed left diaphragmatic hernia diagnosed 16 months after a knife stabbing injury. The patient was successfully treated with video-assisted thoracic surgery, resulting in the absence of residual symptoms. We also review recent published literature on acquired diaphragmatic rupture.

Case Presentation

A 26-year-old male visited the emergency department due to left lower chest tingling pain for 3 days, exacerbated by bending down, with mild shortness of breath. Initial surveillance through a hemogram and electrocardiogram showed no remarkable findings. However, chest X-ray showed a mass lesion at the left costophrenic angle (Figure 1). Upon tracing the patient's history, it was discovered that he had been stabbed in the left chest with a knife during a brawl. He had been admitted for the management of post-traumatic hemopneumothorax with thoracostomy 16 months prior to this visit. After 17 days of admission, the patient was discharged home without thoracotomy, and there was neither an acute complication nor abnormality noted in the image study during the follow-up period (Figure 2). Due to the patient's traumatic history and the findings on chest X-ray, a chest computed tomography (CT) study was scheduled, and revealed a left lateral diaphragmatic hernia with herniation of omental fat and without bowel incarceration (Figure 3). A thoracic surgeon was consulted for possible surgical intervention.

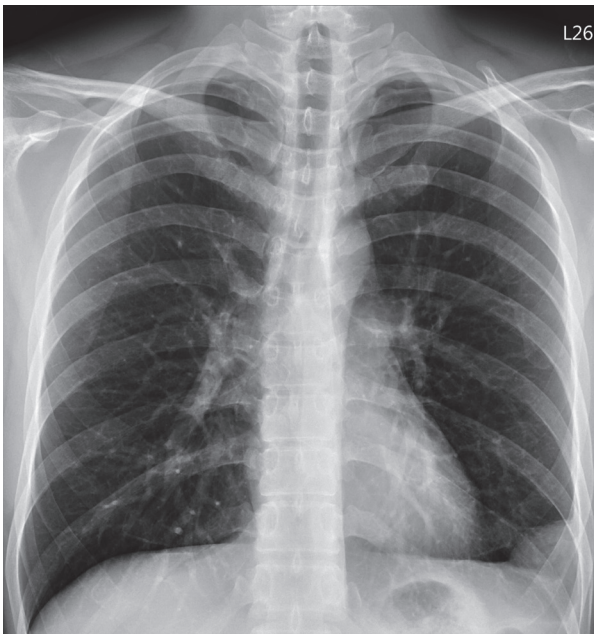

Fig. 1. Chest X-ray showed a mass lesion at the left costophrenic angle.

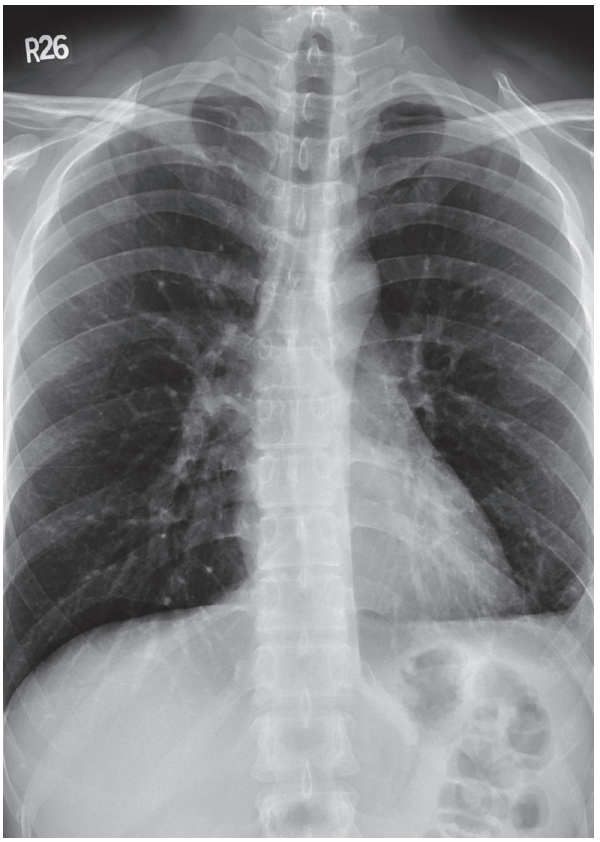

Fig. 2. Chest X-ray showed resolution of the left hemopneumothorax of the previous trauma.

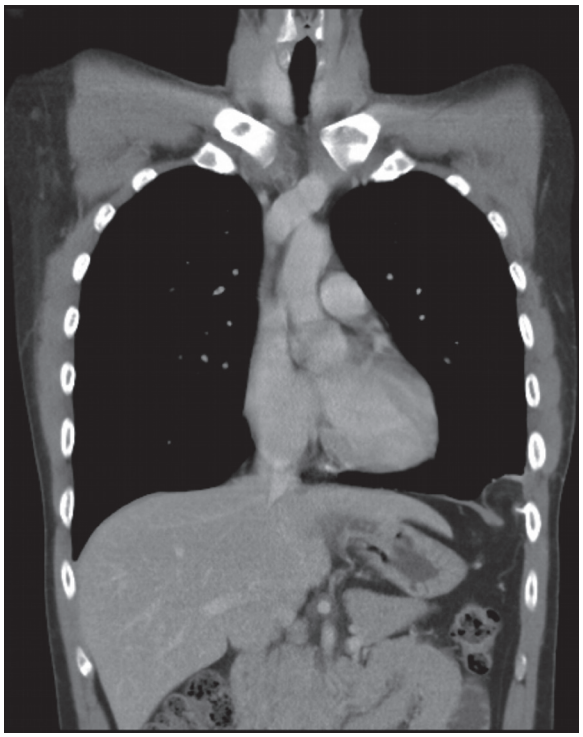

Fig. 3. Chest computed tomography showed a left lateral diaphragmatic hernia with herniation of the omental fat.

Considering the patient's stable vital signs and low risk of abdominal organ involvement, a minimally invasive procedure with video-assisted thoracoscopic surgery for repair of the diaphragmatic hernia was scheduled 2 weeks later. During the operation, a trocar was first inserted from the 7th intercostal space at the posterior axillary line. A mini-thoracotomy was carried out at the 6th intercostal space of the anterior axillary line. A diaphragm defect, about 3 x 2 cm in size, near the left costophrenic angle, with partial omentum herniation, was noted. Cauterization was used for adhesiolysis, and the herniated viscera was softly reduced manually (Figure 4). The diaphragmatic defect was closed and repaired with 3 interrupted 1-0 silk stitches. The closed defect was covered and reinforced with an 8.5 x 10.5 cm vicryl mesh. A 20 Fr. straight chest tube was left at the trocar

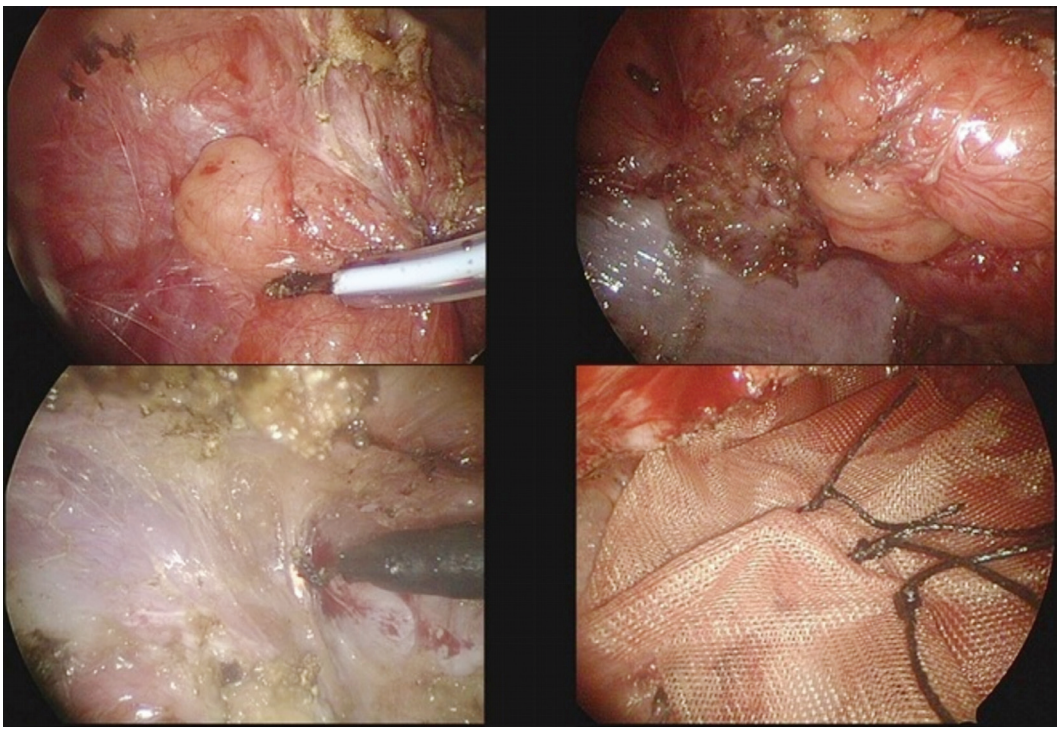

Fig. 4. Adhesiolysis and reduction of herniated omental fat under video-assisted thoracoscopic surgery with mesh and suture repair of the defect.

hole after the surgery. No acute postoperative complication was noted and the left chest tube was removed smoothly 4 days later. During the 3-month follow-up period at the outpatient department, the symptoms resolved. No recurrence of herniation was observed in the chest CT scan performed 3 months after surgery.

Discussion

Acquired diaphragmatic hernia is a rare complication that results mostly from trauma, and occurs in around 1% of traumatic patients. The majority of traumatic diaphragmatic hernias are caused by blunt traumas, such as a traffic accident, while the others are caused by penetrating trauma, like a stab wound. Males are prone to experiencing a traumatic diaphragmatic hernia. The left side is also more likely to develop this type of hernia than the right, probably due to the lack of protection that the liver provides on the right side, or the higher prevalence of right-handed assassins.

Image findings include soft tissue opacity in the chest, pneumothorax, and rib fractures from the index injury. CT scan shows the organ herniating into the thoracic cavity, and the "collar sign", also known as the "hour glass sign"[5], named as a result of the distorted appearance of the herniated organs. MRI, despite taking more time to produce the image and prone to being affected by motion artifacts, can still provide a diagnosis under T1-weighted images [6].

Once the diagnosis of diaphragmatic hernia is made, the patient should undergo surgical repair [2]. Most patients receive laparotomy management for acute traumatic diaphragmatic hernia due to the concomitant intraabdominal organ damage. As for chronic and relatively stable patients, minimally invasive management with laparoscopy or thoracoscopic repair could be considered. After repairing the diaphragm via primary suturing, additional mesh reinforcement is considered, especially with large defects. In a retrospective review by Palanivelu C, *et al*. involving 21 patients, including 3 with chronic traumatic diaphragmatic hernia who underwent laparoscopic repair, reinforcing the defect with mesh was considered to reduce the risk of recurrence, and therefore was widely used [7].

In our literature review, we searched for case reports from 2020 to 2023 on PubMed using the keywords "acquired diaphragmatic hernia" and "acquired diaphragmatic rupture", and compiled data regarding the patient's age, nature of injury, time from injury to symptom onset, site of herniation, and how the herniation was treated. A total of 26 results were found, but only 20 patients were reviewed after excluding those patients without sufficient data. The basic characteristics are listed in Table 1. There were 17 male and 3 female patients aged from 20 to 66 years old. The median age was 30 years. The most reported causal mechanism was blunt injury from a traffic accident or a falling event in 14 patients, while the remaining 6 patients suffered from penetrating trauma due to a stabbing wound. The predominant clinical presentations of these patients were dyspnea, chest pain, abdominal pain, or a combination of these symptoms. Left-side herniation constituted of 80% of cases.

Diaphragmatic hernia could be classified into 2 groups, acute and delayed, based on whether the onset of symptoms was within 14 days or not. Twelve patients (60%) had acute diaphragmatic hernia, and most of them suffered from symptomatic hernia on the same day as the traumatic event. In contrast, 8 patients

Table 1. The Characteristics of Patients with Acquired Diaphragmatic Hernia Reported in Studies Published Between 2020 and 2023

No	Gender	Age (years)	Traumatic mechanism	Time from trauma to symptomatic hernia	Symptoms	Management	Ref.
1	Female	39	Traffic accident	The same day	Blood pressure instability. Chest and right shoulder pain	Exploratory laparotomy	[10]
2	Male	20	Blunt injury	The same day	Abdominal pain and dyspnea	Laparoscopic surgery	[11]
3	Female	28	Traffic accident	The same day	Dyspnea	Exploratory laparotomy	[12]
4	Male	27	Blunt trauma	9 years	Right chest pleuritic pain and RUQ pain	Exploratory laparotomy	[13]
5	Male	35	Traffic accident	The same day	Dyspnea, abdominal tenderness, and muscle guarding	Laparoscopic surgery	[14]
6	Female	23	Traffic accident	The same day	Dyspnea, chest and abdominal pain	Exploratory laparotomy	[15]
7	Male	25	Stabbed in the back with a knife	4 days	Sharp periumbilical pain radiating to the left chest, vomiting, and dyspnea	Exploratory laparotomy	[16]
8	Male	57	Traffic accident	2 years	Dyspnea, hiccups, and cough for 15 days	Exploratory laparotomy	[17]
9	Male	59	Stabbed in the right chest	29 years	Post-prandial epigastric pain for 6 months	Laparoscopic surgery	[18]
10	Male	58	Fall from bicycle	The same day	Dyspnea and left chest pain for 1 day	Thoracotomy	[19]
11	Male	30	Traffic accident	5 years	Dyspnea for 5 years, worsening in the most recent month	Exploratory laparotomy	[20]
12	Male	24	Traffic accident	The same day	Chest pain	Video-assisted thoracoscopic surgery, then thoracotomy	[21]
13	Male	36	Traffic accident	10 years	Chest pain	Laparoscopic and thoracoscopic surgery	[22]
14	Male	26	Stabbed in the left chest	2 days	Dyspnea	Exploratory laparotomy	[23]
15	Male	36	Fall (from 18 meters above)	The same day	Dyspnea	Exploratory laparotomy	[24]
16	Male	30	Fall (from 6 meters above)	8 days	Dyspnea, chest, abdominal pain, and food content leakage from chest tube	Exploratory laparotomy	[25]
17	Male	54	Stabbed in the left subcostal region	3 months	Dyspnea, abdominal and thoracic pain	Exploratory laparotomy	[26]
18	Male	23	Stabbed in the left chest	3 years	Progressive flatulence and defecation disturbance for 2 years	Exploratory laparotomy	[27]
19	Male	66	Falling event	4 days	Left back and shoulder pain	Laparoscopic surgery	[28]
20	Male	26	Stabbed in the left chest	16 months	Left chest pain and dyspnea	Video-assisted thoracoscopic surgery	Our case

(40%) suffered from delayed diaphragmatic hernia. The median time from the traumatic event to symptomatic hernia was 4 years, ranging from 3 months to 29 years. Most patients (N=12, 60%) underwent exploratory laparotomy, while 5 patients (25%) received laparoscopic surgery. One patient received video-assisted thoracoscopic surgery, but shifted to thoracotomy during the operation. Interestingly, our analysis did not uncover a case report that documented the management of delayed diaphragmatic hernia exclusively using thoracoscopic techniques.

Shah R, *et al*. conducted a literature review of 980 patients with traumatic diaphragmatic hernia, finding that 14.6% of the patients had a delayed diagnosis, and the overall mortality rate was 17% [8]. In another case series, Beauchamp G, *et al*. reported 2 mortality cases due to delayed diagnosis of the hernia, 1 resulting in cardiac arrest and the other in septic shock. [9]. Given the possibility that traumatic hernias remain dormant for a long period, and considering the morbidity risk, it is important for physicians to be increasingly aware when encountering patients with a history of trauma, even if the inciting event occurred years ago.

Conclusion

Delayed diaphragmatic hernia, despite its rarity, may still cause fatality if left untreated. Considering that it can be fully reversed with a surgical approach, the importance of a prompt diagnosis through history-taking and image survey of the patient is therefore emphasized. Our case may contribute to raising physician awareness that a delayed diaphragmatic hernia should be considered when the patient has a previous traumatic history, and highlight the possibility of managing such a condition via minimally-invasive thoracoscopic surgery in selected patients.

References

1. Kozak O, Mentes O, Harlak A, *et al*. Late presentation of blunt right diaphragmatic rupture (hepatic hernia). Am J Emerg Med 2008; 26(5): 638 e3-5.
2. Simon LV, Lopez RA, Burns B. Diaphragm rupture. StatPearls [Internet]. 2023.
3. Lu J, Wang B, Che X, *et al*. Delayed traumatic diaphragmatic hernia: a case-series report and literature review. Medicine (Baltimore) 2016; 95(32): e4362.
4. Zhao L, Han Z, Liu H, *et al*. Delayed traumatic diaphragmatic rupture: diagnosis and surgical treatment. J Thorac Dis 2019; 11(7): 2774-7.
5. Venkatasamy A, Huynh TT, Caron B, *et al*. The hourglass sign. Abdom Radiol (NY) 2018; 43(6): 1508-9.
6. Eren S, Kantarci M, Okur A. Imaging of diaphragmatic rupture after trauma. Clin Radiol 2006; 61(6): 467-77.
7. Palanivelu C, Rangarajan M, Rajapandian S, *et al*. Laparoscopic repair of adult diaphragmatic hernias and eventration with primary sutured closure and prosthetic reinforcement: a retrospective study. Surg Endosc 2009; 23(5): 978-85.
8. Shah R, Sabanathan S, Mearns AJ, *et al*. Traumatic rupture of diaphragm. Ann Thorac Surg 1995; 60(5): 1444-9.
9. Beauchamp G, Khalfallah A, Girard R, *et al*. Blunt diaphragmatic rupture. Am J Surg 1984; 148(2): 292-5.
10. Aolayan K, Almohammadi T, Alotaibi A. A diaphragmatic hernia in a traumatic patient simulating a hemorrhage: a case report. Trauma Case Rep 2023; 43: 100754.
11. Charara RH, Ibrahim R, Zaarour R, *et al*. Laparoscopic repair of acute traumatic diaphragmatic hernia: a case report. Cureus 2023; 15(6): e40959.
12. Chellasamy RT, Rajarajan N, Pio Samy NM, *et al*. A rare case of traumatic pericardio-diaphragmatic injury following a road traffic accident. Cureus 2023; 15(5): e39125.
13. Soomro FH, Hassan A, Nazir I, *et al*. Intra-thoracic symptomatic gallstones in a right-sided post-traumatic diaphragmatic hernia: a case report. Cureus 2022; 14(12): e32824.

14. Chitrambalam TG, George NM, Joshua P, *et al*. An interesting case of laparoscopic management of traumatic diaphragmatic rupture in an acute setting. Trauma Case Rep 2023; 43: 100775.
15. Naik Mude N, Prakash S, Shaikh O, *et al*. Traumatic diaphragmatic rupture with pericardial tear and transdiaphragmatic herniation of the stomach. Cureus 2022; 14(9): e29473.
16. Machaku D, Gnanamuttupulle M, Wampembe E, *et al*. A rare case report of perforated viscerothorax in a traumatic diaphragmatic rupture. Int J Surg Case Rep 2022; 99: 107688.
17. Yunus Shah M, Abdrabou AA, Obalappa P. Delayed presentation of post-traumatic multiorgan left diaphragmatic hernia: a case report and literature review. Cureus 2022; 14(7): e26814.
18. Jain N, Raju BP, Dhanda S, *et al*. Delayed presentation of a post-traumatic large right diaphragmatic hernia displacing liver and gallbladder - a case report. Asian J Endosc Surg 2022; 15(2): 388-92.
19. Lee SH, Lee SG, Kim DH, *et al*. Diaphragmatic hernia with stomach rupture after blunt chest trauma at a short interval: a case report. J Chest Surg 2022; 55(1): 85-7.
20. Alsuwayj AH, Al Nasser AH, Al Dehailan AM, *et al*. Giant traumatic diaphragmatic hernia: a report of delayed presentation. Cureus 2021; 13(12): e20315.
21. Innes R, Kulkarni M. Liver in the chest: a case of a large traumatic diaphragmatic rupture. Cureus 2021; 13(8): e17028.
22. Kumar A, Parshad R, Suhani, *et al*. Thoracolaparoscopic repair of diaphragmatic hernias. Indian J Thorac Cardiovasc Surg 2021; 37(5): 558-64.
23. Nappi F, Fiore A, Avtaar Singh SS. Diaphragmatic rupture: too much to stomach. Ann Thorac Surg 2021; 112(5): e391.
24. Handaya AY, Fauzi AR, Andrew J, *et al*. Clinical findings and management of diaphragmatic rupture with hernia caused by safety body harness: a case report. Ann Med Surg (Lond) 2021; 66:102429.
25. Agrawal S, Gajula B, Chongtham AK, *et al*. Unusual complication of intercostal tube drainage of penetrating chest injury: a case report. Cureus 2021; 13(3): e13813.
26. Nusretoğlu R, Dönder Y. Faecopneumothorax due to missing diaphragmatic hernia: a case report. J Med Case Rep 2021; 15(1): 19.
27. Dorgam Maués CA, de Vasconcelos ELC, da Silva Galvão R, *et al*. Diaphragmatic herniation after 3 years of penetrating trauma managed through laparotomy: a case report. Int J Surg Case Rep 2021; 79: 58-61.
28. Nishikawa S, Miguchi M, Nakahara H, *et al*. Laparoscopic repair of traumatic diaphragmatic hernia with colon incarceration: a case report. Asian J Endosc Surg 2021; 14(2): 258-61.

Osmotic Demyelination Syndrome Following Oral Sodium Phosphate Solution Administration for Colon Preparation: A Case Report and Literature Review

Hsiu-Li Wu[1], Chen-Chun Lin[2]

Osmotic demyelination syndrome (ODS) is a rare neurological disorder characterized by non-inflammatory demyelination of the pons. Etiological factors for ODS include rapid correction of hyponatremia, alcoholism, hypertonic or hypotonic syndrome, acquired immunodeficiency syndrome, liver transplantation, refeeding syndrome, and electrolyte imbalances. In this report, we present the case of an elderly individual who fell into a coma following ingestion of 90 ml of oral sodium phosphate solution for colon preparation prior to colonoscopy. Brain magnetic resonance imaging and laboratory data analysis confirmed the diagnosis of ODS, with hyperphosphatemia identified as a contributing factor. A comprehensive literature review was conducted to explore the underlying mechanisms and risk factors for ODS. ***(Thorac Med 2024; 39: 256-261)***

Key words: central pontine myelinolysis, osmotic demyelination syndrome, hyperphosphatemia

Introduction

Osmotic demyelination syndromes (ODS) consist of central pontine myelinolysis and extrapontine myelinolysis. These syndromes were first described by Adams *et al*., who noted the destruction of myelin sheaths in the central part of the basis pontine in alcoholic patients without any signs of inflammation [1]. While rapid correction of hyponatremia is a well-known cause of ODS, it is not the only contributing factor. Other clinical conditions associated with ODS include hyperglycemic hypertonic syndrome, refeeding syndrome, alcoholism, hypokalemia, and liver transplant. ODS is often underdiagnosed in clinical settings and can be fatal due to its imperceptible nature [2]. In this report, we present the case of an elderly patient who developed central pontine myelinolysis following the administration of 90 mL of oral sodium phosphate solution for colon preparation prior to colonoscopy.

Case Report

A 78-year-old male with a medical history

[1]Department of Nursing, Shin Kong Wu Ho-Su Memorial Hospital, Taiwan. [2]Division of Pulmonary Medicine, Department of Internal Medicine, Shin Kong Wu Ho-Su Memorial Hospital, Taiwan
Address reprint requests to: Dr. Chen-Chun Lin, No. 95, Wen-Chang Rd., Shih-Lin, Taipei, Taiwan

of type 2 diabetes mellitus and stage 3 chronic kidney disease presented to the emergency department with progressive dyspnea. Laboratory results showed severe anemia (hemoglobin 5.3 g/dL) and hyponatremia (104 mmol/L). The patient was conscious and hemodynamically stable, and normal saline solution was administered at 40 mL/hr. The serial changes in the patient's renal function tests, electrolytes, and osmolarity are presented in Table 1 and Figure 1.

Table 1. Serial Changes in Renal Function tests, Electrolytes, and Osmolarity During Admission

Item/ admission day	Na (mmol/L)	K (mmol/L)	Cl (mmol/L)	P (mg/dl)	BUN (mg/dl)	Cr. (mg/dl)	Ccr	Osmolarity (mOsm/kg)
1	104	4.7		3.4		1.58		228
2	115				34	1.53		248
3	121	3.4			35	1.72		283
5	127	3.5			33	1.63		271
7	132				37	1.63		282
8	137	3.0		11.2	43	2.01	-10.3	298
9	143	2.8		10.4	39	2.67	-11.5	319
10	147	2.8	100	10.2	46	2.72	-3.2	321
11	145	3.6		9.3	57	2.93	3.5	323
12	146	3.4	109	8.3	58	2.82	4.6	321
14	151	3.2	117	5.3	64	2.37		373
17	149	3.4			54	1.91		362
21	144	3.5		2.6	47	1.51		312
24	139	3.6	112	2.6	46	1.46	-0.1	306

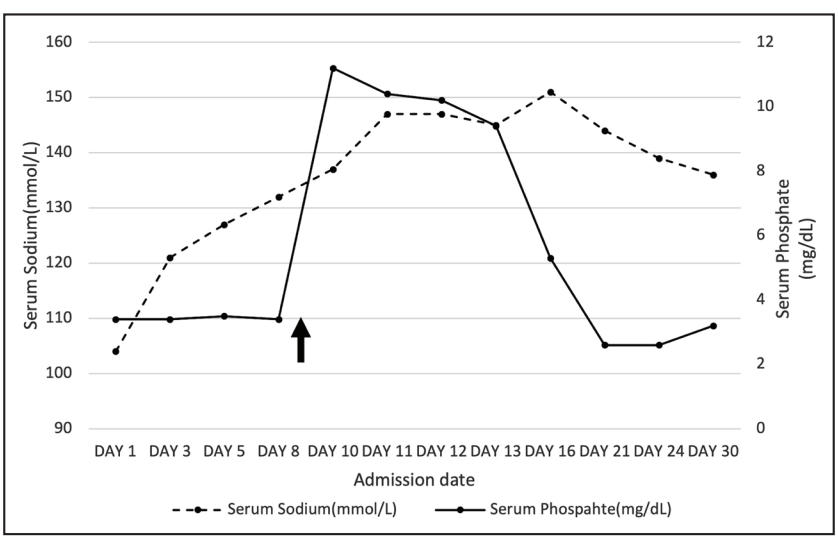

Fig. 1. Changes in serum sodium and phosphate levels over time. Black arrow: day of administration of sodium phosphate solution.

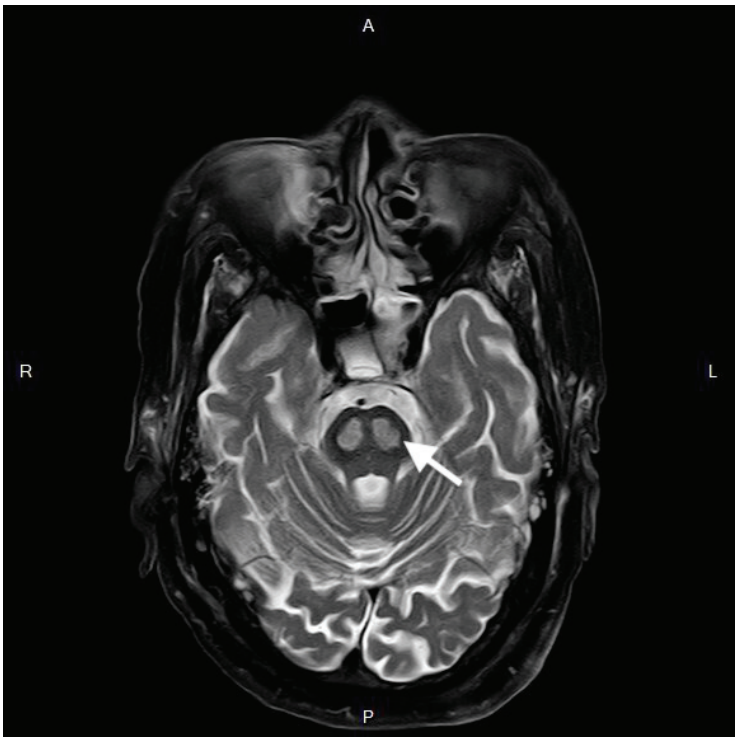

Fig. 2. T2-weighted brain MRI revealed a typical "bat wing" or "butterfly" appearance on coronal view (white arrow).

A colonoscopy was scheduled on the seventh day of admission to investigate the cause of anemia. For colon preparation, the patient was given 90 mL of oral sodium phosphate solution containing 43.2 g of monobasic sodium phosphate (NaH_2PO4) and 16.2 g of dibasic sodium phosphate (Na_2HPO4). However, the patient developed muscle weakness the day after administration of the sodium phosphate solution, and his dysarthria and consciousness disturbance progressed to coma on the eighth day of admission. The patient was transferred to the intensive care unit (ICU) and intubated.

Hypotension and decreased urine output developed on the first day of ICU admission, and norepinephrine infusion was started due to persistent hypotension after fluid resuscitation. Laboratory data revealed high levels of phosphate (11.2 mg/dL) and lactate (146.2 mg/dL), low potassium (2.8 mmol/L), and normal sodium (147 mmol/L). After implementing the best supportive care, the patient regained consciousness on the fifth day of admission to the ICU. Brain MRI revealed a symmetrical hyperintense signal at the pons, consistent with central pontine myelinolysis (Figure 2). Despite receiving several weeks of supportive treatment, the patient remained dependent on mechanical ventilation due to his advanced age and multiple comorbidities.

Discussion

Osmotic demyelination syndrome (ODS) is a complex condition that can have serious consequences for patients. The diagnosis and

management of ODS require a thorough understanding of its pathophysiology and risk factors. While rapid correction of hyponatremia is a well-known cause of ODS, it has also been observed in patients with certain underlying conditions, including chronic kidney disease, diabetes mellitus, malnutrition, liver transplantation, chronic alcoholism, and hypophosphatemia [3-5]. The overall incidence of ODS has been suggested to be 0.5% [6]. Pathologically, ODS is characterized by a symmetric, non-inflammatory loss of myelin with preservation of neuronal cell bodies and axons (myelinolysis) of the central pons, and with sparing of the peripheral fibers and the axons of the corticospinal tracts [7].

The clinical features of ODS can vary depending on the severity and location of the brain lesions and may include symptoms such as weakness, dysarthria, confusion, seizures, and coma. The diagnosis of ODS is usually made as a result of the presence of neurological symptoms following rapid correction of hyponatremia in conjunction with characteristic brain MRI findings. These image features include the presence of symmetrical demyelinating lesions in the brain that frequently exhibit a triangular shape on axial images, as well as a "bat wing" or "butterfly" appearance on coronal views [8].

The precise mechanisms underlying the development of ODS have yet to be fully understood. However, the condition is initiated by osmotic stress, which causes injury to the brain. Glial cells, responsible for regulating extracellular osmolality and electrolyte balance to support the surrounding neurons, are particularly vulnerable to this stress. When glial cells are faced with an osmotic challenge, they activate the Na/K-ATPase pump to adjust intracellular electrolyte levels, resulting in a series of heavy metabolic expenses that can cause glucose to be metabolized into lactate and trigger apoptosis [9]. In addition to the metabolic stress caused by osmotic stress, the release of glutamate and other excitatory neuromodulators can lead to harmful metabolic consequences for both glial cells and neurons [5, 10]. Previous studies have shown that severe hypophosphatemia can adversely affect the Na/K-ATPase pump and initiate apoptosis, which can result in the development of ODS [5].

In our case, the patient developed severe hyperphosphatemia after administration of oral sodium phosphate solution. The mechanisms of hyperphosphatemia that contribute to ODS development are poorly understood. However, one possible mechanism is that the rapid changes in plasma phosphate may lead to osmotic stress in the brain, which may contribute to cellular stress and eventual apoptosis [5]. Sodium phosphate solution is a hypertonic solution that induces bowel evacuation through osmosis by drawing water into the intestinal lumen. If bowel evacuation fails, fluid can pool in the gut, causing dehydration. Furthermore, if sodium phosphate is retained in the gut lumen, it can be potentially absorbed, resulting in sudden and severe hypernatremia and hyperphosphatemia, leading to a further increase in cell stress [11].

The administration of sodium phosphate solution has been associated with various adverse events, including hypocalcemia, hypokalemia, hypernatremia, hypovolemia, hyperphosphatemia, ischemic colitis, acute kidney injury, and acute phosphate nephropathy [12]. In addition, a previous study reported that nearly all elderly patients who receive oral sodium phosphate will exhibit elevated blood phosphate levels, rising from 2.6 to 4.7 mg/dL before oral admin-

istration to 4.5 to 10.4 mg/dL on the second day after administration. Moreover, the increase in blood phosphate levels is positively correlated with a reduction in creatinine clearance (R= -0.52; P = .001) [13]. The US FDA has also issued a safety alert for oral sodium phosphate, cautioning that its use can result in severe electrolyte imbalances, dehydration, metabolic acidosis, renal failure, seizures, and even death [14].

Our patient had an impaired renal clearance rate and mild hyponatremia (132 mmol/L) before his altered mental status (Table 1). On the day of his altered mental status (Day 8), the blood sodium level was 137 mmol/L, but the blood phosphate level was elevated to 11.2 mg/dL, from 3.4 mg/dL, and osmolality increased from 282 to 298 mOsmo/kg. Thus, we postulate that the occurrence of ODS in the patient was not due to the rapid rise of blood sodium, but to dehydration and hyperphosphatemia caused by the administration of sodium phosphate. This resulted in an increase in blood osmotic pressure, which may have been the underlying cause of ODS. Under normal circumstances, the impact of blood phosphate levels on osmolality can be ignored. However, in certain special conditions such as renal failure or diabetes, or in elderly patients, oral sodium phosphate can lead to high blood phosphate levels and further increases in osmolality.

The management of ODS requires a multidisciplinary approach, and may involve supportive care, such as respiratory and hemodynamic support, and careful electrolyte management. Hypertonic solutions, such as sodium phosphate, should be used cautiously, as they can lead to serious adverse events if not administered appropriately. In addition, patients with risk factors for ODS should be carefully monitored, and treatment decisions should be individualized based on their clinical status and underlying conditions.

Conclusion

ODS can result from various electrolyte imbalances, and in the elderly population, the use of sodium phosphate solution for colon preparation prior to colonoscopy can lead to acute changes in serum phosphate levels and volume depletion, causing an acute rise in serum osmolarity and subsequent osmotic stress, ultimately leading to ODS. Administering oral sodium phosphate solution to elderly patients for colon preparation, especially those with concomitant hyponatremia and renal impairment, should be done with caution.

References

1. Adams RD, Victor M, Mancall EL. Central pontine myelinolysis: a hitherto undescribed disease occurring in alcoholic and malnourished patients. AMA Arch Neurol Psychiatry 1959; 81(2): 154-72.
2. Lambeck J, Hieber M, Dressing A, *et al*. Central pontine myelinosis and osmotic demyelination syndrome. Dtsch Arztebl Int 2019; 116(35-36): 600-06.
3. Jacoby N. Electrolyte disorders and the nervous system. Continuum (Minneap Minn) 2020; 26(3): 632-58.
4. Jha AA, Behera V, Jairam A, *et al*. Osmotic demyelination syndrome in a normonatremic patient of chronic kidney disease. Indian J Crit Care Med 2014; 18(9): 609-11.
5. Michell AW, Burn DJ, Reading PJ. Central pontine myelinolysis temporally related to hypophosphataemia. J Neurol Neurosurg Psychiatry 2003; 74(6):820.
6. Bose P. Central pontine myelinolysis and the osmotic demyelination syndromes: an open and shut case? Acta Neurol Belg 2021; 121(4): 849-58.
7. Alleman AM. Osmotic demyelination syndrome: central pontine myelinolysis and extrapontine myelinolysis. Semin Ultrasound CT MR 2014; 35(2): 153-59.

8. Alkali NH, Jibrin YB, Dunga JA, *et al*. Osmotic demyelination syndrome following acute kidney injury with hypernatremia. Niger J Clin Pract 2019; 22(8): 1166-68.
9. Ashrafian H, Davey P. A review of the causes of central pontine myelinosis: yet another apoptotic illness? Eur J Neurol 2001; 8(2): 103-09.
10. Leist M, Nicotera P. Apoptosis, excitotoxicity, and neuropathology. Exp Cell Res 1998; 239(2): 183-201.
11. Mendoza J, Legido J, Rubio S, *et al*. Systematic review: the adverse effects of sodium phosphate enema. Aliment Pharmacol Ther 2007; 26(1): 9-20.
12. Balaban DH. Guidelines for the safe and effective use of sodium phosphate solution for bowel cleansing prior to colonoscopy. Gastroenterol Nurs 2008; 31(5): 327-334; quiz 334-325.
13. Beloosesky Y, Grinblat J, Weiss A, *et al*. Electrolyte disorders following oral sodium phosphate administration for bowel cleansing in elderly patients. Arch Intern Med 2003; 163(7): 803-08.
14. FDA Drug Safety Communications, U.S. Food and Drug Administration, 1 Aug 2014.

Post-COVID-19 Pulmonary Fibrosis: A Case Report and Literature Review

Yung-Hsuan Wang[1], Chih-Bin Lin[1,2]

Severe acute respiratory syndrome coronavirus 2 (SARS-CoV-2) became a global pandemic in December 2019. Pulmonary fibrosis is one of the major long-term complications in patients with coronavirus-induced disease 2019 (COVID-19). There have been some ongoing clinical trials of therapies for post-COVID-19 pulmonary fibrosis. Anti-fibrotic agents such as pirfenidone and nintedanib might be potential treatment options. We reported the case of a patient with COVID-19 that developed severe pulmonary fibrosis and restrictive lung disease. Improvement of pulmonary fibrosis and lung function were noted after pirfenidone was prescribed. ***(Thorac Med 2024; 39: 262-266)***

Key words: SARS-CoV-2, COVID-19, pulmonary fibrosis, pirfenidone

Introduction

After its outbreak in December 2019, severe acute respiratory syndrome coronavirus 2 (SARS-CoV-2) became a global pandemic. The symptoms associated with coronavirus-induced disease 2019 (COVID-19) ranged from upper airway symptoms to acute respiratory distress syndrome. Patients of an older age and with preexisting comorbidities of diabetes, cardiovascular disease, hypertension, or obesity, and those who were immunocompromised, had a higher risk of developing severe COVID-19 [1]. The sequelae of COVID-19 may include abnormal lung function, decreased life quality and lung tissue damage [2]. Pulmonary fibrosis is one of the major long-term complications in patients with COVID-19 [3]. Anti-fibrotic agents such as pirfenidone and nintedanib might have a role in treating fibrosis after SARS-CoV-2 infection [1]. There are some ongoing clinical trials of therapies for post-COVID-19 pulmonary fibrosis [3]. Here, we report the case of a COVID-19 patient with improving pulmonary fibrosis and lung function after pirfenidone was prescribed.

Case Presentation

A 48-year-old Taiwanese businessman who

[1]Division of Chest Medicine, Department of Internal Medicine, Hualien Tzu Chi Hospital, Buddhist Tzu Chi Medical Foundation, Hualien, Taiwan. [2]Buddhist Tzu Chi Medical Foundation and Tzu Chi University.
Address reprint requests to: Dr. Yung-Hsuan Wang, Division of Chest Medicine, Hualien Tzu Chi Hospital, Buddhist Tzu Chi Medical Foundation, Hualien 97004, Taiwan

worked in Vietnam had diabetes and hypertension and had not received coronavirus vaccination. An outbreak of the SARS-CoV-2 Delta variant occurred in his factory in July 2021. He presented with fever, dry cough, exertional dyspnea, anosmia and dysgeusia. His SARS-CoV-2 real-time polymerase chain reaction test (RT-PCR) was positive on July 26, 2021. He was admitted to the hospital in Vietnam for 2 months. Severe COVID-19 pneumonia was diagnosed. High-flow nasal cannula was used to maintain O_2 saturation above 90%. Antibiotics treatment and pulmonary rehabilitation were arranged during the hospitalization. Weight loss of 20 kilograms was recorded during the 2 months in the hospital. After discharge, he still needed O_2 inhalation through a nasal cannula at a rate of 2 liters per minute with persistent symptoms of cough and exertional dyspnea.

The patient returned to Taiwan for further medical treatment in September 2021. His basic blood profile and biochemistry were normal. An infection workup was negative for bacterial, fungal, and viral growth, including Mycoplasma pneumoniae, Legionella pneumophila, Chlamydia pneumoniae, pulmonary tuberculosis, Pneumocystis jirovecii, Aspergillus, cytomegalovirus, and herpes simplex virus. The SARS-CoV-2 nasopharyngeal RT-PCR was still positive, with a cycle threshold value of 32.3 on September 21, 2021. A chest radiograph in September 2021 showed fibrotic changes in bilateral lungs (Figure 1). Chest computed tomography (CT) revealed ground-glass opacities (GGO), traction bronchiectasis and interstitial fibrosis in bilateral lungs (Figure 2A). A diagnosis of post-COVID-19 pulmonary fibrosis was made. After explanation to the patient, self-pay pirfenidone 600 mg daily was started for 14 days. Dosage was gradually titrated to 1200 mg per day from Day 15 to Day 28, then increased to 1800 mg per day beginning on Day 29.

Initial pulmonary function test reported restrictive ventilatory impairment and reduced diffusion capacity of the lungs for carbon monoxide (DLCO) after 2 weeks of treatment. Within 3 months of treatment, forced vital capacity (FVC) increased to 770 ml, DLCO improved to 2.07 mmol/(min*kPa), and 125 meters were added to the patient's 6-minute walking test distance (Table 1). After treatment with pirfenidone for 4 months, chest CT images revealed reductions in the area of GGO and fibrosis (Figure 2). The patient's exercise tolerance was improving, and he tolerated the pirfenidone treatment without severe side effects, including skin rash, hepatitis, or diarrhea.

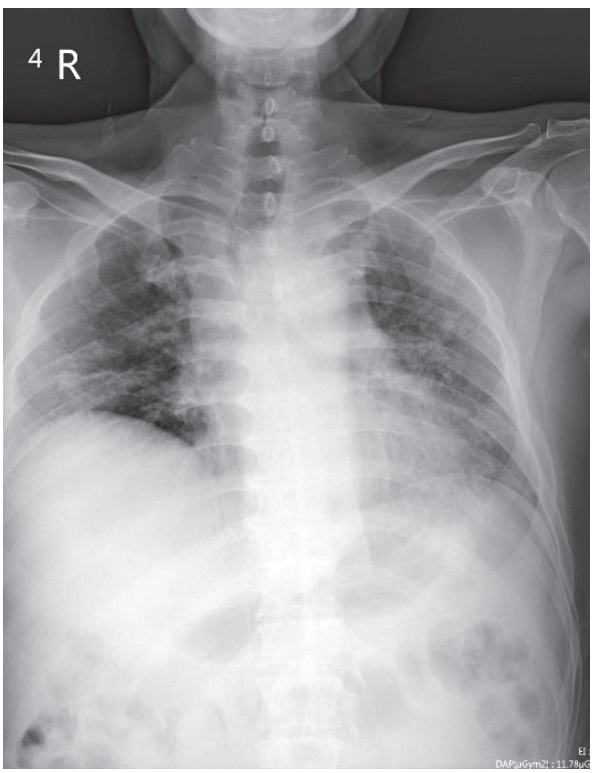

Fig. 1. Chest radiograph showed fibrotic changes in bilateral lungs.

Table 1. Pulmonary Function test. Within 3 Months of Treatment, FVC Increased to 770 ml, DLCO Improved to 2.07 mmol/(min*kPa), and 125 Meters Were Added to the Patient's 6-minute Walking Test (6MWT) Distance

	FVC (liters)	FEV1 (liters)	DLCO (mmol/min*kPa)	6MWT (meters)
Two weeks post-treatment	1.56	1.32	2.81	440
Three months post-treatment	2.33	2.01	4.88	565
Changes	0.77	0.69	2.07	125

A. Twenty days before pirfenidone treatment.

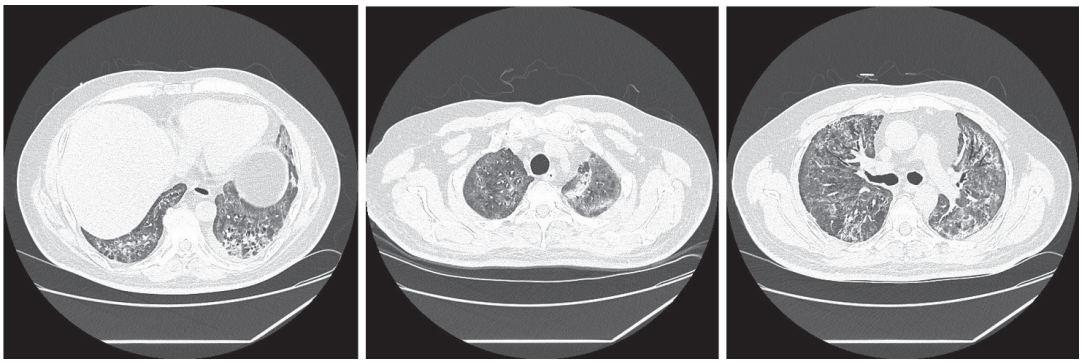

B. Just before pirfenidone treatment.

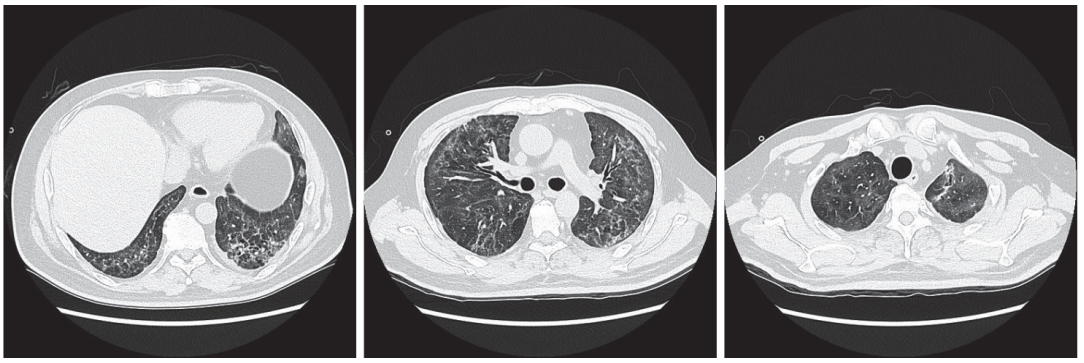

C. Four months after pirfenidone treatment.

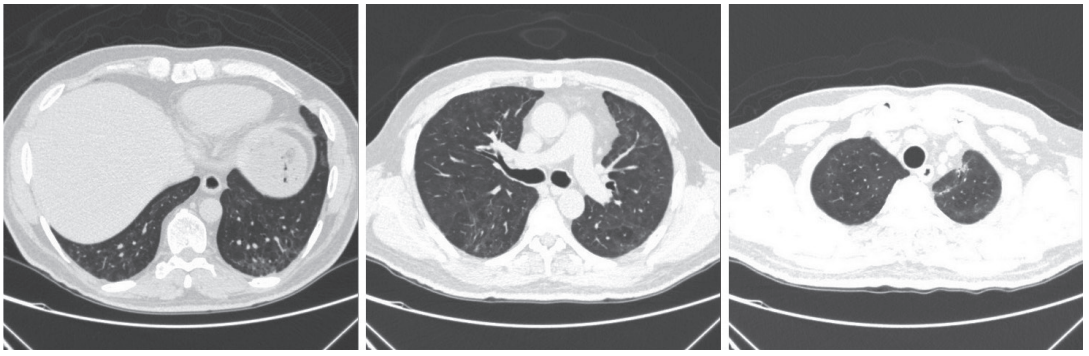

Fig. 2. Serial chest CT images at the lower lobe level, at the carina level and at the upper lobe level, which revealed GGO, traction bronchiectasis and interstitial fibrosis in bilateral lungs. CT images showed reductions in the area of GGO and fibrosis compared to the images obtained before treatment.

Discussion

Severe COVID-19 is associated with risk factors such as older age, male gender, hypertension, diabetes mellitus, and ischemic heart disease [9]. These factors are also linked to the development of progressive lung fibrosis [9, 13].

Pulmonary fibrosis was found in 56% of moderate COVID-19 patients and in 71% of severe patients [6]. SARS-CoV-2 infects type II alveolar epithelial cells to activate macrophages and recruit immune cells, which leads to a cytokine storm [14]. Activation of profibrotic pathways by COVID-19 has the potential to develop pulmonary fibrosis. In COVID-19, the most frequently observed radiological pattern is organizing pneumonia, which can lead to fibrotic remodeling in severe diseases [10]. Chest CT images can reveal reticulations, honeycombing, traction bronchiectasis, parenchymal bands, irregular interfaces, interlobular septal thickening, lung distortion, GGO, meshwork, consolidation, and crazy paving [7]. One year after recovering from COVID-19 pneumonia, persistent radiological findings may vary from GGO and subpleural reticulation to more severe traction bronchiectasis, and honeycombing [11]. Reduction of the DLCO and pulmonary interstitial damage were common respiratory manifestations of COVID-19 [3]. These complications can lead to patient disability. Pulmonary rehabilitation, including exercise training, education, and behavioral changes, can improve the physical and psychological condition of the patient [8].

Anti-fibrotic therapies, including pirfenidone and nintedanib, are known to be effective in inhibiting the reduction of respiratory function and in increasing the life expectancy of patients with idiopathic pulmonary fibrosis [1]. Ongoing clinical trials are surveying what might be adequate therapy for post-COVID-19 pulmonary fibrosis [3]. A multicenter, retrospective study has reported on a survey of the administration of pirfenidone or nintedanib for post-COVID-19 interstitial lung abnormalities [4]. However, the study included only 142 subjects. Larger randomized studies are still required to investigate the long-term efficacy and safety of these treatments.

In considering that the patient's dyspnea was related to pulmonary fibrosis, and also considering current possible medications, we chose pirfenidone as an off-label treatment for his fibrosis. Pirfenidone-related side effects include skin rash, photosensitivity, elevation of liver enzymes and gastrointestinal upset [7]. While the patient is on an anti-fibrotic treatment course, those side effects should be monitored carefully.

Conclusion

We presented the case of a patient with post-COVID-19 pulmonary fibrosis that was treated with pirfenidone, with improvement in pulmonary fibrosis and lung function. Currently available scientific evidence for the efficacy of anti-fibrotic agents for post-COVID-19 pulmonary fibrosis treatment needs more research. We hope the ongoing trials may offer more information about the clinical course of the disease and treatment choices.

References

1. George PM, Wells AU, Jenkins RG. Pulmonary fibrosis and COVID-19: the potential role for antifibrotic therapy. Lancet Respir Med 2020 Aug; 8(8): 807-15.
2. Li X., Shen C., Wang L., *et al*. Pulmonary fibrosis

and its related factors in discharged patients with new coronavirus pneumonia: a cohort study. Respir Res 2021; 22:203.

3. Bazdyrev E, Rusina P, Panova M, *et al*. Lung fibrosis after COVID-19: treatment prospects. Pharmaceuticals (Basel) 2021 Aug 17; 14(8): 807.
4. Dhooria S, Maturu VN, Talwar D, *et al*. A multicenter survey study of antifibrotic use for symptomatic patients with post-COVID-19 interstitial lung abnormalities. Lung India 2022 May-Jun; 39(3): 254-260.
5. Gulati S, Luckhardt TR. Updated evaluation of the safety, efficacy and tolerability of pirfenidone in the treatment of idiopathic pulmonary fibrosis. Drug Healthc Patient Saf 2020 May 7; 12: 85-94.
6. Fu Z, Tang N, Chen Y, *et al*. CT features of COVID-19 patients with two consecutive negative RT-PCR tests after treatment. Sci Rep 2020; 10: 11548.
7. Hama Amin BJ, Kakamad FH, Ahmed GS, *et al*. Post COVID-19 pulmonary fibrosis; a meta-analysis study. Ann Med Surg 2022; 77: 103590.
8. Reina-Gutiérrez S, Torres-Costoso A, Martínez-Vizcaíno V, *et al*. Effectiveness of pulmonary rehabilitation in interstitial lung disease, including coronavirus diseases: a systematic review and meta-analysis. Arch Phys Med Rehabil 2021; 102: 1989-97.
9. Hu J, Wang Y. The clinical characteristics and risk factors of severe COVID-19. Gerontology 2021; 67(3): 255-266.
10. Vadász I, Husain-Syed F, Dorfmüller P, *et al*. Severe organizing pneumonia following COVID-19. Thorax 2021 Feb; 76(2): 201-204.
11. Luger AK, Sonnweber T, Gruber L, *et al*. Chest CT of lung injury 1 year after COVID-19 pneumonia: the CovILD Study. Radiology 2022 Aug; 304(2): 462-470.
12. Fabbri L, Moss S, Khan FA, *et al*. Parenchymal lung abnormalities following hospitalization for COVID-19 and viral pneumonitis: a systematic review and meta-analysis. Thorax 2023 Feb; 78(2): 191-201.
13. Shah AS, Wong AW, Hague CJ, *et al*. A prospective study of 12-week respiratory outcomes in COVID-19-related hospitalisations. Thorax 2021 Apr; 76(4): 402-04.
14. Singh SJ, Baldwin MM, Daynes E, *et al*. Respiratory sequelae of COVID-19: pulmonary and extrapulmonary origins, and approaches to clinical care and rehabilitation. Lancet Respir Med 2023 Aug; 11(8): 709-25.

Diagnostic Lobectomy for Life-threatening Hemoptysis: A Rare Presentation of Pulmonary Arteriovenous Malformation

Ruei-Lin Sun[1,2], Yi-Chen Yeh[2,3], Chung-Wei Chou[1,2*]

A 61-year-old man presented with fever, dyspnea, and blood-streaked sputum for 1 day, and his condition rapidly progressed to massive hemoptysis and respiratory failure on the second day of his stay. Chest computed tomography (CT) revealed predominant consolidation of the left lung without evidence of contrast extravasation. Bronchoscopy revealed blood clots extending from the left main bronchus to the left upper lung (LUL), resulting in total occlusion of the LUL without detectable sources of bleeding. Tests for microbial infection and vasculitis antibodies were negative. The patient underwent a lobectomy of the LUL supported by venovenous extracorporeal membrane oxygenation. Histopathological examination of the resected lung tissue confirmed pulmonary arteriovenous malformation (PAVM). This case report highlights a rare instance of near-fatal recurrent hemoptysis due to PAVM without classic CT findings and diagnosed after surgical intervention. ***(Thorac Med 2024; 39: 267-270)***

Key words: hemoptysis, pulmonary arteriovenous malformation

Introduction

Massive hemoptysis is a medical emergency that is associated with a high mortality risk and necessitates immediate intervention. Common causes of hemoptysis include bronchiectasis; an infection such as a fungal infection, tuberculosis, or necrotizing pneumonia; neoplasms; vasculitis or collagen vascular diseases; and vascular abnormalities [1]. Pulmonary arteriovenous malformation (PAVM) is a vascular abnormality that involves a direct connection between the pulmonary artery and pulmonary vein without capillary intervention. While typically asymptomatic, PAVMs may manifest with dyspnea or, less commonly, epistaxis, particularly in association with hereditary hemorrhagic telangiectasia (HHT) [2]. PAVMs may also lead to massive, potentially fatal hemoptysis [3]. The gold standard for diagnosing PAVMs

[1]Department of Chest Medicine, Taipei Veterans General Hospital, Taipei, Taiwan. [2]School of Medicine, National Yang Ming Chiao Tung University, Taipei, Taiwan. [3]Department of Pathology and Laboratory Medicine, Taipei Veterans General Hospital, 11 Taipei, Taiwan.
Address reprint requests to: Dr. Chung-Wei Chou,Department of Chest Medicine, Taipei Veterans General Hospital No. 201, Sec. 2, Shih-Pai Rd., Taipei, Taiwan.

is contrast-enhanced computed tomography (CT), which typically reveals a feeding artery, a draining vein, and an aneurismal sac. In the present case report, we describe a patient with near-fatal hemoptysis due to a PAVM that was undetected in serial CT scans and ultimately confirmed after surgical resection. We also explore the factors that may have contributed to the prior failure to detect PAVM via imaging.

Case Report

A 61-year-old man, previously in good health and with an 8-pack-per-year smoking history for 40 years, presented with a 1-day history of fever, dyspnea, and blood-streaked sputum. He reported no animal exposure or travel during the preceding few years. His medical history and family history were negative for recurrent epistaxis, respiratory problems, gastrointestinal bleeding, and cerebrovascular events.

Initially suspected of having pneumonia, the patient was given antibiotics upon admission and maintained at 95% oxygen saturation through a nasal cannula at 3 L/min. However, on the following day, he experienced massive hemoptysis, and his oxygen saturation dropped to 88%, despite the administration of oxygen through a non-rebreathing mask, thereby necessitating intubation. Subsequent contrast-enhanced chest CT revealed consolidation of the left lung, but no clear signs of contrast extravasation or vascular abnormalities (Figures 1A and 1B). Comprehensive microbiological testing ruled out bacterial, fungal, viral, and mycobacterial infections. In addition, tests for anti-nuclear, anti-neutrophil cytoplasmic, and anti-glomerular basement membrane antibodies were negative.

During the patient's first week of hospitalization, he experienced recurrent massive hemoptysis, maintaining an average PaO_2 of 90 mmHg on a ventilator set at 80%–90% FiO_2, which precluded further chest CT scans. Instead, bronchoscopy was performed, revealing blood clots from the left main bronchus to the left upper lung (LUL), which caused total occlusion of the LUL without visible sources of active bleeding. Despite multiple attempts to remove these blood clots through bronchoscopy, another CT scan on the 20th day of hospitalization, with a modified CT pulmonary angiography protocol, revealed the same left lung consolidation without evidence of contrast extravasation. By the third week of hospitalization, the patient still exhibited persistent bloody

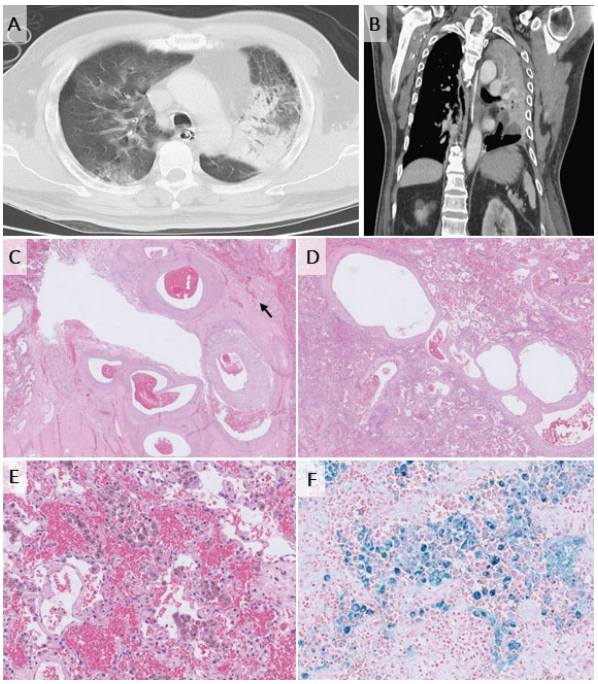

Fig. 1. CT images of the consolidation of the left upper lung: (A) axial view; (B) coronal view. The lobectomy specimen shows dilated bronchi filled with blood clots, as well as a network of irregular, thin-walled vessels, indicative of PAVMs (C, D: hematoxylin and eosin stain, 40×; E: hematoxylin and eosin stain, 400×; F: iron stain, 400×). (C) Microscopic PAVM near the bronchus (arrow)..

secretions and required intermittent high-concentration oxygen, with his lowest PaO_2 recorded at 75 mmHg on 90% FiO_2.

Accordingly, a LUL lobectomy was performed on the 34th day of hospitalization, with peri-operative venovenous extracorporeal membrane oxygenation support to ensure adequate respiratory function during surgery. Pathohistological examination of the resected specimen (Figures 1C–1F) confirmed PAVMs and was negative for microorganisms. The patient's postoperative course was uneventful, and he was successfully extubated without further episodes of hemoptysis.

Discussion

PAVMs are vascular abnormalities that involve direct connections between pulmonary arteries and veins, leading to anatomic right-to-left shunt. With an incidence of 2-3 individuals per 100,000, fewer than 400 cases of PAVMs have been documented [4]. The majority of PAVMs are congenital and are often associated with HHT. Among the common clinical manifestations of PAVMs are epistaxis (mucosal telangiectasia related to HHT), dyspnea, chest pain, and hemoptysis [2]. Massive hemoptysis due to intrabronchial PAVM rupture and hemothorax with spontaneous ruptured subpleural lesions are uncommon, but life-threatening complications.

Diagnosing PAVMs requires the identification of a feeding artery and a draining vein connected to an aneurismal sac. If no overlapping lesions are present, contrast-enhanced CT typically detects 98% of PAVMs, indicating its sensitivity. Utilizing CT with a modified pulmonary angiography protocol aids in the definition of angio-architecture and the planning for further interventions. Currently, catheter angiography is rarely used for diagnostic purposes, but it remains part of the embolization procedure, with radiographically visible PAVMs for vessel obliteration [5]. Surgical resection is reserved for patients with ongoing complications such as severe bleeding, or in cases where embolization is inadequate or unsuitable because of the extent of the disease [2].

It is imperative to note that the patient in our case presented with a microscopic AVM, which could not be visualized on CT images. This underscores the limitation of imaging modalities in detecting such small vascular abnormalities, particularly in the context of lung collapse and consolidation caused by hemoptysis, and that its nature was not grossly seen but histologically found. Despite the high sensitivity of CT scans in diagnosing PAVMs, microscopic AVMs may evade detection, thus necessitating alternative diagnostic approaches such as surgical exploration or other imaging modalities.

Overall, our literature review revealed 2 cases in which PAVMs were not initially detected by CT scans, but were later confirmed through microscopic examination after lobectomy [4, 6]. These cases were either asymptomatic or presented with mild to moderate hemoptysis. To our knowledge, the present paper is the first report of a PAVM with life-threatening hemoptysis, but without notable feeding vessels detected through serial CT imaging. This condition was confirmed through histopathological examination after surgery, suggesting a microscopic PAVM near the bronchus (Figure 1C).

Conclusion

Although CT imaging is typically sensitive in detecting PAVMs, the unique nature of the

present case, with its high oxygenation parameters and an absence of classic feeding vessels, precluded image-based diagnosis. Because PAVMs are rare, massive recurrent hemoptysis should prompt clinicians to consider surgical intervention, not only as a treatment option, but also as a diagnostic measure in critical cases with near-fatal hemoptysis.

References

1. Radchenko C, Alraiyes AH, Shojaee S. A systematic approach to the management of massive hemoptysis. J Thorac Dis 2017; 9(Suppl 10):S1069-s1086, 10.21037/jtd.2017.06.41.
2. Shovlin CL, Condliffe R, Donaldson JW, *et al*. British Thoracic Society clinical statement on pulmonary arteriovenous malformations. Thorax 2017; 72(12): 1154-1163, 10.1136/thoraxjnl-2017-210764.
3. Ference BA, Shannon TM, White RI, *et al*. Life-threatening pulmonary hemorrhage with pulmonary arteriovenous malformations and hereditary hemorrhagic telangiectasia. Chest 1994; 106(5): 1387-1390, https://doi.org/10.1378/chest.106.5.1387.
4. Kuhajda I, Milosevic M, Ilincic D, *et al*. Pulmonary arteriovenous malformation--etiology, clinical four case presentations and review of the literature. Ann Transl Med 2015; 3(12): 171, 10.3978/j.issn. 2305-5839.2015.06.18.
5. Majumdar S, McWilliams JP. Approach to pulmonary arteriovenous malformations: a comprehensive update. J Clin Med 2020; 9(6): 1927, 10.3390/jcm9061927.
6. Aya-ay EV, Luna AD, Pineda MJ. A case of right middle lobe pulmonary arteriovenous malformation presenting as non-resolving pneumonia. Pathology 2012; 44:S107, https://doi.org/10.1016/S0031-3025(16)32902-6.

Spontaneous Hemopneumothorax Following Electronic Cigarette Use: A Case Report and Literature Review

Wei-Hsiang Feng[1], Yuan-Ming Tsai[1]

Spontaneous pneumothorax, characterized by the accumulation of air in the chest leading to lung collapse, is a known condition. Spontaneous hemopneumothorax (SHP), a less common subtype, historically affects approximately 0.5–11.6% of patients with spontaneous pneumothorax, often involving more than 400 mL of blood within the pleural space. While cigarette smoking is a well-established risk factor for spontaneous pneumothorax, the contribution of electronic cigarettes (e-cigarettes or vaping) use to the development of SHP remains poorly understood. Herein, we present the case of a patient with life-threatening SHP possibly triggered by the inhalation of substances present in e-cigarette aerosol. ***(Thorac Med 2024; 39: 271-274)***

Key words: electronic cigarette, vaping, spontaneous hemopneumothorax, foreign body giant cell

Introduction

Spontaneous pneumothorax, characterized by the accumulation of air in the pleural space resulting in lung collapse, is a well-recognized clinical entity. It can manifest as primary spontaneous pneumothorax (PSP) or secondary spontaneous pneumothorax, each with its distinct etiologies and risk factors. Spontaneous hemopneumothorax (SHP), a less common subtype of pneumothorax, historically affects approximately 0.5–11.6% of patients with spontaneous pneumothorax, and often involves more than 400 mL of blood within the pleural space [1]. While cigarette smoking is a well-established risk factor for spontaneous pneumothorax [2], the emergence of electronic cigarettes (e-cigarettes or vaping) use has introduced new complexities to this landscape.

E-cigarettes deliver an aerosolized mixture of 3 main components: nicotine, propylene glycol, and glycerin, compared to traditional cigarettes, which contain over 7000 chemical compounds [3]. The pulmonary effects of e-cigarette

[1]Division of Thoracic Surgery, Department of Surgery, Tri-Service General Hospital, National Defense Medical Center, Taipei, Taiwan
Address reprint requests to: Dr. Yuan-Ming Tsai, Division of Thoracic Surgery, Department of Surgery, Tri-Service General Hospital, National Defense Medical Center, Taipei, Taiwan.

use have garnered significant attention, with mounting evidence suggesting associations with respiratory symptoms, lung injury, and acute respiratory distress syndrome. Despite evidence suggesting that e-cigarettes can be as damaging to pulmonary structures as traditional cigarettes [3-4], it remains uncertain whether vaping is a risk factor for spontaneous pneumothorax. This knowledge gap underscores the importance of elucidating the potential contributions of e-cigarette use to the development of pneumothorax, including its pathophysiological mechanisms and clinical implications. Herein, we present a compelling case of life-threatening SHP in a young adult with a history of both cigarette smoking and occasional e-cigarette use.

Case Presentation

A 26-year-old man, with a 3-year history of smoking half a pack of regular cigarettes daily and occasional e-cigarette use, presented to our emergency department with sudden-onset chest pain and shortness of breath during sleep. Examination and diagnostic tests, including blood sampling, electrocardiogram, and chest X-ray, revealed PSP with pleural effusion on the right side (Figure 1). A pig-tail catheter was inserted and connected to an underwater sealed system, initially releasing a significant amount of air. Subsequent high-resolution computed tomography (CT) identified blebs over the bilateral apical lungs and right-side pleural effusion (Figure 2a, 2b). After applying suction to the chest drainage tube, approximately 600 mL of bloody effusion was drained.

Following explanation and informed consent, emergency video-assisted thoracoscopic surgery with decortication and wedge resection of the right upper lobe was performed. Intra-

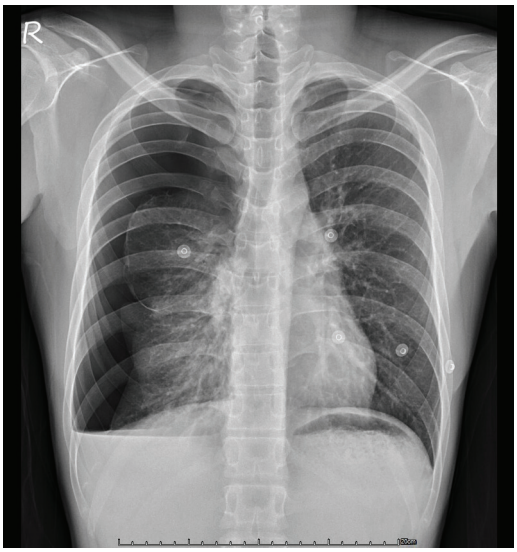

Fig. 1. Pneumothorax with pleural effusion on the right side.

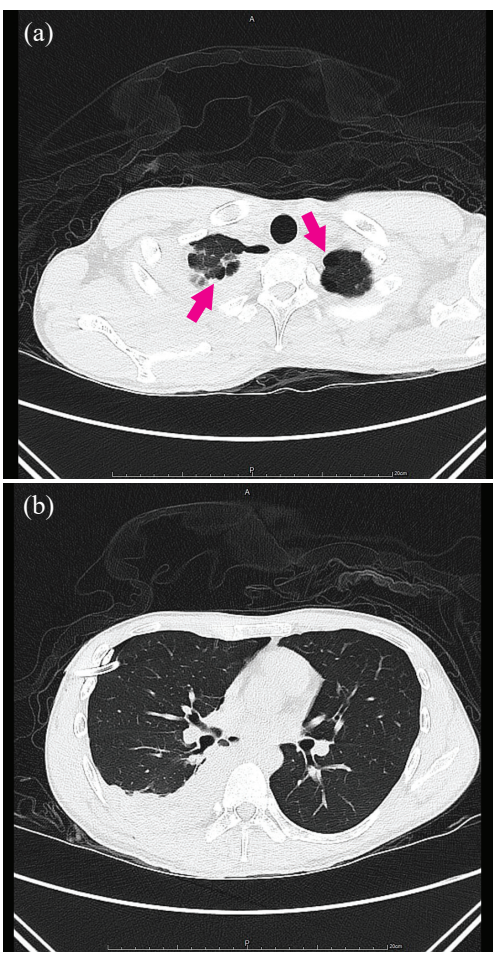

Fig. 2. (a) Blebs at bilateral apical lungs (red arrow). (b) Right-side pleural effusion.

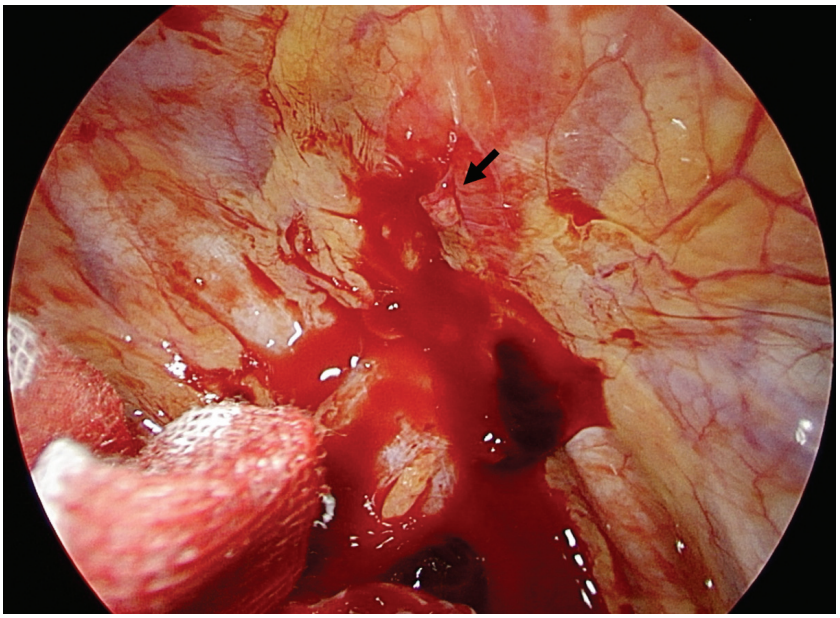

Fig. 3. An active bleeder (black arrow) at the apical parietal pleura.

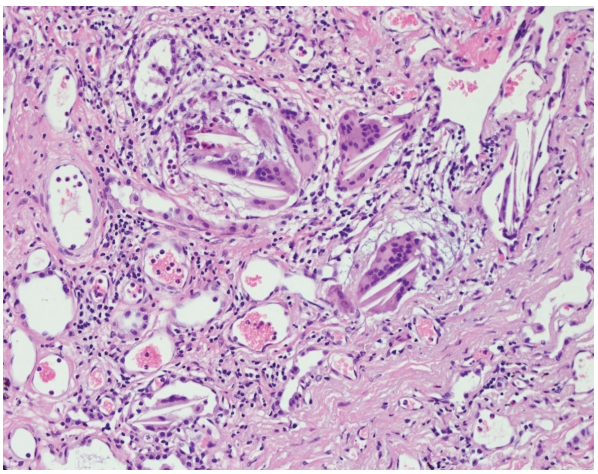

Fig. 4. Foreign body giant cells with cholesterol cleft-like material, focal fibrosis, and intra-alveolar hemorrhage.

operatively, blood clots were discovered in the pleural cavity, along with an active bleeder at the apical parietal pleura (Figure 3). Hemostasis was achieved by electrocautery, and blebs resection was performed smoothly with endostaplers. The postoperative course was uneventful, and the chest drainage tube was removed on the 3rd postoperative day. The patient was discharged the following day.

Histopathological examination revealed foreign body giant cells with cholesterol cleft-like material, focal fibrosis, and intra-alveolar hemorrhage (Figure 4). No evidence of malignancy was found, and the patient provided informed consent for publication of his case.

Discussion

Spontaneous pneumothorax, classified as primary or secondary, is associated with various risk factors, including age, gender, cigarette smoking, and low body mass index. Smoking has been implicated in increased bleb formation, consistent with our case's CT findings. SHP often results from the rupture of a vascularized bulla or a torn adhesion between the visceral and parietal pleura, leading to life-threatening conditions such as hypovolemic shock [5].

The use of electronic cigarettes has surged, especially among adolescents and young adults. Bonilla *et al*. reported the potential for the vaping-related Muller maneuver driving spontaneous pneumothorax [6]. In addition, vaping-

associated lung injury is characterized by foamy macrophages and pneumocyte vacuolization, thus serving as useful diagnostic clues [7]. The presence of foreign body giant cells, characterized by the fusion of macrophages in response to persistent stimuli, suggests a chronic inflammatory response within the lung tissue, possibly triggered by the inhalation of substances present in e-cigarette aerosol. Notably, the foreign body giant cells in our patient were associated with cholesterol cleft-like material, hinting at the possibility of lipid or cholesterol deposits. The origin of these deposits may be related to the composition of e-cigarette fluids. Compounds delivered through the electronic cigarette may induce an innate inflammatory response in the lung.

In conclusion, the pathological findings of foreign body giant cells, cholesterol cleft-like material, focal fibrosis, and intra-alveolar hemorrhage in our case underscore the potential pulmonary consequences associated with e-cigarette use. While these findings do not definitively establish a causal relationship between vaping and SHP, they raise important questions about the potential risks and mechanisms underlying vaping-related lung injury.

It is essential to recognize that the presence of foreign body giant cells is not specific to a vaping-related lung pathology, but may represent a chronic inflammatory response to inhaled substances present in e-cigarette aerosol. Therefore, clinicians should remain vigilant in assessing and counseling patients regarding the potential risks associated with vaping, particularly in light of emerging evidence linking e-cigarette use to respiratory symptoms and lung injury.

Furthermore, continued research efforts are warranted to better understand the complex interactions between e-cigarette constituents, pulmonary physiology, and the development of respiratory complications. Ongoing investigations will be crucial in informing public health policies, clinical guidelines, and preventive strategies aimed at mitigating the potential harms of e-cigarette use relative to respiratory health.

References

1. Williams EW, Ramphal PS, Williams-Johnson J, *et al*. Spontaneous haemo-pneumothorax: a rare but life-threatening phenomenon. West Indian Med J 2005; 54(5): 346-7.
2. Cheng YL, Huang TW, Lin CK, *et al*. The impact of smoking in primary spontaneous pneumothorax. J Thorac Cardiovasc Surg 2009; 138(1): 192-5.
3. Reinikovaite V, Rodriguez IE, Karoor V, *et al*. The effects of electronic cigarette vapour on the lung: direct comparison to tobacco smoke. Eur Respir J 2018; 51(4).
4. Cherian SV, Kumar A, Estrada YMRM. E-cigarette or vaping product-associated lung injury: a review. Am J Med 2020; 133(6): 657-63.
5. Boersma WG, Stigt JA, Smit HJ. Treatment of haemothorax. Respir Med 2010; 104(11): 1583-7.
6. Bonilla A, Blair AJ, Alamro SM, *et al*. Recurrent spontaneous pneumothoraces and vaping in an 18-year-old man: a case report and review of the literature. J Med Case Rep 2019; 13(1): 283.
7. Butt YM, Smith ML, Tazelaar HD, *et al*. Pathology of vaping-associated lung injury. N Engl J Med 2019; 381(18): 1780-1.

Carbon Monoxide Poisoning Induces Myocardial Injury With ECG ST Elevation: A Case Report and Literature Review

Pei-Yi Shen[1], Po-Hsin Lee[1,2,3,4,5#], Tsai-Yun Lee[1,5], Yi-Wen Chen[1,5], Chun-Shih Chin[1,5]

In patients with carbon monoxide (CO) poisoning, tailored evaluation is needed due to the high likelihood of symptoms overlapping with myocardial infarction. Here, we reported a 58-year-old man who presented to the emergency room after smoke inhalation. His complaints were shortness of breath, hoarseness, sore throat, dizziness, and general weakness. Laboratory results showed elevated cardiac enzymes, metabolic acidosis and elevated serum carboxyhemoglobin. CO poisoning was diagnosed accordingly. Electrocardiography (ECG) revealed atypical territories involvement with II, III, aVF, and V2-V5 ST elevation. His coronary angiography, however, showed patent coronary arteries. It is difficult to distinguish myocardial injury caused by CO poisoning from true acute myocardial infarction. Ischemic patterns in atypical territories on an ECG can offer a crucial clue in this differentiation. However, angiography and revascularization should still be considered in patients with highly suspected acute myocardial infarction. ***(Thorac Med 2024; 39: 275-280)***

Key words: Carbon monoxide poisoning, CO poisoning-related cardiac injury, myocardial injury, myocardial injury with ST elevation

Introduction

One third of individuals that experience moderate to severe CO poisoning suffer from myocardial injury, which leads to a higher long-term mortality rate [1] and a higher risk of congestive heart failure [2]. Differentiating CO poisoning-related myocardial injury from acute myocardial infarction is challenging, due to their similar cardiovascular symptoms and signs, and limited diagnostic tools. Here, we present the case of a male patient displaying myocardial injury resembling ST elevation myocardial infarction (STEMI) secondary to

[1]Division of Chest Medicine, Department of Internal Medicine, Taichung Veterans General Hospital, Taichung, Taiwan. [2]College of Medicine, National Yang Ming Chiao Tung University, Taipei, Taiwan. [3]Doctoral Program in Translational Medicine, National Chung Hsing University. [4]Rong Hsing Translational Medicine Research Center, National Chung Hsing University. [5]Division of Pulmonary and Critical Care Medicine, and Hyperbaric Oxygen Therapy Center, Department of Internal Medicine, Taichung Veterans General Hospital, Taichung, Taiwan
Address reprint requests to: Dr. Po-Hsin Lee, Division of Chest Medicine, Department of Internal Medicine, Taichung Veterans General Hospital, No.1650, Sect. 4, Taiwan Boulevard, Taichung 407, Taiwan.

CO intoxication, which highlights the complexity in differentiating and managing these conditions. This case report aimed to delve into the mechanisms, clinical presentation, diagnostic approaches, and treatment modalities regarding CO-induced myocardial injury.

Case Presentation

A 58-year-old man with no systemic disease visited our emergency department after hours of an unfortunate exposure to dense smoke while repairing electrical circuits. He complained about shortness of breath after just a 10-meter walk. He had a voice, but also hoarseness, a sore throat, red eyes, a red face, dizziness, and general weakness. He denied chest pain, chest distress or back pain. During physical examination, a substantial amount of carbon particles were found in his mouth, nose, trunk and 4 limbs. He used accessory muscles during breathing. Results of laboratory tests were as follows: white blood cell count, 16.20 K/μL; hemoglobin, 16.5 g/dL; platelets, 149 K/μL; neutrophils, 89.8%; alanine aminotransferase (ALT), 43 U/L; total bilirubin, 1.80 mg/dL; and procalcitonin, 1.02 ng/mL. His renal function was within normal range. His arterial blood gas revealed pH 7.346; partial pressure of oxygen (PaO_2), 34.9 mmHg; oxygen saturation (SpO_2), 79%; partial pressure of carbon dioxide ($PaCO_2$), 45.3 mmHg; bicarbonate ions (HCO_3-), 19.3 mmol/L; excess bases (BE), -6.6mEq/L; and markedly elevated lactates of 36.5 mg/dL. These results were compatible with metabolic lactic acidosis. Cardiac enzymes showed abnormal elevations: CK (creatine kinase), 259 U/L; CK-MB, 7.3 U/L; and troponin-I, 60.9 ng/L. The initial serum carboxyhemoglobin (HbCO) level was 8.7%. Chest plain film showed increased right upper lobe infiltrations. The first electrocardiography (ECG) showed ST elevation in leads II, III and aVF.

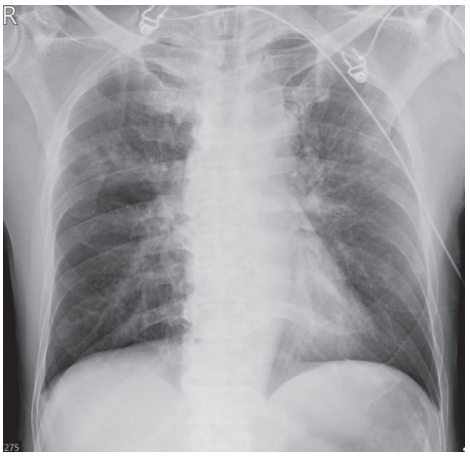

Fig. 1. Initial chest plain film taken at the emergency room.

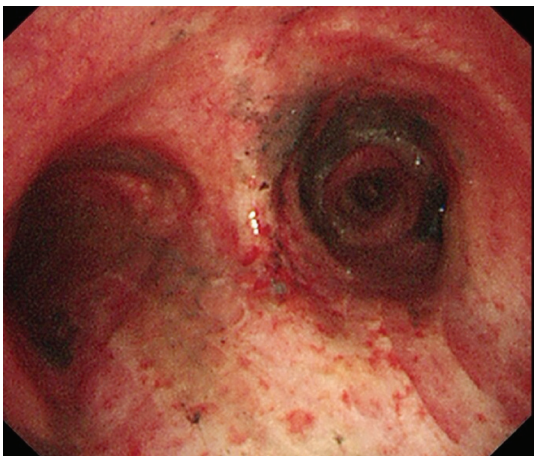

Fig. 2. Bronchoscopic examination showed respiratory tract burn injury with mucosal erosion and carbonaceous sputum.

For airway protection, the patient was promptly intubated at the emergency room (ER), and was subsequently admitted to the intensive care unit (ICU). After endotracheal intubation, bronchoscopic examination was performed. Results showed burning injury of the respiratory tract, with mucosal erosion and carbonaceous sputum. Two hours later, his cardiac enzymes showed further elevations in CK (350 U/L) and

troponin-I (127.7 ng/L), and ECG showed ST elevation in leads II, III, aVF and V2-V5. A coronary angiogram was performed the following day to rule out acute coronary syndrome, and revealed patent coronary arteries. The possibility of STEMI was hence ruled out. Cardiac enzyme levels, as followed up regularly during the patient's 3 days at the ICU, showed a progressive decline in levels: troponin T dropped from 24.04 to 14.95 ng/L; and CK dropped from 647 to 489 U/L. At the same time, the ECG showed no remarkable change. Hyperbaric oxygen therapy (HBOT) was performed twice after the accident. The patient finally was extubated smoothly and discharged without any chest distress.

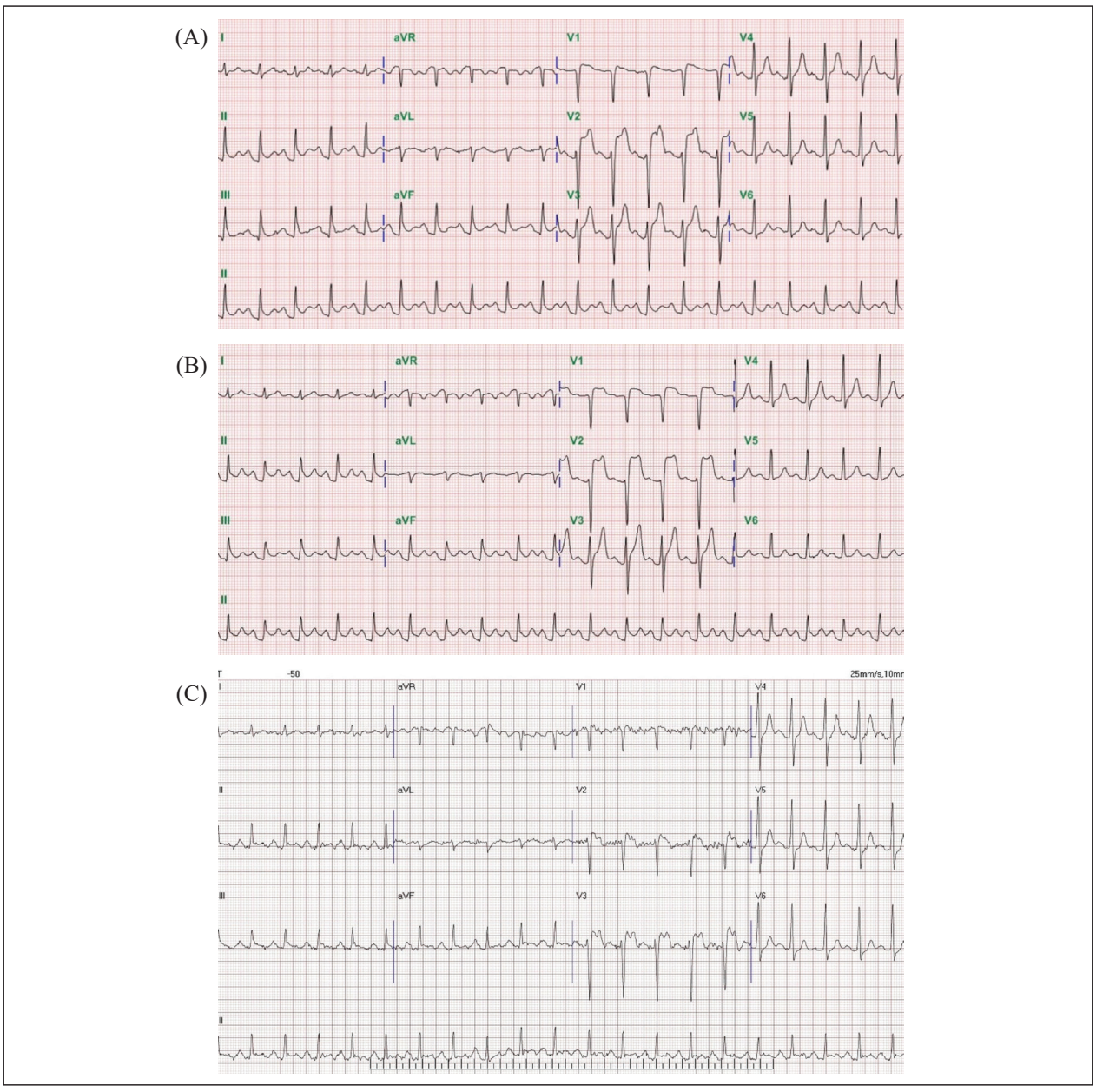

Fig. 3. Patient's consecutive ECG changes on Day 1: (A) ECG on arrival; (B) ECG 2 hours after arrival (A); (C) ECG taken 2 days after admission.

Discussion

Mechanisms of CO poisoning-related cardiac injury

Myocardial ischemia and cardiac dysfunction in CO poisoning involve several mechanisms that interplay between binding affinity with hemoglobin and myocytes; mitochondrial dysfunction and platelet activation underscore their combined role in neurological and cardiac damage.

1. High binding affinity of CO with hemoglobin

CO has an affinity for hemoglobin >200 times greater than oxygen. It forms HbCO, which displaces oxygen and hence reduces the blood's oxygen-carrying capacity [3], leading to a left shift in the oxygen-Hb dissociation curve that increases overall oxygen demand and heightens myocardial contractility [4].

2. Mitochondrial inhibition and myoglobin binding

CO disrupts adenosine triphosphate (ATP) production by binding to ferrous heme a3 at the active site of cytochrome c oxidase (COX). This interaction inhibits mitochondrial respiration in myocardial myoglobin, impairs oxidative phosphorylation, and results in ROS production that intensifies oxidative stress. The consequence is cardiac dysfunction and myocardial infarction [5-6].

3. Platelet activation

Excessive CO activates platelets, initiating an inflammatory cascade by displacing nitric oxide from the platelets' surface hemoproteins. The inflammatory cascade leads to the release of myeloperoxidase (MPO) from neutrophils. MPO could induce additional ROS release, contributing to neurological and cardiac injuries [7].

Diagnosis of CO poisoning-related myocardial injury

Common cardiovascular complications include myocardial stunning, acute myocardial ischemia, left ventricular dysfunction, and arrhythmia [8]. Angina stands out as a primary symptom, with a direct relationship with CO exposure [9]. In one study, chest pain emerged in 34% of patients; it started approximately 90 minutes after CO exposure, and was resolved within 2 days [10].

Both elevated troponin-I and CK-MB indicate myocardial injury. They are effective in gauging severity of injury and short-term prognosis. ECG changes include repolarization disturbances (e.g., T-wave change), ischemic patterns (e.g., ST segment deviation), and alterations in QT interval, which is correlated with HbCO levels. These changes persist for 3 to 7 days.

In our case, the cause-effect mechanism regarding myocardial injury resulting from smoke inhalation remains unclear. There are many potential causes, including exposure to other toxins such as cyanide, and stress-related factors. Although the patient's HbCO level was not elevated upon arrival, this may be attributed to delayed presentation, considering that more than 2 half-lives had elapsed since exposure. This suggests that the initial HbCO concentration may have exceeded 30%. Therefore, it is still likely that CO was the primary cause of the patient's myocardial injury. The patient's ECG revealed ST elevation in leads II, III, aVF, and V2-V5, which are atypical presentations of acute myocardial infarction. Typically, evidence of inferior wall ischemia on an ECG includes

ST- or T-wave changes in leads II, III, and aVF. Conversely, ST elevation in leads V2-V5 indicates anterior wall ischemia. When ischemic patterns involve atypical territories on an ECG, they can provide valuable clues in differentiating between myocardial injury related to CO exposure and acute coronary syndrome. Patients with atypical territory involvement on an ECG may potentially avoid immediate cardiac catheterization. However, individuals with persistent left ventricular dysfunction, a history of pre-existing coronary artery disease (CAD), or risk factors for CAD, should still undergo cardiac catheterization to accurately differentiate true myocardial infarction [11-12].

Treatment for CO poisoning-related myocardial injury

The current guidelines recommend oxygen therapy (both normobaric and hyperbaric) to remove CO from the blood at a faster rate by increasing the partial pressure of oxygen until the HbCO concentration drops to 3%, or until clinical symptoms are completely resolved. HBOT is preferred for patients with neurological deficits, cardiac ischemia, loss of consciousness, metabolic acidosis, and HbCO levels >25% [14]. Patients who are suspected of having acute coronary syndrome due to risk factors and clinical presentation may require percutaneous coronary intervention for both diagnosis and treatment [11-12].

Follow-up of CO poisoning-related myocardial injury

Myocardial injury from CO poisoning is linked to higher long-term cardiovascular mortality [8], as well as an elevated risk of congestive heart failure during the first month of follow-up, which should be continued for >2 years [13]. In addition, there is a subsequent risk of developing arrhythmia [14]. It is advisable to recommend that patients participate in cardiac rehabilitation programs, and to have the patients followed and co-managed by cardiologists due to a high risk of myocardial fibrosis and exercise intolerance [15-16].

Conclusion

For patients with CO poisoning, findings of elevated cardiac enzymes and an abnormal ECG indicate myocardial injury. The atypical territories of ST-segment changes on an ECG potentially distinguish CO poisoning-related myocardial injury from acute coronary syndrome. However, patients at high risk of CAD are advised to undergo coronary angiography, and revascularization in cases of true myocardial infarction.

References

1. Henry CR, Satran D, Lindgren B, *et al*. Myocardial injury and long-term mortality following moderate to severe carbon monoxide poisoning. JAMA 2006; 295(4): 398-402.
2. Huang CC, Chen TH, Ho CH, *et al*. Increased risk of congestive heart failure following carbon monoxide poisoning. Circ Heart Fail 2021; 14(4): e007267.
3. Weaver LK. Clinical practice. Carbon monoxide poisoning. N Engl J Med 2009; 360(12): 1217-25.
4. Smithline HA, Ward KR, Chiulli DA, *et al*. Whole body oxygen consumption and critical oxygen delivery in response to prolonged and severe carbon monoxide poisoning. Resuscitation 2003; 56(1): 97-104.
5. Rose JJ, Wang L, Xu Q, *et al*. Carbon monoxide poisoning: pathogenesis, management, and future directions of therapy. Am J Respir Crit Care Med 2017; 195(5): 596-606.
6. Tritapepe L, Macchiarelli G, Rocco M, *et al*. Functional and ultrastructural evidence of myocardial stunning after

acute carbon monoxide poisoning. Crit Care Med 1998; 26(4): 797-801.
7. Thom SR, Bhopale VM, Han ST, *et al*. Intravascular neutrophil activation due to carbon monoxide poisoning. Am J Respir Crit Care Med 2006; 174(11): 1239-48.
8. Garg J, Krishnamoorthy P, Palaniswamy C, *et al*. Cardiovascular abnormalities in carbon monoxide poisoning. Am J Ther 2018; 25(3): e339-e48.
9. Koskela R-S, Mutanen P, Sorsa J-A, *et al*. Factors predictive of ischemic heart disease mortality in foundry workers exposed to carbon monoxide. Am J Epidemiol 2000; 152(7): 628-32.
10. Henz S, Maeder M. Prospective study of accidental carbon monoxide poisoning in 38 Swiss soldiers. Swiss Med Wkly 2005; 135(27-28): 398-406.
11. Satran D, Henry CR, Adkinson C, *et al*. Cardiovascular manifestations of moderate to severe carbon monoxide poisoning. J Am Coll Cardiol 2005; 45(9): 1513-6.
12. Dziewierz A, Ciszowski K, Gawlikowski T, *et al*. Primary angioplasty in patient with ST-segment elevation myocardial infarction in the setting of intentional carbon monoxide poisoning. J Emerg Med. 2013; 45(6): 831-4.
13. Huang C-C, Chen T-H, Ho C-H, *et al*. Increased risk of congestive heart failure following carbon monoxide poisoning. Circ Heart Fail 2021; 14(4): e007267.
14. Lee FY, Chen WK, Lin CL, *et al*. Carbon monoxide poisoning and subsequent cardiovascular disease risk: a nationwide population-based cohort study. Medicine (Baltimore). 2015; 94(10): e624.
15. Henry TD, Satran D. Acute carbon monoxide poisoning and cardiac magnetic resonance. JACC: Cardiovasc Imaging 2021; 14(9): 1771-3.
16. Wang YM, Huang CC, Liu KF, *et al*. Exercise-induced myocardial ischemia presenting as exercise intolerance after carbon monoxide intoxication and smoke inhalation injury: case report. BMC Cardiovasc Disord 2022; 22(1): 570.

Malignant Pleural Mesothelioma in a Young Adult: A Case Report and Literature Review

Jin-Hao Xu[1], Chia-Yu Chiu[2], Jen-Hsien Lin[1], Wei-Yi Lee[3]

Classic malignant pleural mesothelioma (MPM) is typically diagnosed in patients >70 years old. Here, we presented a case of MPM diagnosed at age 30, with asbestos exposure 10 years previous. We also reviewed the published literature on MPM at age <40 (young MPM). Compared with the historical cohort, young MPM has a shorter latency period (15 vs. 32 years), less known asbestos exposure (38% vs. 80%), and more surgical opportunities (31% vs. 18%). Although asbestos has been gradually prohibited in developed countries, clinicians should be aware that MPM can still occur after short-term exposure to asbestos in young adults. ***(Thorac Med 2024; 39: 281-291)***

Key words: asbestos exposure, asbestos inhalation, occupational exposure, brake linings, asbestos bans

Introduction

Malignant pleural mesothelioma (MPM), a cancer that arises from the pleura, is predominantly caused by asbestos inhalation. The latency period between asbestos exposure and mesothelioma onset is approximately 30-40 years, with the median age at diagnosis being 74 years [1-2]. However, MPM could occur at a younger age if there was high intensity or early age exposure [2-3]. Young MPM (defined as MPM that occurs at age < 40) is rare, accounting for less than 2% of all cases [3]. Young MPM patients often have more exposure to non-occupational asbestos or environmental sources than classic MPM patients [3]. This includes secondary exposure (through household members) and environmental exposure (living near mines and factories; or using asbestos-containing products [such as ironing on asbestos-coated boards or using building materials]) [4]. Some young MPM is secondary to radiation therapy or occurs in those with a genetic predisposition [3, 5]. Treatment for MPM generally involves a combination of surgery, radiation, chemotherapy, and immunotherapy [6-7]. In addition, a study showed young MPM patients have a better prognosis than classic MPM pa-

[1]Department of Internal Medicine, Kaohsiung Armed Forces General Hospital, Kaohsiung, Taiwan. [2]Division of Public Health, Infectious Diseases, and Occupational Medicine, Department of Medicine, Mayo Clinic, Rochester, Minnesota, USA. [3]Department of Surgery, Kaohsiung Armed Forces General Hospital, Kaohsiung, Taiwan.
Address reprint requests to: Dr. Jin-Hao Xu, Department of Internal Medicine, Kaohsiung Armed Forces General Hospital, No.2, Zhongzheng 1st Rd., Lingya Dist., Kaohsiung City 80284, Taiwan.

tients (median survival time 11 months vs. 8 months, $p<0.0001$) [3].

In Taiwan, asbestos consumption peaked in the mid-1980s at around 40,000 metric tons annually, with widespread use in ships, insulation, brake linings, cement, and textiles. In 2018, Taiwan implemented a national policy banning all types of asbestos [8]. Herein, we report the case of a 30-year-old male diagnosed with MPM that was linked to high-intensity, unprotected exposure to asbestos in brake linings for 2 years. To explore the unique aspects of this condition in this demographic group, we critically reviewed the published cases of MPM in patients under age 40.

Case Report

A 30-year-old male soldier, previously in good health, was referred to our emergency department (ED) for persistent right pleural effusion (Figure 1A, 1B) discovered during a rou-

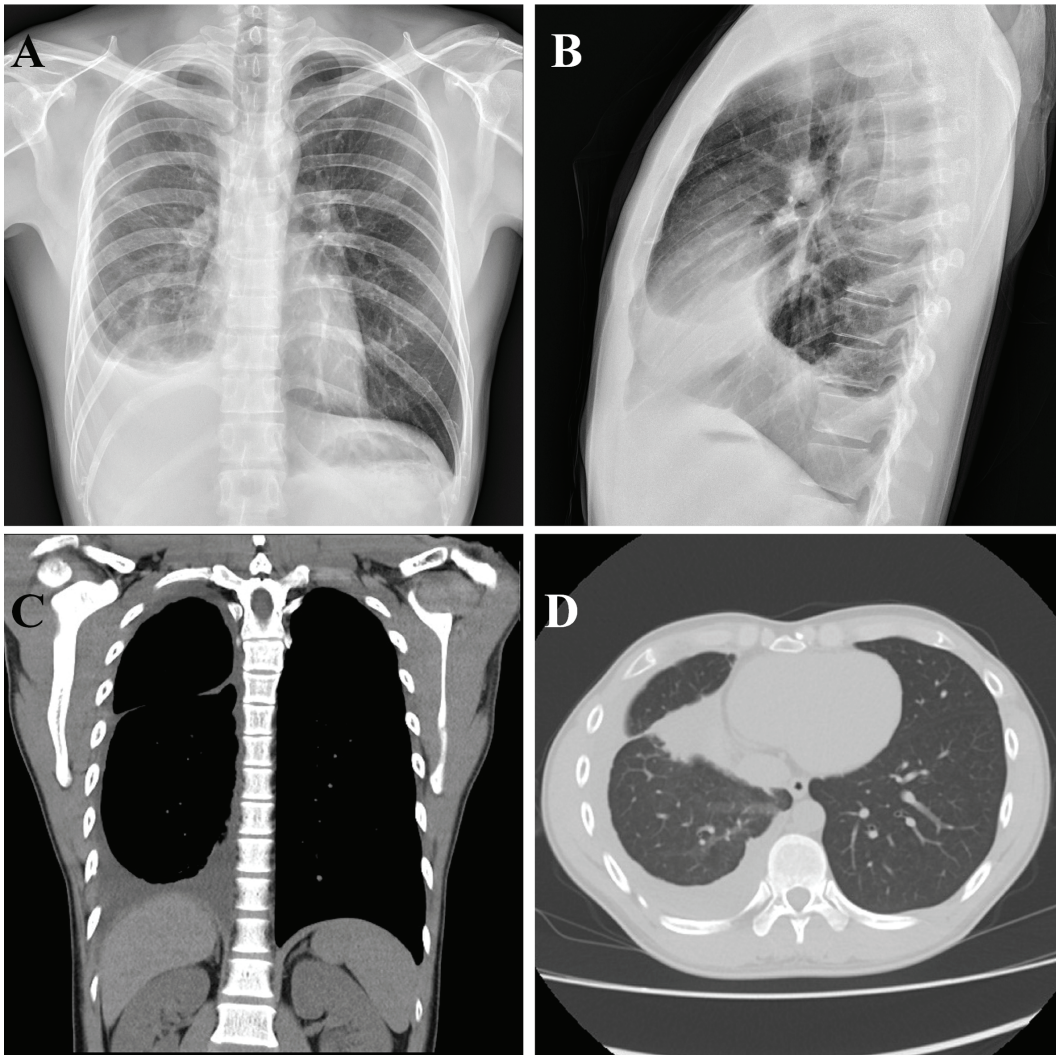

Fig. 1. Image findings in the present case. A, B: Chest X-ray showed right-side pleural effusion. C, D: Computed tomography scans showed right-side pleural effusion with right lower lobe consolidation.

tine military physical examination. The patient experienced a 6-month history of progressive exertional dyspnea, cough, and right chest pain. At the ED, his vital signs were stable, with a fever of 37.8oC (100oF).

Physical examination revealed decreased breathing sounds and dullness on percussion on the right side of his chest, consistent with pleural effusion. Computed tomography (CT) scans confirmed right pleural effusion, consolidation in the right lower lobe (RLL), and subsegmental atelectasis (Figure 1C, 1D). Upon admission, empirical antibiotic therapy with amoxicillin-clavulanic acid was initiated to address potential pulmonary infection. The patient underwent bronchoscopy with endobronchial brushing and lavage on the second day of hospitalization. The stains and cultures for bacteria and mycobacterium both showed negative results.

Thoracentesis yielded exudative effusion with lactate dehydrogenase of 578 U/L, total protein of 6.7 g/dL, and malignant cells on cytology, raising a suspicion of carcinoma. He denied a history of smoking, but his occupational history was significant for employment at a brake linings factory for 2 years (at age 19-20 years), indicating substantial asbestos exposure.

On the seventh day of hospitalization, video-assisted thoracoscopic surgery (VATS) with wedge resection of the RLL was performed. During the surgery, pleural plaques and thickening (Figure 2A, 2B) with 700 ml of dark-

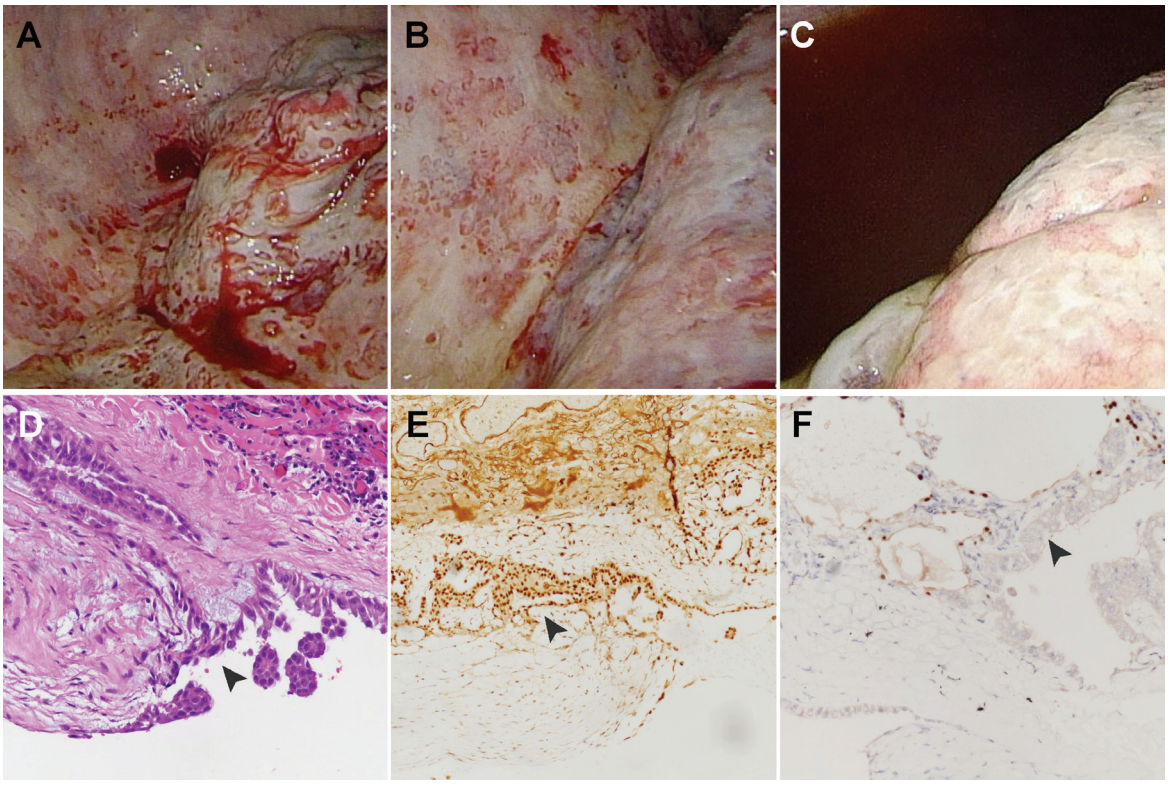

Fig. 2. Surgical findings and pathology findings in the present case. A, B: Pleural plaques and pleural thickening. C: Dark-red pleural effusion. D: Papillary and glandular structures infiltrated from the outer pleura to the internal fibrous pulmonary stroma (arrowhead) (H&E, x200). E: Immunohistochemistry staining was positive for WT1 (arrowhead). F: Immunohistochemistry staining was positive for TTF-1 (thyroid transcription factor-1) (arrowhead).

red pleural effusion (Figure 2C) were noted. In addition, there were some adhesions from the right upper lobe (RUL) to the anterior/medial aspect of the chest wall.

Histopathological examination revealed tumor cells arranged in papillary and glandular structures, infiltrating from the outer pleura to the internal fibrous pulmonary stroma (Figure 2D). Thickening of the pleura with fibrosis was also noted. Immunohistochemistry (IHC) staining was positive for cytokeratin (CK), CK 5/6, and WT1 (Figure 2E), and negative for thyroid transcription factor-1 (TTF-1) (Figure 2F), confirming the diagnosis of epithelioid mesothelioma. The patient underwent a whole-body bone scan and brain magnetic resonance imaging for cancer staging. Finally, his cancer staging was determined to be cT3N0M0, pT2N0M0, Stage IB.

He was subsequently transferred to the tertiary medical center. He underwent a second VATS (wedge resection of the RUL), and hyperthermic intrathoracic chemotherapy (cisplatin) was administered during surgery. Currently, this patient is receiving intravenous cisplatin and pemetrexed for mesothelioma treatment.

Discussion

We performed a literature search from the inception to November 2023 using PubMed, Embase, Scopus, Cochrane Library, and ClinicalTrials.gov. The search protocol was (pleural mesothelioma AND young adult) OR (pleural mesothelioma AND teenagers) OR (pleural mesothelioma AND young). Only patients under 40 years old and articles written in English with the full text available were included.

We identified a total of 16 cases, including ours. The majority of young MPM patients were male (11 patients, 69%), with a median age of 26 years (interquartile range [IQR] 16 – 32 years). The distribution of MPM cases included 6 patients (38%) from Asia (Taiwan, India, Japan), 6 patients (38%) from Europe (UK, Turkey, Greece, Germany), 2 patients (13%) from the USA, 1 patient (6%) from Israel, and 1 patient (6%) from Mexico. Asbestos exposure was identified in 6 patients (38%), of whom 3 (19%) were exposed to asbestos-containing building materials, 2 (13%) had occupational exposure, and 1 (6%) was exposed to asbestos through household members. The latency period was available for 5 (31%) patients, with a median of 15 years (IQR 8.5 – 20 years). Smoking was noted in 4 patients (25%). The symptoms were chest pain (11 patients, 69%), fever (9 patients, 56%), cough (8 patients, 50%), and dyspnea (7 patients, 44%). Due to the above nonspecific symptoms, 6 patients (38%) were initially treated as infectious conditions (pneumonia, empyema, or fever of unknown origin). Right-side disease occurrence was noted in 9 patients (56%). Pleural effusion was noted in 12 patients (75%). Thoracoscopy was the primary diagnostic method, used for 7 patients (44%), followed by image-guided biopsy (5 patients, 31%) and open lung biopsy (4 patients, 25%).

The histopathologic type was available for 13 (81%) patients, and included 10 (63%) patients with epithelioid, 2 (13%) with a deciduoid subtype, and 1 (6%) with a biphasic type. Disease staging varied at diagnosis. Cancer staging was available for 9 (56%) patients, including 2 (13%) at Stage I, 3 (19%) at Stage III, and 4 (25%) at Stage IV. Cancer-directed surgery was performed for 5 patients (31%).. The detailed characteristics are summarized in Table 1.

MPM is a cancer highly associated with

Table 1. Characteristics of Young Malignant Pleural Mesothelioma Cases in This Review (N = 16)

Case	Author, Year, Country [reference no.]	Age, Gender, Comorbidities	Occupation, Asbestos exposure	Other associated risk factors	Clinical manifestations	Image finding of MPM	Cell type	Diagnosis method	Stage	Treatment
1	Xu, *et al*., 2023, Taiwan, Our presented case	30, M, None	Soldier, brake linings worker for 2 years 10 years ago	None	Cough, chest pain, dyspnea, fever	R pleura	Epithelioid	Thoracoscopy	cT3N0M0, pT2N0M0, Stage IB	Wedge resection, hyperthermic intrathoracic cisplatin, systemic cisplatin and pemetrexed
2	Hayat *et al*., 2023, UK, [22]	34, M, Thyroidectomy for thyroid cancer, leukemia	No	Total body irradiation therapy for leukemia	Cough, dyspnea, fever	L pleura	Epithelioid	Thoracoscopy	T4N1M0, Stage IIIB	No
3	Pérez-Guzmán *et al*., 2015, Mexico [23]	17, M, Allergic rhinitis and bronchial hyper-reactivity	No	Smoking	Cough, chest pain, dyspnea, fever, headache	R pleura	NA	Open lung biopsy	NA	Systemic cisplatin, pleurodesis
4	Patra *et al*., 2015, India [24]	18, F, None	Lived in a house with asbestos roofing for 2 years	None	Chest pain, cough, fever, swelling of neck, weight loss	R pleura, mediastinum	Epithelioid	CT-guided biopsy	Stage IV	Systemic cisplatin and pemetrexed
5	Singhal *et al*., 2014, India [25]	26, F, None	Housewife. Lived with her miner father for 3 months, 15 years ago.	None	Chest pain, dyspnea, puffiness over face	R lung, R pleura,	Epithelioid	Lung biopsy	Stage IV (liver and pelvic metastasis)	Systemic cisplatin and pemetrexed
6	Kanbay *et al*., 2014, Turkey [26]	26, M, None	No	None	Chest pain, dyspnea	R pleura	Epithelioid	Thoracoscopy	T3N3M0, Stage IIIC	Systemic cisplatin and pemetrexed
7	Voulgaridis *et al*., 2013, Greece [27]	33, M, None	Farmer. Lived in a warehouse with an asbestos roof for 20 years.	Smoking 10 pack/years	Chest pain, fever	L pleura, mediastinum	Epithelioid	Open lung biopsy	Stage IV	Systemic cisplatin and pemetrexed
8	Rosas-Salazar *et al*., 2013, USA [28]	16, M, Ataxia-telangiectasia	No	None	Chest pain, cough, fever, hypoxemia	R pleura, pericardium	Epithelioid	Ultrasound-guided biopsy	NA	Systemic cisplatin and pemetrexed

9	Kumar *et al.* 2013, USA, [29]	35, F, None	No	None	Chest pain, cough, fever, weight loss	R pleura	Epithelioid	Thoracoscopy	NA	NA
10	Zarogoulidis *et al.*, 2011, Greece [30]	26, M, None	From age 6 to 12, due to building construction	None	Chest pain, fatigue, painful supraclavicular lump	R pleura, mediastinum	NA	Biopsy of supraclavicular lymph node	Stage IV	Systemic carboplatin, gemcitabine, and pemetrexed, followed by carboplatin and docetaxel
11	Bitchatchi *et al.*, 2010, Israel [31]	27, F, None	white-collar worker from age 20 to 27, due to dust and asbestos in the military	None	Dyspnea, upper back pain	R lung, R pleura	Epithelioid	Thoracoscopy	T1bN0M0, Stage IA	Extra-pleural pneumonectomy and intrapleural cisplatin
12	Tsai *et al.*, 2010, Taiwan [32]	13, M, None	No	None	Chest pain, trunk deviation and scoliosis	R lung, R pleura	Deciduoid (Epithelioid)	Thoracoscopy and pleurectomy	NA	Systemic cisplatin and pemetrexed, followed by surgical resection
13	Nagata *et al.*, 2005, Japan [33]	16, M, None	No	Smoking and inhalation of paint thinner	Chest pain, cough, fever	L lung, L pleura	Biphasic	Thoracoscopy	NA	Extra-pleural pneumonectomy
14	Gloeckner-Hofmann *et al.*, 2000, Germany [34]	40, F, None	No	Smoking 9 pack/years	Dyspnea	Mediastinum	Deciduoid (Epithelioid)	Open lung biopsy	NA	Systemic carboplatin, etoposide, vindesine, followed by 5-fluorouracil, radiotherapy, and surgical resection
15	Varan *et al.*, 1999, Turkey [35]	14, M, None	No	None	None	L pleura	Epithelioid	Pleural biopsy	NA	Systemic vincristine, ifosfamide, cisplatin and adriamycin
16	Tewari *et al.*, 1989, India [36]	15, M, Seizures, rheumatic heart disease	No	None	Cough, dysphagia, fever, weight loss	R pleura, mediastinum	NA	Open lung biopsy	T4N1M0, Stage IIIB	NA

Acronyms: CT, computed tomography; F, female; L, left; M, male; NA, not available; R, right; UK, United Kingdom; USA, United States of America; VATS, video-assisted thoracoscopic surgery

asbestos exposure. In our review, there were 6 (38%) patients with a clear history of asbestos exposure, a percentage significantly lower than the approximate 80% exposure history typically observed in classic MPM patients [1, 3]. Environmental or secondary exposure (i.e., family household members working in an asbestos-related industry) is usually unrecognized compared to primary occupational exposure. Studies showed that even with minimal asbestos exposure, young MPM might have a genetic predisposition, such as germline mutations in the gene encoding BRCA1-associated protein-1 (BAP1) [3, 5-7]. In our review, 11 young MPM patients (69%) were diagnosed by surgery, as it could not be confirmed from initial thoracentesis. Therefore, our review reminds clinicians that MPM should also be included in the differential diagnosis when young patients present with pleural lesions. When patients present with recurrent unexplained pleural effusion or radiographic evidence of pleural thickening, further diagnostic procedures, including thoracentesis, pleural biopsy, or VATS, are indicated to assess these abnormal findings [9].

There are 4 primary histological types of malignant mesothelioma (MM): epithelioid (most common), sarcomatoid, mixed/biphasic, and desmoplastic [10]. In our review, the majority of young MRM were the epithelioid type, which aligned with previous studies [3, 10]. The diagnosis of MPM is based on IHC biomarkers [9]. The positive biomarkers included were WT1, calretinin, and CK 5/6. The negative biomarkers included polyclonal carcinoembryonic antigen (CEA), TTF-1, and claudin-4.23-25 [9]. In our case, the patient tested positive for CK 5/6 and WT1, and negative for TTF-1.

The treatment options for young MPM are similar to those for classic MPM, and include surgery (pleurectomy/decortication or extrapleural pneumonectomy), chemotherapy (pemetrexed plus cisplatin or carboplatin), immunotherapy (pembrolizumab or nivolumab +/- ipilimumab), and radiotherapy [9]. The choice of treatment depends on the stage of the disease, histology, and the patient's performance status. In classic MPM, radical surgical resection is usually not feasible, and the surgery approach is generally viewed as a palliative approach [6]. In our review, cancer-directed surgery in young MPM was more common than in classic MPM (31% vs. 18%) [3]. This observation suggests that classic MPM (older age) may present more comorbidities, making them unresectable, and contribute to a poorer prognosis than for young MPM. For our patient (stage IB), first-line therapy is surgery and systemic chemotherapy with cisplatin and pemetrexed [9]. In addition, hyperthermic intrathoracic chemotherapy (cisplatin) during surgery may have contributed to a potentially prolonged survival in those with epithelioid MPM histologic subtype stage IB [11-12].

The strongest prognostic factors in MPM are cancer stage and histologic subtype. The stage affects treatment options and the possibility of undergoing surgery. Patients with epithelioid MPM tend to have better outcomes compared to those with sarcomatoid and biphasic types [9, 10]. Other prognostic factors include Eastern Cooperative Oncology Group performance status, chest pain, dyspnea, platelet count > 400,000/μL, weight loss, serum lactate dehydrogenase levels > 500 IU/L, pleural involvement, low hemoglobin levels, high white blood cell count, and age >75 years [13]. These factors were also incorporated into the prognostic scoring systems developed by the European Organisation for Research and Treatment of

Cancer (EORTC) and the Cancer and Leukemia Group B (CALGB) [14-15]. Furthermore, recent research has explored IHC targets as potential indicators of prognosis. For instance, epithelioid MPM patients with a loss of BAP1 by IHC and a retained p16 expression by IHC have prolonged survival [9].

For unresectable MPM, a combination of nivolumab (a PD-1 inhibitor) and ipilimumab (a CTLA-4 inhibitor) improved overall survival compared to standard platinum-based chemotherapy [6, 7]. Bevacizumab, an antibody that targets VEGF, combined with standard chemotherapy, has demonstrated a survival benefit in unresectable MPM and has just been newly added to the treatment guidelines [9, 16]. Other targeted therapies, focusing on genomic alterations in MPM, have been explored but not widely accepted for clinical use, especially those targeting BAP1 (MiST trial), cyclin-dependent kinase inhibitor 2/alternative reading frame (CDKN2A/ARF) (MiST trial) [16], and neurofibromatosis 2 (NF2) (COMMAND trial) [16].

Our 30-year-old patient, diagnosed with MPM in 2023 and with a history of working in brake linings from 2011 to 2013, calls attention to a less-known issue in Taiwan: that brake linings contain asbestos. The lack of awareness of this reality led to difficulties in obtaining an asbestos exposure history and to insufficient protection for these patients in work environments. Our patient had 2 years of asbestos exposure and a 10-year latency period. In our review, young MPM also had a shorter latency period compared to classic MPM (median latency period 15 years for young MPM vs. 32 years for classic MPM) [3]. There is also a subgroup of young MPM without known exposure to asbestos. It is probable that other pathogenetic mechanisms are involved. These may include radiation exposure, non-asbestos mineral fibers like erionite, simian virus 40 [3], or genetic predisposition (such as germline mutations in the BAP1 gene) [3].

Denmark was the first country to ban asbestos for insulation in 1972, followed by a complete ban in 1986 [17]. The United States prohibited the production of asbestos in 1992 [17]. From 1994−2005, European Union member countries gradually implemented asbestos bans [17]. In Asia, Japan, South Korea, and Hong Kong banned asbestos in 2004, 2009, and 2014, respectively [17]. Between 2002 and 2012, China progressively enacted laws to ban asbestos use in vehicle braking systems and buildings [17]. Taiwan prohibited the manufacture of asbestos boards, pipes, and cement in 2008, and implemented a total ban in 2018. In addition, the import licenses for products containing asbestos have been suspended in Taiwan since 2023 [17]. As of 2022, a total of 82 countries and regions had established laws and policies to control the use of asbestos, and 62 countries had almost strictly prohibited the production, import, and sale of asbestos [18]. Countries were likely to ban asbestos when they encountered a surge in mesothelioma-related deaths within 1-5 years before the ban [19].

Implementing asbestos bans has reduced the incidence of MPM in the past decade, especially in industrialized countries with advanced economies and industries [18]. Due to the latency period after exposure, the MPM epidemic in Taiwan peaked between 2012 and 2020 [8]. From 1990 to 2019, the global age-standardized incidence rate (ASIR) decreased from 0.49 to 0.43 cases per 100,000 person-years [18]. However, despite a declining incidence, the number of newly diagnosed mesothelioma patients still

increased from 19,072 (1990) to 34,511 cases (2019) because of the long latency of asbestos exposure and an aging population [18]. These findings indicate that in countries with a long history of asbestos use, the overall number of MPM cases remained stable in the past decade [20]. Nowadays, the risk factors associated with MPM shift from asbestos exposure to genetic mutation, other carcinogenic materials (other than asbestos) or radiation therapy [20].

Between 2012 and 2021, the annual average number of malignant pleural tumor cases was 80 (IQR 70– 92) in Taiwan, with a peak of 102 cases recorded for 2021, according to the latest data available in cancer registry reports [21]. The 102 cases of malignant pleural tumors in 2021 accounted for 0.08% of all cancer cases and 0.55% of cases in the respiratory system and intrathoracic organs. Among males, the median age for diagnosing malignant pleural tumor was 69 years, with a global ASIR of 0.37 cases per 100,000 person-years [21]. Among these 102 cases of malignant pleural tumors, there were 92 cases of MPM, 8 of sarcoma, and 2 of unknown histology. Given that MPM occurs decades after exposure, we anticipate that the annual cases of MPM will remain at a peak for years in Taiwan.

TThere are several limitations to our study. First, although genetic factors are associated with young MPM, the reviewed cases usually did not provide genetic details. Second, we only focused on pleural MPM in our study, but asbestos exposure can also cause peritoneal mesothelioma [1]. Third, the outcome of these young MPM cases was usually not available in these reports.

In conclusion, our review highlighted the distinct epidemiological and clinical features of MPM in patients under 40 years old. It emphasizes the importance of considering MPM in the differential diagnosis for young patients presenting with pleural lesions, particularly in those with a history of asbestos exposure, even in countries where asbestos use is prohibited.

References

1. Lin, R.T., K. Takahashi, A. Karjalainen, *et al*., Ecological association between asbestos-related diseases and historical asbestos consumption: an international analysis. Lancet, 2007. 369(9564): p. 844-49.
2. Lacourt, A., E. Lévêque, E. Guichard, *et al*., Dose-time-response association between occupational asbestos exposure and pleural mesothelioma. Occup Environ Med, 2017. 74(9): p. 691-97.
3. Thomas, A., Y. Chen, T. Yu, *et al*., Distinctive clinical characteristics of malignant mesothelioma in young patients. Oncotarget, 2015. 6(18): p. 16766-73.
4. Liu, B., M. van Gerwen, S. Bonassi, *et al*., Epidemiology of Environmental Exposure and Malignant Mesothelioma. J Thorac Oncol, 2017. 12(7): p. 1031-45.
5. Panou, V., M. Gadiraju, A. Wolin, *et al*., Frequency of Germline Mutations in Cancer Susceptibility Genes in Malignant Mesothelioma. J Clin Oncol, 2018. 36(28): p. 2863-71.
6. Janes, S.M., D. Alrifai, and D.A. Fennell, Perspectives on the Treatment of Malignant Pleural Mesothelioma. N Engl J Med, 2021. 385(13): p. 1207-18.
7. Tsao, A.S., H.I. Pass, A. Rimner, *et al*., New Era for Malignant Pleural Mesothelioma: Updates on Therapeutic Options. J Clin Oncol, 2022. 40(6): p. 681-92.
8. Lin, R.T., Y.Y. Chang, J.D. Wang, *et al*., Upcoming epidemic of asbestos-related malignant pleural mesothelioma in Taiwan: A prediction of incidence in the next 30 years. J Formos Med Assoc, 2019. 118(1 Pt 3): p. 463-70.
9. National Comprehensive Cancer Network. Mesothelioma: Pleural (Version 1.2024). 2023; Available from: https://www.nccn.org/professionals/physician_gls/pdf/meso_pleural.pdf.
10. Paliogiannis, P., C. Putzu, G.C. Ginesu, *et al*., Deciduoid mesothelioma of the thorax: A comprehensive review of

the scientific literature. Clin Respir J, 2018. 12(3): p. 848-56.
11. Aprile, V., A. Lenzini, F. Lococo, *et al*., Hyperthermic Intrathoracic Chemotherapy for Malignant Pleural Mesothelioma: The Forefront of Surgery-Based Multimodality Treatment. J Clin Med, 2021. 10(17).
12. Järvinen, T., J. Paajanen, I. Ilonen, *et al*., Hyperthermic Intrathoracic Chemoperfusion for Malignant Pleural Mesothelioma: Systematic Review and Meta-Analysis. Cancers (Basel), 2021. 13(14).
13. Herndon, J.E., M.R. Green, A.P. Chahinian, *et al*., Factors predictive of survival among 337 patients with mesothelioma treated between 1984 and 1994 by the Cancer and Leukemia Group B. Chest, 1998. 113(3): p. 723-31.
14. Edwards, J.G., K.R. Abrams, J.N. Leverment, *et al*., Prognostic factors for malignant mesothelioma in 142 patients: validation of CALGB and EORTC prognostic scoring systems. Thorax, 2000. 55(9): p. 731-5.
15. Curran, D., T. Sahmoud, P. Therasse, *et al*., Prognostic factors in patients with pleural mesothelioma: the European Organization for Research and Treatment of Cancer experience. J Clin Oncol, 1998. 16(1): p. 145-52.
16. Borea, F., M.A. Franczak, M. Garcia, *et al*., Target Therapy in Malignant Pleural Mesothelioma: Hope or Mirage? Int J Mol Sci, 2023. 24(11).
17. Kazan-Allen, L. Chronology of asbestos bans and restrictions. Updated March 29, 2023 [cited 2024 January 4]; Available from: http://www.ibasecretariat.org/chron_ban_list.php.
18. Han, Y., T. Zhang, H. Chen, *et al*., Global magnitude and temporal trend of mesothelioma burden along with the contribution of occupational asbestos exposure in 204 countries and territories from 1990 to 2019: Results from the Global Burden of Disease Study 2019. Crit Rev Oncol Hematol, 2022. 179: p. 103821.
19. Chimed-Ochir, O., E.M. Rath, T. Kubo, *et al*., Must countries shoulder the burden of mesothelioma to ban asbestos? A global assessment. BMJ Glob Health, 2022. 7(12).
20. Carbone, M., H. Yang, H.I. Pass, *et al*., Did the Ban on Asbestos Reduce the Incidence of Mesothelioma? J Thorac Oncol, 2023. 18(6): p. 694-7.
21. Health Promotion Administration, m.o.h.a.w., Cancer registry annual report, Taiwan. 2023.
22. Hayat, R., S. Ahmed, R. Badiger, *et al*., A case of malignant mesothelioma in a young patient with childhood leukaemia who had received total body irradiation. Oxf Med Case Reports, 2023. 2023(5): p. omac151.
23. Pérez-Guzmán, C., R. Barrera-Rodríguez, and J. Portilla-Segura, Malignant pleural mesothelioma in a 17-year old boy: A case report and literature review. Respir Med Case Rep, 2016. 17: p. 57-60.
24. Patra, A., S. Kundu, A. Pal, *et al*., Mesothelioma with superior vena cava obstruction in young female following short latency of asbestos exposure. J Cancer Res Ther, 2015. 11(4): p. 940-2.
25. Singhal, B., S. Kohli, A. Singhal, *et al*., Malignant pleural and peritoneal mesothelioma consequential to brief indirect asbestos exposure. J Clin Imaging Sci, 2014. 4: p. 35.
26. Kanbay, A., Z. Ozer Simsek, N. Tutar, *et al*., Non-asbestos-related malignant pleural mesothelioma. Intern Med, 2014. 53(17): p. 1977-9.
27. Voulgaridis, A., V. Apollonatou, D. Lykouras, *et al*., Pleural mesothelioma in a young male patient. Monaldi Arch Chest Dis, 2013. 79(2): p. 96-9.
28. Rosas-Salazar, C., S.W. Gunawardena, and J.E. Spahr, Malignant pleural mesothelioma in a child with ataxia-telangiectasia. Pediatr Pulmonol, 2013. 48(1): p. 94-7.
29. Kumar, A., C. Carcano, A. Hadeh, *et al*., Unusual presentation and location pleural malignant mesothelioma. BMJ Case Rep, 2013. 2013.
30. Zarogoulidis, P., M. Orfanidis, T.C. Constadinidis, *et al*., A 26-year-old male with mesothelioma due to asbestos exposure. Case Rep Med, 2011. 2011: p. 951732.
31. Bitchatchi, E., K. Kayser, M. Perelman, *et al*., Mesothelioma and asbestosis in a young woman following occupational asbestos exposure: Short latency and long survival: Case Report. Diagn Pathol, 2010. 5: p. 81.
32. Tsai, L.Y., Y.L. Yang, M.Y. Lu, *et al*., Deciduoid mesothelioma of the pleura in an adolescent boy. Pediatr Hematol Oncol, 2010. 27(2): p. 132-7.
33. Nagata, S. and R. Nakanishi, Malignant pleural mesothelioma with cavity formation in a 16-year-old boy. Chest, 2005. 127(2): p. 655-7.
34. Gloeckner-Hofmann, K., X.Z. Zhu, H. Bartels, *et al*., Deciduoid pleural mesothelioma affecting a young female

without prior asbestos exposure. Respiration, 2000. 67(4): p. 456-8.
35. Varan, A., A. Kara, M. Haliloğlu, *et al*., Malignant mesothelioma in an adolescent boy. Pediatr Int, 1999. 41(6): p. 693-5.
36. Tewari, S.C., G. Kurian, R. Jayaswal, *et al*., Malignant mesothelioma in the young (with prosthetic aortic valve an unusual association). J Assoc Physicians India, 1989. 37(2): p. 187-9.

Right Hydropneumothorax with Epigastric Pain: Primary Surgical Repair or Minimally Invasive Endoscope Management: A Case Report

Che-Hung Lin[1]

Spontaneous esophageal perforation, also known as Boerhaave syndrome or effort rupture of the esophagus, is most lethal if treatment is delayed. Different perforation regions contribute to a variety of clinical symptoms and signs. The rarity and variability of the clinical signs of esophageal perforation may lead to a delay in diagnosis. According to a previous literature review, the mortality rate was significantly lower when a primary repair was performed within 24 hours after perforation. Here, we reported on the emergency surgical repair of a 40-year-old man diagnosed with Boerhaave syndrome with right epigastric pain and coffee-ground vomitus after meals. ***(Thorac Med 2024; 39: 292-297)***

Key words: Boerhaave syndrome, spontaneous esophageal perforation, hydropneumothorax

Introduction

Esophageal perforation is a medical challenge due to its accompanying high morbidity and mortality: it can be fatal if diagnosis and treatment are delayed. Esophageal perforations are rare, with an incidence of 3.1 per 1,000,000 per year [1]. There are 3 types of esophageal perforation: spontaneous, traumatic and iatrogenic, and their mortality rates have been 36%, 19% and 7%, respectively [2]. Iatrogenic injury to the esophagus was the most common cause of esophageal perforation, with instrumentation accounting for 59% of all patients. Approximately 15% of esophageal perforations are spontaneous. Spontaneous esophageal perforation, also known as Boerhaave syndrome or effort rupture of the esophagus, is most lethal if treatment is delayed [2].

There are 3 types of esophageal perforation based on their location: cervical, thoracic and intra-abdominal. The different perforation regions contribute to the variety of clinical symptoms and signs. The rarity and variability of the clinical signs of esophageal perforation may lead to a delay in diagnosis. Here, we present the case of a 40-year-old man diagnosed with Boerhaave syndrome with the main complaints

[1]Division of Thoracic Surgery, MacKay Memorial Hospital, Taipei, Taiwan
Address reprint requests to: Dr. Che-Hung Lin, Division of Thoracic Surgery, MacKay Memorial Hospital, Taipei, Taiwan, Sec. 2, Zhongshan N. Rd., Zhongshan Dist., Taipei City 10

of right epigastric pain and coffee-ground vomitus after meals.

Case Report

The patient was a 40-year-old male with a medical history of schizophrenia and GERD. He also had undergone open heart surgery for valvular heart diseases more than 20 years ago. According to his family, progressive epigastric pain and coffee-ground vomitus after dinner were mentioned. In the emergency room, decreased blood pressure (systolic/diastolic: 88/55 mmHg), sinus tachycardia, and shortness of breath were noted. A complete blood count and biochemistry revealed leukocytosis, anemia, an elevated serum C-reactive protein level, and hypokalemia. Cardiac enzyme findings were negative. Abdominal radiography showed mild distention and intestinal gas, and chest radiography incidentally revealed right-side hydropneumothorax (Fig. 1). Chest computed tomography showed diffuse wall thickening of the esophagus and massive right hydropneumothorax with passive atelectasis of the right lung (Fig. 2).

The patient underwent a tube thoracostomy, and a total of 700 ml of turbid effusions with a bile-like appearance drained into the chest bottle initially. His blood pressure showed mild improvement after chest tube placement and intravenous fluid resuscitation. Under the impression of severe sepsis and suspected esophageal perforation, he was transferred to the intensive care unit (ICU).

In the ICU, there was a persistent air-leak and turbid effusion from the chest tube. The gastroenterologist and thoracic surgeon then were consulted. An esophagogastroduodenoscopy (EGD) examination was arranged and revealed an esophageal perforation about 2 cm

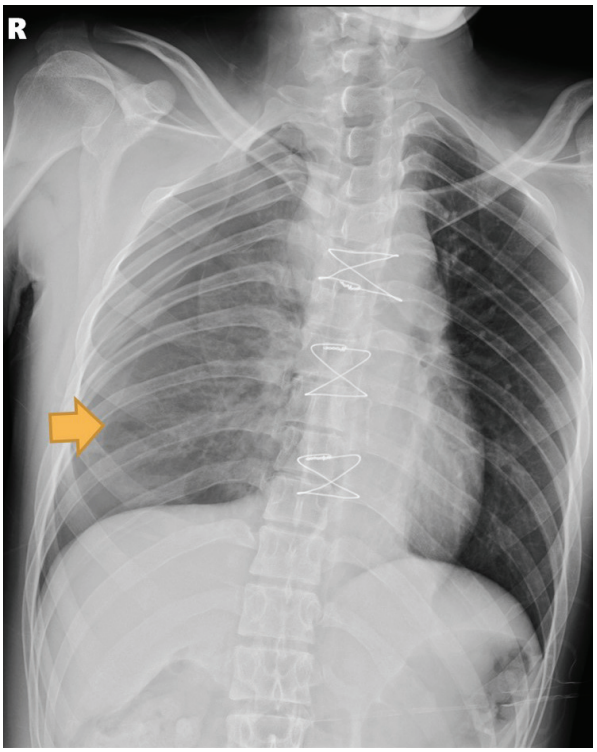

Fig. 1. Hydropneumothorax can be seen in the chest x-ray.

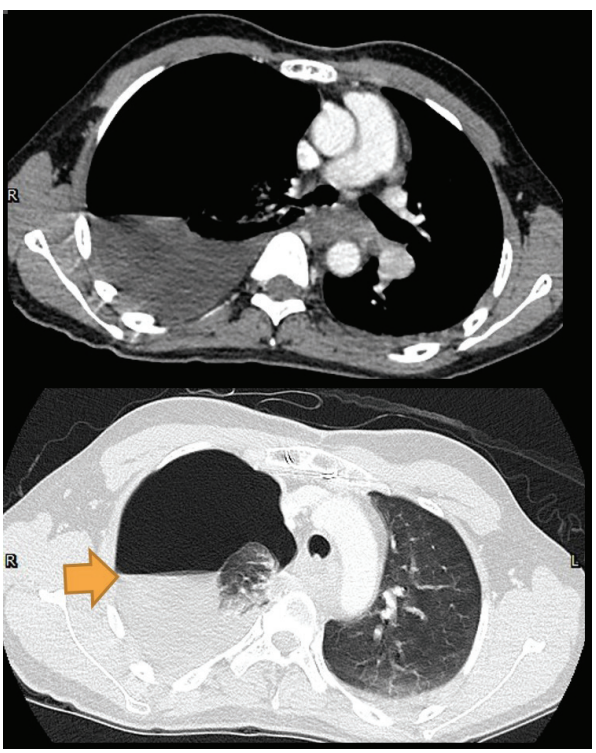

Fig. 2. Massive right hydropneumothorax with passive atelectasis of the right lung.

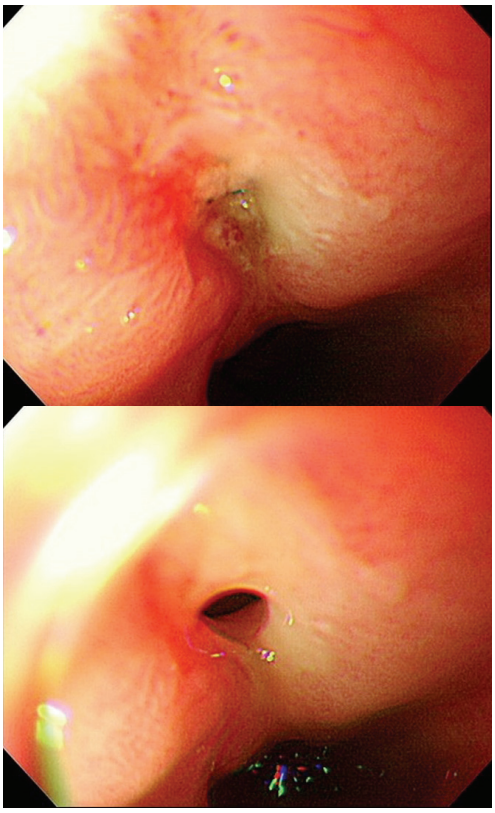

Fig. 3. Perforation above the EG junction.

above the [esophago-gastric (EG)] junction; persistent fluid throughout could be seen from this hole (Fig. 3). Emergency surgery was suggested by the thoracic surgeon for the repair of the ruptured esophagus. A right mini-thoracotomy with primary repair and a pleural flap was performed. The operative findings included an empyema with thickened peels between the posterior mediastinum and the right lower lung near the diaphragm. A perforation (at least 4 cm in diameter) was noted in the esophagus after the peels were removed, approximately 4 cm above the esophagogastric junction. Suture repair, feeding jejunostomy and intra-operative EGD were performed (Fig. 4).

On postoperative day 2 (POD 2), endotracheal tube weaning and jejunostomy feeding were started. The patient was transferred to the general ward on POD 4. Oral feeding and chest tube removal were performed in the second

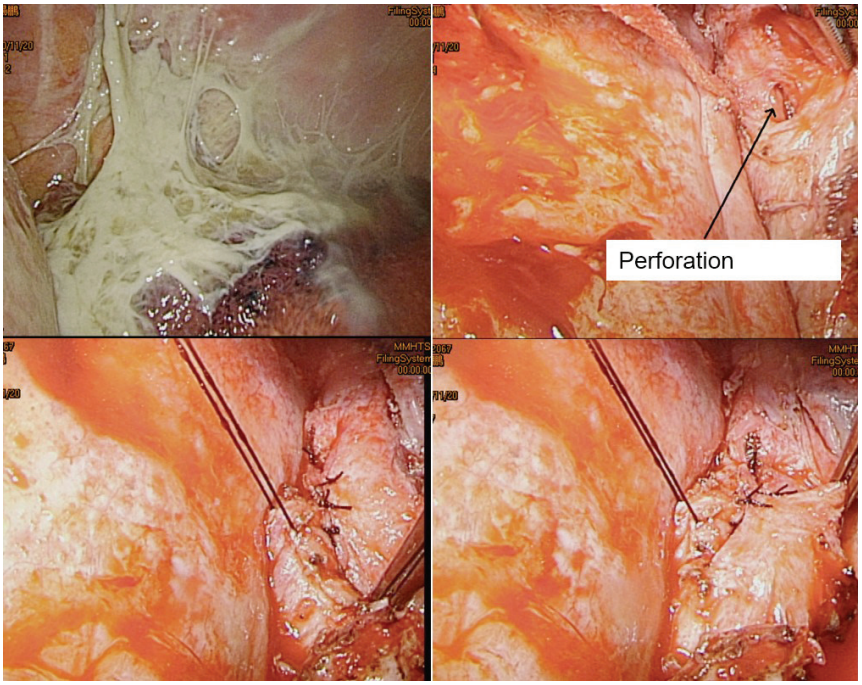

Fig. 4. Peels formation covered the hole and the primary suture repair with a pleural flap.

week of this admission. The patient was discharged in stable condition on POD 12 and has been followed up in our outpatient clinic, with no re-intervention.

Discussion

The different regions of esophageal perforation contribute to the variety of clinical symptoms and signs. The rarity and variability of the clinical signs of esophageal perforation may lead to a delay in diagnosis. Larsen K and colleagues found that a delay in diagnosis was associated with a higher risk (from 16-51%) of complications and mortality [3]. In the real world, traumatic injury of the esophagus has been diagnosed earlier than spontaneous and iatrogenic types. This indicates why the spontaneous type of esophageal perforation has a higher mortality rate (39%) than the traumatic type of injury (9%) [2].

There are 3 types of esophageal perforation based on location: cervical, thoracic and intra-abdominal. Thoracic esophageal perforation is the most common (72.6%), followed by cervical (15.2%), and abdominal (12.5%) [18, 19]. The cervical type has the lowest mortality rate (6%), due to the limited spread of infection resulting from the anatomical limitations of the neck. The presentation of cervical subcutaneous emphysema, neck pain, and dysphagia or dysphonia can be found in cervical esophageal perforation patients [20]. If the perforation can be accurately localized without distal obstruction, primary surgical repair is warranted. In addition, drainage of the perforation is sufficient to control the leak in patients not suitable for primary repair [2]. In the thoracic group, intractable retrosternal, pleuritic and mid-epigastric pain are presented. Physical examination reveals mediastinal crackles with each heartbeat. Positive imaging studies have revealed hydropneumomediastinum, left hydropneumothorax and pleural effusions. Surgical strategies include primary surgical repair, diversion with and without esophagectomy traditionally, and endoscopic management with esophageal stenting. Intra-abdominal perforation mimics the acute abdomen. Laparotomy is the preferred approach to repair an intra-abdominal esophageal perforation.

Brinster CJ and colleagues [2] found higher mortality rates in the thoracic (34%) and intra-abdominal (29%) groups than in the cervical group (6%). The sometimes non-specific nature of the symptoms may contribute to a delayed diagnosis and poor outcome. The degree of leakage and the time that has elapsed since injury are of concern. A history of severe vomiting after drinking or eating is always a concern. However, approximately 25-45% of patients have had no history of vomiting [5]. This lack of a history of vomiting has also led to a delay in diagnosis.

Boerhaave syndrome most commonly occurs as full-thickness tears along the left aspect of the distal intrathoracic esophagus, near the gastroesophageal junction (GEJ) [21]. Left-side hydropneumothorax is most common. Our patient suffered right-side hydropneumothorax, which also led to a delay in diagnosis and treatment. Boerhaave syndrome is suspected only when patients develop sepsis-related symptoms, such as fever, tachypnea, tachycardia, and hypotension. The above symptoms and signs and pleural effusion can be detected several hours after injury [6].

For patients with a stable hemodynamic status, initial medical strategies consist of total avoidance of all oral intake, parenteral nutri-

tion support, broad-spectrum antibiotics, proton pump inhibitors and drainage of extraluminal infectious fluids, and surgical consultation with an experienced thoracic surgeon [7]. Brinster CJ, *et al*. reported that the mortality rate was significantly lower when a primary repair was performed within 24 hours of perforation, compared to repair after 24 hours (4% vs 27%) [2]. The time interval between emergency surgery and the onset of symptoms in our patient was 18 hours.

Medical treatment has been successfully applied in selected patients, including those with stable hemodynamic status, and without symptoms and signs of sepsis, leakage in the neck, and leakage surrounding perforation of the thoracic esophagus without extending to the pleural cavity. In addition, early consultation with an experienced thoracic surgeon is recommended if the patient deteriorates, since emergency surgery may be necessary [8]. Recently, the use of endoscopic treatment for those who are unlikely to tolerate surgery (due to extensive underlying comorbidities) for esophageal perforations has become more popular, and has included placement of fully covered esophageal stents, through-the-scope (TTS) clips, over-the-scope (OTS) clips, and endoscopic suturing [9]. Gurwara S, *et al*. concluded that for perforations less than 1 cm in size, TTS clips are the preferred approach. For larger defects, OTS clips allow for greater closing force, thus facilitating closure [10]. The success of stenting in the treatment of esophageal perforation has been documented in several studies, some of which report esophageal salvage rates of over 80% [11]. For a further look, Chiu, *et al*. have reviewed their experience with placing esophageal stents in combination with minimally-invasive surgical drainage to treat delayed (> 24 hours) spontaneous esophageal perforations [21].

The median time to oral nutrition and to esophageal stent removal was 43 and 66 days, respectively. There was no stent migration or hospital mortality. Endoscopic vacuum therapy (EVT) is more successful in closing small perforations than in closing larger ones [12, 13]. Aziz M, *et al*. reported that EVT was associated with successful closure of esophageal defects in 89.4% of cases, with an average treatment duration of 20 days [14]. However, some studies have reported that a significant proportion of patients treated endoscopically require re-intervention [9, 15, 16]. In one study that included 340 patients with an esophageal perforation, endoscopic stenting had a success rate of 81%, but reintervention was required in 91 (27%) patients [17].

Conclusion

Boerhaave syndrome is associated with high morbidity and mortality, and is fatal if diagnosis is delayed. The most common cause of death is sepsis, leading to multi-organ failure. The location of the perforation and the etiology of the perforation have different risks and require different treatment strategies. Recently developed endoscopic treatment provides another minimally invasive treatment for delayed spontaneous esophageal perforations and for highly selective patients, but has higher re-intervention rates. The sometimes non-specific nature of the symptoms may contribute to a delay in diagnosis and a poor outcome. Early consultation with an experienced thoracic surgeon is recommended.

References

1. Vidarsdottir H, Blondal S, Alfredsson H, *et al*. Oesophageal perforations in Iceland: a whole population study on incidence, aetiology and surgical outcome. Thorac Cardiovasc Surg 2010; 58: 476.
2. Brinster CJ, Singhal S, Lee L, *et al*. Evolving options in the management of esophageal perforation. Ann Thorac Surg 2004; 77: 1475.
3. Larsen K, Skov Jensen B, Axelsen F. Perforation and rupture of the esophagus. Scand J Thorac Cardiovasc Surg 1983; 17: 311.
4. Salo JA, Isolauri JO, Heikkilä LJ, *et al*. Management of delayed esophageal perforation with mediastinal sepsis. Esophagectomy or primary repair? J Thorac Cardiovasc Surg 1993; 106: 1088.
5. Wilson RF, Sarver EJ, Arbulu A, *et al*. Spontaneous perforation of the esophagus. Ann Thorac Surg 1971; 12: 291.
6. McGovern M, Egerton MJ. Spontaneous perforation of the cervical oesophagus. Med J Aust 1991; 154(4): 277-8.
7. Lindenmann J, Matzi V, Neuboeck N, *et al*. Management of esophageal perforation in 120 consecutive patients: clinical impact of a structured treatment algorithm. J Gastrointest Surg 2013; 17(6): 1036-43.
8. Ivey TD, Simonowitz DA, Dillard DH, *et al*. Boerhaave syndrome. Successful conservative management in three patients with late presentation. Am J Surg 1981; 141(5): 531-3.
9. Barakat MT, Girotra M, Banerjee S. (Re)building the wall: recurrent Boerhaave syndrome managed by over-the-scope clip and covered metallic stent placement. Dig Dis Sci 2018; 63: 1139.
10. Gurwara S, Clayton S. Esophageal perforations: an endoscopic approach to management. Curr Gastroenterol Rep 2019 Nov; 21(11): 57
11. Liang DH, Hwang E, Meisenbach LM, *et al*. Clinical outcomes following self-expanding metal stent placement for esophageal salvage. J Thorac Cardiovasc Surg 2017 Sep; 154(3): 1145-50.
12. Ooi G, Burton P, Packiyanathan A, *et al*. Indications and efficacy of endoscopic vacuum-assisted closure therapy for upper gastrointestinal perforations: EndoVAC for upper GI perforations. ANZ J Surg 2018 Apr; 88(4):E257-63.
13. Loske G, Schorsch T, Dahm C, *et al*. Iatrogenic perforation of esophagus successfully treated with Endoscopic Vacuum Therapy (EVT). Endosc Int Open 2015 Dec; 3(6): E547-51.
14. Aziz M, Haghbin H, Sharma S, *et al*. Safety and effectiveness of endoluminal vacuum-assisted closure for esophageal defects: systematic review and meta-analysis. Endosc Int Open 2021 Sep; 09(09): E1371-80.
15. Ali JT, Rice RD, David EA, *et al*. Perforated esophageal intervention focus (PERF) study: a multi- center examination of contemporary treatment. Dis Esophagus 2017; 30: 1.
    [[The original reference 15 was repeated from reference 9 above.]]
16. Hauge T, Kleven OC, Johnson E, *et al*. Outcome after stenting and débridement for spontaneous esophageal rupture. Scand J Gastroenterol 2018; 53: 398.
17. Dasari BV, Neely D, Kennedy A, *et al*. The role of esophageal stents in the management of esophageal anastomotic leaks and benign esophageal perforations. Ann Surg 2014; 259: 852.
18. Sdralis EIK, Petousis S, Rashid F, *et al*. Epidemiology, diagnosis, and management of esophageal perforations: systematic review. Dis Esophagus 2017 Aug; 30(8) :1-6.
19. Chen S, Shapira-Galitz Y, Garber D, *et al*. Management of iatrogenic cervical esophageal perforations: a narrative review. JAMA Otolaryngol Head Neck Surg 2020 May; 146(5): 488-94.
20. Brauer RB, Liebermann-Meffert D, Stein HJ, et al. Boerhaave's syndrome: analysis of the literature and report of 18 new cases. Dis Esophagus 1997; 10(1): 64.
21. Chiu CH, Leow OQY, Wang YC. Esophageal stenting with minimally-invasive surgical intervention for delayed spontaneous esophageal perforation. J Thorac Dis 2023 Mar 31; 15(3): 1228-35.